MASTERARBEIT | MASTER'S THESIS

Titel | Title

Screening of natural products and derivatives as GPR84 receptor modulators

verfasst von | submitted by

Marvin Csar BSc

angestrebter akademischer Grad | in partial fulfilment of the requirements for the degree of

Magister pharmaciae (Mag. pharm.)

Wien | Vienna, 2025

Studienkennzahl lt. Studienblatt | Degree programme code as it appears on the student record sheet:	UA 066 605
Studienrichtung lt. Studienblatt | Degree programme as it appears on the student record sheet:	Masterstudium Pharmazie
Betreut von | Supervisor:	Univ.-Prof. Dr. Verena Dirsch
Mitbetreut von | Co-Supervisor:	Mag. Dr. sc. ETH Alexander Franz Perhal

Declaration on the use of AI in the writing process

During the preparation of this thesis, the author used DeepL to improve the language and readability of the text. The author subsequently reviewed and edited all content and takes full responsibility for the final version of the thesis.

Abstract (English)

The GPR84 receptor, which is primarily expressed on cells of the innate immune system, is a G protein-coupled receptor that triggers an enhanced pro-inflammatory immune response upon activation. Much about this receptor remains unknown, but it is associated with various inflammatory diseases, some of which are severe, such as colitis, acute lung injury (ALI), and atherosclerosis. This study aimed to identify potential agonists and antagonists of the GPR84 receptor by screening various natural products and their derivatives. This could help gain insight into the pathophysiological relevance of the receptor and potentially discover pharmacologically relevant compounds for further investigation.

The screening was conducted via photometric measurement of intracellular cAMP levels using an EPAC-based FRET biosensor in a stably transfected GPR84-HEK cell line. Since GPR84 is a Gi-type G protein-coupled receptor, its activation decreases the level of cAMP in the cells, while its inactivation increases it. Binding of cAMP to the biosensor induces a shift in the wavelength of emitted light. Thus, photometric measurements can indicate agonistic or antagonistic activity of the substances under investigation. Substances that exhibited activity in the EPAC screening were then tested in a neutrophil migration assay. Specifically, we investigated whether test substances activated and stimulated isolated neutrophil granulocytes to migrate through a monolayer of Calu-3 cells. This experiment determines whether a substance exhibits chemotactic activity and confirms the pro- or anti-inflammatory effects of the substances being tested.

As a result, oxidative metabolites of linoleic acid (OXLAMs), primarily known for their role in inflammatory reactions, were found to be linked to agonistic activity at the GPR84 receptor. Additionally, the natural compounds Pinoresinol and imbricaric acid were identified as potential antagonists of the GPR84 receptor. According to the literature, these substances have been described as having anti-inflammatory effects. However, more research is needed to determine if these effects are associated with the GPR84 receptor. Similarly, the potential relationship between OXLAMs and this orphan receptor is an area of ongoing research that could provide insight into its physiological function.

Abstract (Deutsch)

Der GPR84-Rezeptor ist ein G-Protein-gekoppelter Rezeptor, der hauptsächlich auf Zellen des angeborenen Immunsystems exprimiert wird und bei Aktivierung eine verstärkte pro-inflammatorische Immunantwort auslöst. Über diesen Rezeptor ist noch nicht viel bekannt, er wird jedoch mit verschiedenen entzündlichen Erkrankungen in Verbindung gebracht, von denen einige schwerwiegend sind, wie beispielsweise Colitis, akute Lungenverletzung (ALI) und Atherosklerose. Ziel dieser Arbeit war die Identifizierung potenzieller Agonisten und Antagonisten des GPR84-Rezeptors durch das Screening verschiedener Naturstoffe und ihrer Derivate. Dies könnte dazu beitragen, Einblicke in die pathophysiologische Bedeutung des Rezeptors zu gewinnen und potenziell pharmakologisch relevante Verbindungen für weitere Untersuchungen zu identifizieren.
Das Screening erfolgte durch photometrische Messung des intrazellulären cAMP-Spiegels mit einem EPAC-basierten FRET-Biosensor in einer stabil transfizierten GPR84-HEK-Zelllinie. Da GPR84 ein G-Protein-gekoppelter Rezeptor vom Gi-Typ ist, verringert seine Aktivierung die Menge an cAMP in den Zellen, während seine Inaktivierung sie erhöht. Die Bindung von cAMP an den Biosensor führt zu einer Verschiebung der Wellenlänge des emittierten Lichts. Somit können photometrische Messungen die agonistische oder antagonistische Aktivität der untersuchten Substanzen anzeigen. Substanzen, die im EPAC-Screening Aktivität zeigten, wurden anschließend in einem Granulozyten-Migration Assay getestet. Konkret wurde untersucht, ob die Testsubstanzen isolierte neutrophile Granulozyten aktivieren und zur Migration durch eine einfache Zellschicht aus Calu-3-Zellen anregen. Mit diesem Experiment lässt sich feststellen, ob eine Substanz chemotaktische Aktivität aufweist, wodurch auch die pro- oder antiinflammatorische Wirkung der getesteten Substanzen bestätigt wird.

Es konnte nachgewiesen werden, dass oxidative Metaboliten der Linolsäure (OXLAMs), die vor allem für ihre Rolle bei Entzündungsreaktionen bekannt sind, eine agonistische Aktivität am GPR84-Rezeptor aufweisen. Darüber hinaus konnten die Naturstoffe Pinoresinol und imbricic acid als potenzielle Antagonisten des GPR84-Rezeptors identifiziert werden. In der Literatur wird diesen Substanzen eine entzündungshemmende Wirkung zugeschrieben. Es sind jedoch weitere Untersuchungen erforderlich, um festzustellen, ob diese Wirkungen mit dem GPR84-Rezeptor zusammenhängen. Auch der potenzielle Zusammenhang zwischen OXLAMs und diesem Rezeptor bedarf weiteren Untersuchungen und könnte Aufschluss über die physiologische Funktion dieses Rezeptors geben.

Table of contents

1 Introduction

1.1 The GPR84 receptor

The GPR84 receptor is an immune-modulating G-protein-coupled receptor primarily expressed in myeloid cells of the innate immune system, such as macrophages, monocytes, and neutrophil granulocytes. Unlike other immune-modulating G protein-coupled receptors, GPR84 is an inhibitory receptor of the Gi-type. The expression of the GPR84 receptor significantly increases under acute inflammatory stimuli, such as lipopolysaccharides, which leads to the assumption that it may be related to inflammatory and fibrotic diseases[1–3]. According to Wang et al., the GPR84 receptor plays an important role in the development of inflammatory lung diseases, such as acute lung injury (ALI) and acute respiratory distress syndrome (ARDS), the latter of which has a high mortality rate. The authors demonstrate that GPR84 is significantly increased in cells obtained from the bronchoalveolar lavage fluid of mice with lipopolysaccharide (LPS)-induced ALI. However, blocking or downregulating GPR84 significantly reduces inflammation in lung tissue[4,5]. Zhang et al. demonstrated that GPR84 is highly upregulated in the inflamed colon tissue of patients with ulcerative colitis and in mice with dextran sulfate sodium (DSS)-induced colitis. They also found that GPR84 knockout mice were resistant to DSS-induced colitis[1]. However, it was also found that GPR84 plays an important role in the phagocytosis of cancer cells by macrophages[6,7]. However, it should be noted that opinions about the function and effects of this receptor are widespread and controversial. For example, it has been shown that receptor activation has anti-atherosclerotic effects due to stimulation of reverse cholesterol transport[8]. Additionally, reports indicate that activating GPR84 can have anti-inflammatory and antifibrotic effects[9]. Although the receptor has been known for almost 25 years, its physiological role and endogenous ligands remain unknown. Therefore, it is classified as an orphan receptor[8,10].

1.1.1 Ligands of GPR84

1.1.1.1 Fatty acids (potential endogenous ligands)

Several studies have found that GPR84 is activated by medium-chain fatty acids (MCFAs) containing 9-14 carbon atoms, but not by short-chain (SCFAs) or long-chain (LCFAs) fatty acids. Using cryo-electron microscopy, Zhang et al. discovered that fatty acids with more than 14 carbon atoms are too large to fit into the ligand-binding pocket. However, short-chain fatty acids are not long enough because their hydrophobic tails are too short to reach the end of the binding pocket, which is essential for activating the receptor[6]. Additionally, Wang et al.'s experiments showed that fatty acids shorter than C9 and longer than C14 did not affect the GPR84 receptor[11]. Suzuki et al. demonstrated that hydroxylated fatty acids are more potent agonists than non-hydroxylated fatty acids[12].

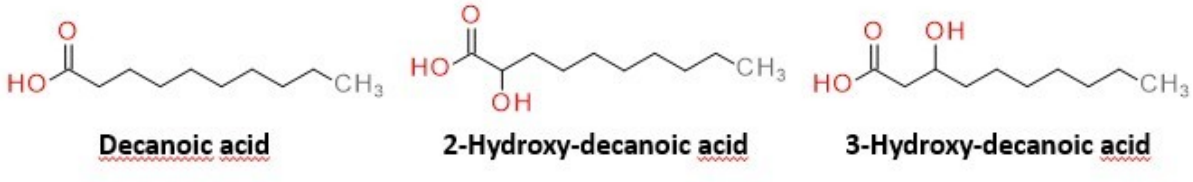

Figure 1: Structures of potential endogenous GPR84 ligands. Created in BIOVIA Draw 2019.

Several ligands of the GPR84 receptor have already been identified, but the receptor's endogenous ligands remain unknown. It is assumed that medium-chain fatty acids (MCFAs) could be the natural ligands, but the high concentrations necessary to activate the receptor exceed normal physiological levels, which makes this assumption questionable[8].

1.1.1.2 Other ligands

Other ligands were also discovered, such as the synthetic agonist 6-(octylamino)-2,4(1H,3H)-pyrimidinedione (6-OAU), which has been described in several publications[1,4,6,10,13–15]. Later, 2-(hexylthio)pyrimidine-4,6-diol, a structurally related compound, was identified as a GPR84 agonist[10,16]. Diindolylmethane, a natural compound found in green vegetables like broccoli, has been identified as an allosteric agonist of GPR84. It likely acts via an allosteric binding site since it is not similar to fatty acids[10,11,16,17]. Embelin, another natural product and a secondary metabolite originally isolated from the plant Embelia ribes (Primulaceae), was

proven to be a moderately potent GPR84 agonist. In addition to activating GPR84, embelin has been reported to exhibit antimicrobial, anthelmintic, analgesic, antiapoptotic, and anti-inflammatory activities[8,17].

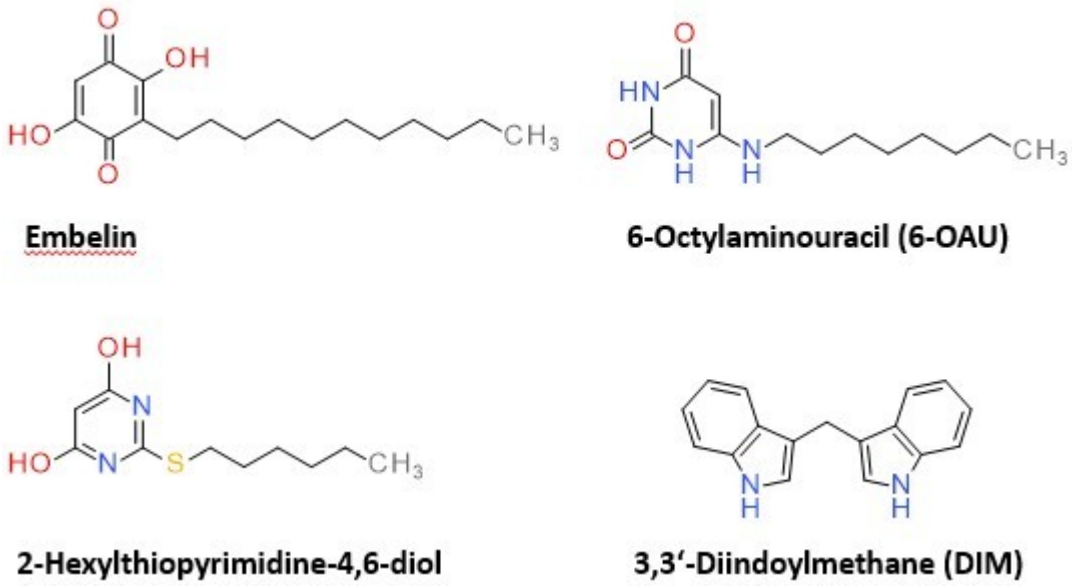

Figure 2: Structures of reported GPR84 agonists. Created in BIOVIA Draw 2019.

1.1.2 Downstream Signaling Pathways of GPR84

1.1.2.1 G Protein signaling

GPR84 is believed to be involved in many biological pathways; however, its primary function and role in physiology are not fully understood. Like many other G protein-coupled receptors, GPR84 inhibits the production of cAMP by blocking adenylyl cyclase through Gi.

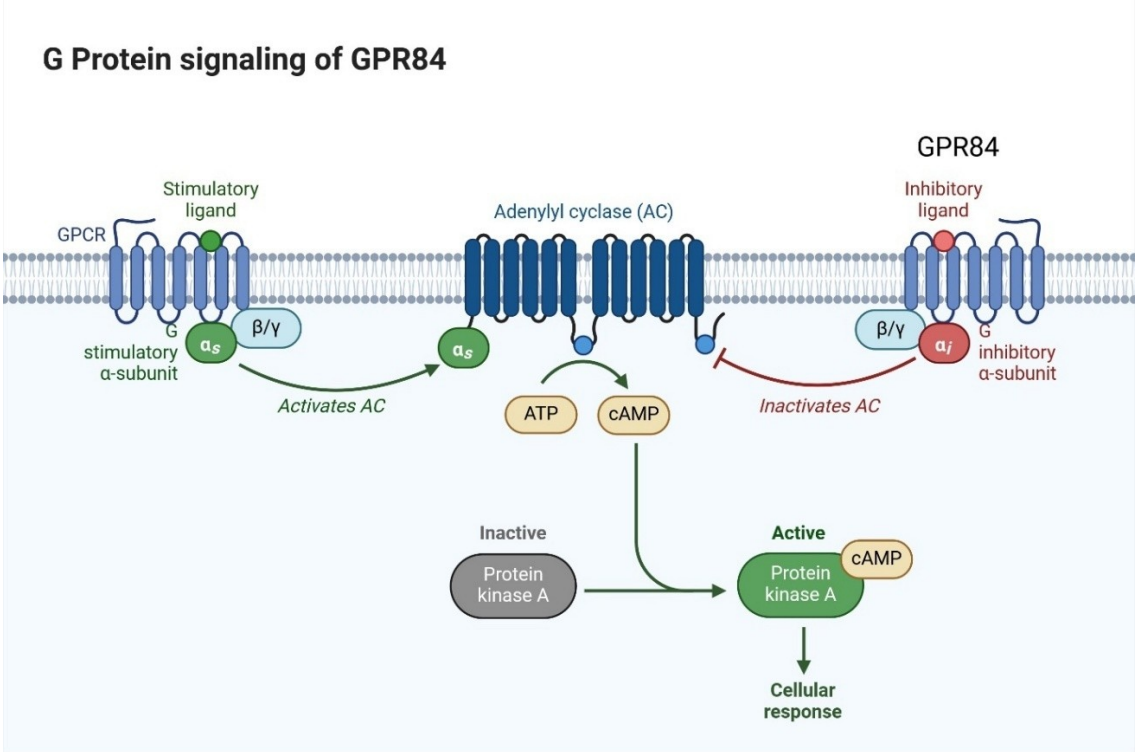

Figure 3: Graphical scheme of the G Protein signaling of GPR84. A G protein-coupled receptor (GPCR) like GPR84 (shown on the right) can bind to agonist ligands, which cause the release of the α-subunit that inactivates adenylyl cyclase (AC). Conversely, stimulatory ligands activate AC by releasing the α-subunit of a Gs-coupled GPCR (shown on the left). AC transforms ATP into cAMP, which activates protein kinase A (PKA). This subsequently leads to a cellular response. Thus, activation of GPR84 by an agonist results in the inactivation of AC, lower levels of cAMP, and ultimately, a reduced cellular response to PKA activation. Created in https://BioRender.com

As shown in Figure 3, activation of GPR84 by an agonistic ligand causes adenylyl cyclase to be inactivated by Gi. As a result, less ATP is converted to cAMP, resulting in less PKA activation for a cellular response[8,15,16,18].

1.1.2.2 AKT, ERK1/2 and NFκB pathways

Although much remains unknown about the exact mechanisms, it has been discovered that the GPR84 receptor influences the AKT and ERK1/2 pathways. In their experiments, Recio et al. compared the AKT and ERK1/2 phosphorylation of wild-type and GPR84-/- macrophages when exposed to the GPR84 agonist 6-OAU. The researchers demonstrated that the GPR84 receptor plays a significant role in activating these kinases. A similar effect was observed with the translocation of the p65 subunit of NF-κB. An increased nuclear translocation of p65 was observed when treated with 6-OAU, indicating NF-κB activation by the reported GPR84 agonist[4,8,10,15,19].

1.1.2.3 NLRP3 inflammasome

Activation of GPR84 leads to the release of numerous inflammatory mediators, including reactive oxygen species (ROS) and proinflammatory cytokines such as IL-1β, IL-6, IL-18, and TNF-α[1,4,20,21]. Researchers found that the receptor mediates the formation of the NLRP3 inflammasome complex in the presence of pathogens. The NLRP3 inflammasome is a protein complex that contains a cytosolic receptor belonging to the Nod-like receptor (NLR) family. Its activation triggers the activation of caspase-1 and the secretion of interleukin (IL)-1β and IL-18. This plays an important role in the pathogenesis of inflammatory diseases. In their experiments, Zhang et al. proved that GPR84 activation with 6-OAU significantly increased IL-1β secretion in a concentration-dependent manner[1,10,20].

1.1.2.4 β -Arrestin signaling

Several GPR84 agonists, such as 6-OAU, have been found to effectively recruit β-arrestins to the receptor. These proteins form complexes with G protein-coupled receptors after agonist binding and receptor phosphorylation by G protein-coupled receptor kinases. This process results in downregulation via receptor internalization. In other words, repeated activation of the GPR84 receptor or use of high concentrations of agonists causes desensitization and subsequently reduced effects[6,10,16,22,23].

1.1.2.5 Potential anti-atherosclerotic function

Gaidarov et al. demonstrated that GPR84 agonists can increase the expression of cholesterol transporters, such as ABCA1 and ABCG1, and promote cholesterol efflux in macrophages. This could lead to reverse cholesterol transport, which has an anti-atherosclerotic effect[8].

There may be even more pathways affected by this receptor. More research is necessary to determine how all the pathways are linked and what this receptor's physiological function is.

1.2 Linoleic acid

Linoleic acid (LA) is the most common polyunsaturated fatty acid in the human diet. It is an essential fatty acid that must be consumed because the body cannot synthesize it on its own[24,25]. In the human body, LA has several functions. Like all fatty acids, it can be used for energy, but it is also a component of cell membranes[25]. In general, linoleic acid is an essential component of a healthy diet because it plays an important role in several physiological processes[26]. It is a precursor to arachidonic acid, which is then converted into other biological mediators, such as eicosanoids, prostaglandins, and leukotrienes[25]. Furthermore, it is suggested that LA is an important nutrient for early human development[27]. However, it was found that an extremely high intake of linoleic acid can cause severe health issues due to the formation of OXLAMs and free radicals[26]. Chronic inflammatory diseases, such as cardiovascular disease and Alzheimer's disease, are often reported as possible consequences of excessive LA consumption[28].

1.3 OXLAMs

OXLAM is an abbreviation for "oxidized linoleic acid metabolites." As shown in Figure 4, there are four different substances included in the OXLAM group: 9- and 13-hydroxyoctadecadienoic acid (9- and 13-HODE), and 9- and 13-oxo-octadecadienoic acid (9- and 13-oxo-ODE).There are reports of additional metabolites, such as 9,10,13-trihydroxyoctadecenoic acid (9,10,13-triHOME), 9,10-dihydroxyoctadecenoic acid (9,10-DiHOME), and 12,13-dihydroxyoctadecenoic acid (12,13-DiHOME), but they were not considered in this thesis[29]. These OXLAMs are linked to inflammatory diseases, such as cardiovascular disease, chronic pain, Alzheimer's disease, and non-alcoholic steatohepatitis[26,30]. Studies also show that a high intake of OXLAM can affect cerebral lipid peroxidation and accumulation[31]. Although the exact mechanisms are not fully understood, Schuster et al. found that higher OXLAM levels increase oxidative stress and subsequent inflammatory processes in the blood. Their results also showed that higher OXLAM consumption leads to greater NLRP3 inflammasome activation and, consequently, greater caspase-1 activation[26].

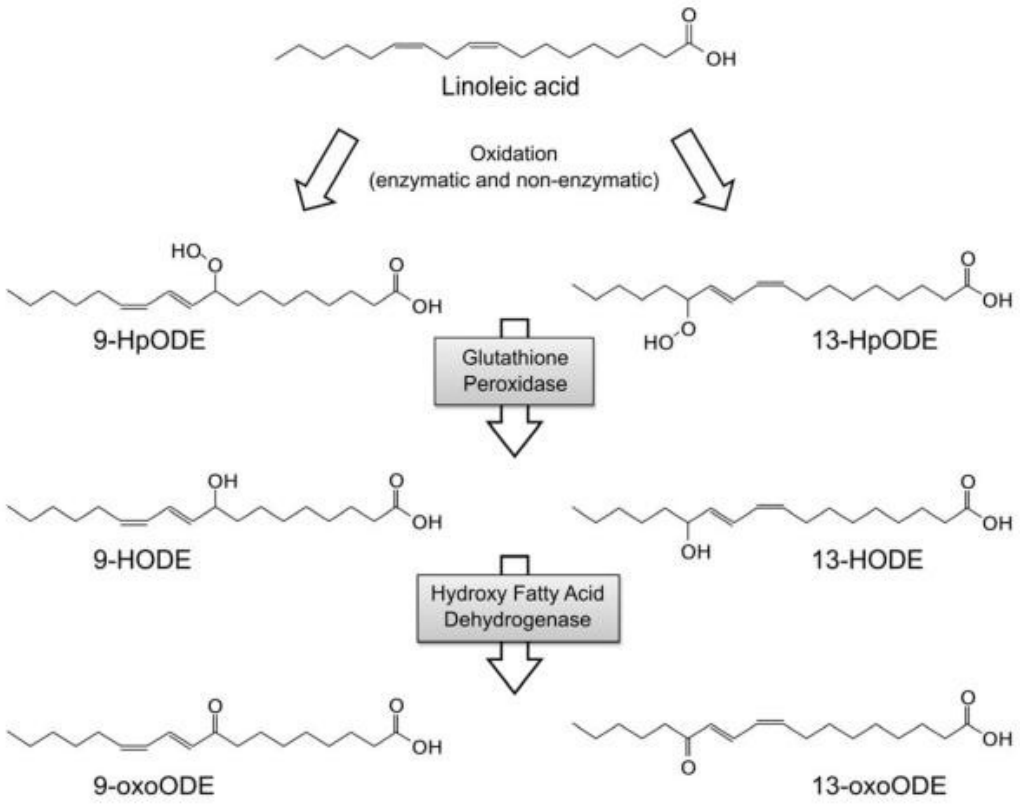

Figure 4: Oxidative metabolism of linoleic acid (LA). In vivo, linoleic acid undergoes enzymatic and non-enzymatic oxidation. This process results in the formation of either 9-HpODE or 13-HpODE. The enzyme glutathione peroxidase then metabolizes these structures into 9-HODE or 13-HODE. In a subsequent metabolic step, hydroxy fatty acid dehydrogenase converts them into 9-oxo-ODE and 13-oxo-ODE. These substances are collectively known as OXLAMs (oxidized linoleic acid metabolites)[24].

1.4 Imbricaric acid

Several lichen species, such as *Cetrelia monachorum* (Parmeliaceae), produce imbricaric acid. Lichens are known to contain a variety of secondary metabolites with reported pharmacological properties, including antifungal, antibiotic, antiviral, anti-inflammatory, antipyretic, and antioxidant effects. Oettl et al. identified imbricaric acid as a contributor to the positive effects of *Cetrelia monachorum* extracts, particularly the antipyretic activity. The researchers tested imbricaric acid for its inhibitory effects on the mPGES-1, 5-LO, and NFκB pathways. The substance exhibited inhibitory activity in all three pathways, making it a promising candidate for further investigation[32].

1.5 Pinoresinol

Pinoresinol diglucoside (PDG) is a key lignan extracted from the bark of *Eucommia ulmoides* (Eucommiaceae), a traditional Chinese medicinal herb. Previous research has demonstrated that PDG exhibits various pharmacological effects, including anti-inflammatory, antihypertensive, osteoporotic-preventive, and tumor-suppressive properties[33,34]. In Lei et al.'s experiments, PDG notably decreased Toll-like receptor 4 (TLR4) expression and nuclear factor-κB (NF-κB) activation, while enhancing nuclear factor E2-related factor 2 (Nrf2) and heme oxygenase 1 (HO-1) expression. These results demonstrate PDG's ability to reduce neuroinflammation, neuronal apoptosis, and oxidative stress by modulating the TLR4/NF-κB and Nrf2/HO-1 signaling pathways[34]. Haapakorva et al. demonstrated that pinoresinol stimulates the growth of human keratinocytes in vitro and decreases the expression of TNF-α and, to a lesser extent, IL-1β in peripheral blood mononuclear cells[35]. Chen et al. found that PDG administration suppressed the activation of the AKT/mTOR/NF-κB signaling pathway in vivo and in vitro. The researchers concluded that pinoresinol might be a promising therapeutic intervention for conditions such as hypertrophic cardiomyopathy[36].

2 Aim of the study

The study aimed to test a large database of various natural products and their derivatives (DNTI database from the Division of Pharmacognosy, Department of Pharmaceutical Sciences of the University of Vienna) on GPR84-transfected HEK cells, in order to identify compounds with agonistic or antagonistic activity. The focus was on antagonists, as attenuating inflammation seemed more therapeutically relevant. However, this study tested substances for both agonistic and antagonistic activity. During the course of the project, a number of interesting compounds with agonistic activity were discovered, prompting further investigation of these compounds. Meanwhile, screening for more substances continued and potential antagonists were found. Due to time constraints and technical issues, however, the investigation of these antagonistic compounds could not be completed and remains a subject of interest for further research.

3 Materials and Methods

3.1 Materials

Table 1: Summary of all reagents used

Name	Ingredients	Amount/Concentration	Provider
DMEM Complete Medium for HEK cells	Dulbecco's Modified Eagle's Medium with 4.5 g/l glucose and phenol red	500 ml	Lonza (Basel, Switzerland)
	Glutamine solution 2 mM	5 ml	
	Penicillin	100 U/ml	
	Streptomycin	100 µg/ml	
	FBS	50 ml	
DMEM/F12 Complete Medium for Calu 3 cells	Dulbecco's Modified Eagle's Medium with 4.5 g/l glucose and phenol red	250 ml	Lonza (Basel, Switzerland)
	Ham's F12 Medium with L-glutamine	250 ml	
	Glutamine solution 2 mM	5 ml	
	Penicillin	100 U/ml	
	Streptomycin	100 µg/ml	
	FBS	50 ml	

RPMI stripped + HEPES Medium	Roswell Park Memorial Institute Medium with L-glutamine	500 ml	Lonza (Basel, Switzerland)
	Glutamine solution 2 mM	5 ml	Lonza (Basel, Switzerland)
	Penicillin	100 U/ml	Lonza (Basel, Switzerland)
	Streptomycin	100 µg/ml	Lonza (Basel, Switzerland)
	HEPES	1.31 g	Sigma-Aldrich (St. Louis, USA)
	Charcoal stripped FBS	25 ml	Gibco (Waltham, CA, USA)
	NaOH ad pH 7.2	quantum satis	
PBS	NaCl	7.2 g	Carl-Roth (Karlsruhe, Germany)
	Na_2HPO_4	1.48 g	
	KH_2PO_4	0.43 g	
	ddH_2O	1000 ml	
	NaOH ad pH 7.4	quantum satis	
Trypsin/EDTA solution	Trypsin	0.5 g	Gibco (Waltham, CA, USA)
	Na_2-EDTA	0.2 g	
	PBS	1000 ml	
10X FURA buffer	NaCl	40.3 g	Carl-Roth (Karlsruhe, Germany)

	KCl	1.86 g	Carl-Roth (Karlsruhe, Germany)
	$MgCl_2$ anhydrous	0.47 g	Sigma-Aldrich (St. Louis, USA)
	$CaCl_2$ x 2 H_2O	1.17 g	Fluka Analytical (St. Gallen, Switzerland)
	Glucose anhydrous	5 g	Sigma-Aldrich (St. Louis, USA)
	HEPES (free acid)	23.8 g	Carl-Roth (Karlsruhe, Germany)
	NaOH	q.s.	Carl-Roth (Karlsruhe, Germany)
1X FURA buffer	10X FURA buffer	50 ml	
	ddH_2O	450 ml	
10X RBC (red blood cell) lysis buffer	NH_4Cl	41.3 g	Department of Pharmaceutical Sciences Univ. Prof. Judith Rollinger
	$NaHCO_3$	5 g	Carl-Roth (Karlsruhe, Germany)
	EDTA 0.5 M	1 ml	Carl-Roth (Karlsruhe, Germany)
	ddH_2O	ad 500 ml	
1X RBC (red blood cell) lysis buffer	10X RBC (red blood cell) lysis buffer	50 ml	
	ddH_2O	450 ml	

P/F/E-buffer	PBS	500 ml	
	FBS	5 ml	Lonza (Basel, Switzerland)
	EDTA 0.5 M pH = 8	1 ml	Carl-Roth (Karlsruhe, Germany)
Lymphopure		500 ml	BioLegend (San Diego, USA)
DMSO		1000 ml	Carl Roth (Karlsruhe, Germany)
Forskolin			MCE (New Jersey, USA)
Embelin			Cayman Chemical (Michigan, USA)
Capric acid (decanoic acid)			Cayman Chemical (Michigan, USA)
6-OAU			Cayman Chemical (Michigan, USA)
9-HODE		100 µg in 100 µl EtOH	Cayman Chemical (Michigan, USA) Batch: 0579560-31
9-OxoODE		25 µg in 250 µl EtOH	Cayman Chemical (Michigan, USA) Batch: 0467447-59
ALA			Biomol (Hamburg, Germany)
LA			Biomol (Hamburg, Germany)

AA			Biomol (Hamburg, Germany)
EPA			Biomol (Hamburg, Germany)
DHA			Biomol (Hamburg, Germany)
fMLP			Sigma-Aldrich (St. Louis, USA)
IL-8			Milteny Biotec (Bergisch Gladbach, Germany) Batch: 130-122-353
Luminol			Sigma-Aldrich (St. Louis, USA)
CD11b Antibody (APC Vio770)			Milteny Biotec (Bergisch Gladbach, Germany) LOT: 5220902765
CD14 Antibody (APC)			Milteny Biotec (Bergisch Gladbach, Germany) LOT: 5220805954
CD16 Antibody (PE Vio770)			Milteny Biotec (Bergisch Gladbach, Germany) LOT: 5220708881
CD45 Antibody (Vio Blue)			Milteny Biotec (Bergisch Gladbach, Germany) LOT: 5220809903

CD66b Antibody (FITC)			Milteny Biotec (Bergisch Gladbach, Germany) LOT: 5220902789

Table 2: Table of used devices

Name	Provider
Biological Safety Cabinets Herasafe™	Thermo Fisher Scientific Inc. (Waltham, CA, USA)
Heracell™ 150 Incubator	Thermo Fisher Scientific Inc. (Waltham, CA, USA)
Vi-Cell™ XR Cell Viability Analyzer	Beckmann Coulter (Fullerton, CA, USA)
Light Microscope Olympus CKX31	Olympus Europa GmbH (Hamburg, Germany)
Centrifuge Heraeus™ Multifuge 1 S-R	Thermo Fisher Scientific Inc. (Waltham, CA, USA)
Tecan Spark™ plate reader	Tecan (Mannedorf, Switzerland)
EVOM2 Voltohmmeter	WPI Germany (Berlin, Germany)
VWR VM-3000™ Mini Vortexer	VWR International (Radnor, US)
MACSQuant Analyzer	Miltenyi Biotec (Bergisch Gladbach, Germany)
Fisherbrand 500 ml filter unit 0,2 µm	Fisher scientific (Massachusetts, USA)
TC-Inserts 24 Well PET 3 µm	Sarstedt (Nümbrecht, Germany)

3.2 Buffer and Media

3.2.1 10X FURA Buffer

A stock solution of 10X FURA buffer was prepared and frozen. The substances listed in Table 1 were then dissolved in ddH_2O. Then, the pH was adjusted to 7.4 with HCl or NaOH, and the solution was taken to the cell culture lab for sterile filtration. In the laminar airflow hood, the solution was filtered using a sterile filtration kit and divided into ten 50-ml falcon tubes. The falcon tubes were labeled and frozen, making them ready to use as needed.

3.2.2 1X FURA Buffer

When a fresh 1X FURA buffer solution was needed, one of the prepared 10X FURA buffer solution flasks was thawed and diluted with 450 mL of deionized water (ddH_2O). Then, the dilution was adjusted to pH 7.4 with HCl or NaOH. Then, the dilution was sterile-filtered under a laminar airflow using a sterile filtration kit similar to the one used for the 10X FURA buffer. The filtrate was then divided into 10 50-ml falcon tubes and stored at 4°C.

3.2.3 PBS (phosphate buffered saline)

To prepare this substance, 7.2 g of NaCl, 1.48 g of Na_2HPO_4, and 0.43 g of KH_2PO_4 were dissolved in 1,000 mL of deionized water and sterilized by autoclaving.

3.2.4 Complete media for cell culture

To prepare the DMEM complete medium, a 500-ml bottle of DMEM was mixed with 5-ml aliquots of a 2-mM glutamine solution and an antibiotic solution containing penicillin and streptomycin, as well as 50-ml of FBS. This was done under a laminar airflow hood to ensure sterility of the medium. After labeling, the medium was stored in the refrigerator at 4°C.

For the DMEM/F12 complete medium, a sterile bottle with a capacity of over 1000 mL was placed under the laminar airflow and filled with 500 mL of DMEM and 500 mL of Ham's F12 medium. Then, 100 mL of FBS, 10 mL of 2 mM glutamine solution, and an antibiotic solution were added. The mixture was sterile-filtered, divided into two bottles, labeled, and stored at 4°C.

3.2.5 RPMI stripped + HEPES

Five hundred milliliters of RPMI were mixed with 1.31 grams of HEPES and 25 milliliters of charcoal-stripped FBS. Then, 5 mL each of glutamine and antibiotic solutions (penicillin and streptomycin) were added. After thoroughly mixing, the pH of the medium was adjusted to 7.2 with HCl or NaOH, and then it was sterile filtered under a laminar airflow. After filtration, the medium was transferred to the bottle in the filtration kit and stored at 4°C in the refrigerator.

3.2.6 10X RBC lysis buffer

The 10X RBC lysis buffer is a highly concentrated stock solution intended for storage and should be diluted 1:10 before use. Therefore, 41.3 g of NH_4Cl, 5 g of $NaHCO_3$, and 1 mL of 0.5 M EDTA were dissolved in 500 mL of ddH_2O and sterilized by sterile filtration.

3.2.7 1X RBC lysis buffer

Before performing the migration assay, 50 mL of 10X RBC lysis buffer was diluted with 450 mL of ddH_2O to obtain 1X RBC lysis buffer. This buffer was used to lyse red blood cells during the neutrophil extraction process.

3.3 Used Cell Lines

3.3.1 HEK-293-GPR84-EPAC Cell Line

This cell line is a human embryonic kidney cell line that was stably transfected with the GPR84 receptor. The cells also stably express an EPAC-based FRET biosensor, which is important for screening possible agonistic or antagonistic effects on the GPR84 receptor (see 3.5.1 for a description). The HEK cell line is human, which is advantageous because the observed effects are easier to translate to the human organism. Furthermore, this cell line grows quickly and is easy to handle, making it suitable for the experiments performed.

3.3.2 HEK-293-EPAC Cell Line

This cell line contains the EPAC-based FRET biosensor, but not the GPR84 receptor. It is used to compare the effects observed in the HEK-293-GPR84-EPAC cell line with a cell line that does not express the receptor. Experiments have been performed with both cell lines to determine whether the effect is caused by the GPR84 receptor, another pathway, or an endogenously expressed receptor in the cells.

3.3.3 Calu-3 Cell Line

This cell line consists of human lung cancer cells and was used in the neutrophil migration assay. Unlike HEK cells, these cells grow slowly, which limits this assay. However, they were necessary for this experiment because they form dense layers with tight junctions. This is important because the cell layer must imitate the lung epithelium, which needs to be penetrated by neutrophils in the presence of pro-inflammatory substances.

3.3.4 Neutrophil granulocytes

Primary neutrophil granulocytes cannot be grown in a cell culture because their lifespan is too short. Instead, they were extracted from fresh human blood each time the migration assay was performed (see section 3.6.4.1 for a description of the extraction process). The cells were used to determine whether a compound of interest could induce neutrophil migration.

3.4 Cell Culture work

Aseptic conditions were crucial to ensure appropriate conditions for the cell lines while working. Therefore, each step of the cell culture process was performed under a laminar airflow workbench (HERAsafe™ KS18). Before beginning, the workbench was turned on and the surfaces were cleaned with 1% Hexaquart Plus and disinfected with 70% ethanol.
All necessary materials were disinfected with 70% ethanol before being placed under the laminar airflow to prevent contamination.
To prevent cell damage, all necessary liquids were warmed to 37°C in a water bath beforehand (usually half an hour before use).

Between work steps, the cells were cultured in Sarstedt T-175 culture flasks with DMEM complete medium. The flasks were then stored in a Heracell™ 150 incubator at 37 °C with 5% CO_2 to provide optimal growth conditions for the cells.

Cell splitting and passaging:

To prevent confluence, the cells were split or passaged every two to three days.

After cleaning the workbench as described, the cells were washed with PBS (phosphate-buffered saline) to remove the remaining complete medium. To detach the cells from the culture flask, a trypsin and EDTA solution was used. After a short 2-5 minute incubation step, the cell suspension was diluted with fresh complete medium (approximately twice the volume of the trypsin/EDTA solution used) to stop the trypsinization. The suspension was then centrifuged using a Heraeus™ Multifuge 1 S-R centrifuge to form a pellet of cells at the bottom

of the falcon tube. The supernatant was removed to eliminate any remaining trypsin in the liquid phase. The pellet was resuspended in 11 mL of complete medium.
Approximately 1 mL of this suspension was used for cell counting in the ViCell™ XR Cell Viability Analyzer, which determined the cell concentration of the suspension. The 11 mL of medium used in the previous step was chosen to simplify the calculation of the concentration of the remaining 10 mL of cell suspension. To culture new cell flasks for continual breeding, 6 to 8 million cells were re-seeded. The necessary amount of cell suspension was pipetted into a new flask, which was then filled to 20 mL with complete medium. The number of culture flasks was chosen depending on the amount of cells needed for the following experiments. The remaining cell suspension was used for the assays, as described below.

3.5 EPAC Assay

3.5.1 Principle of the Assay

For the EPAC assay, HEK 293A cells stably transfected with an EPAC-based FRET sensor were used. This sensor emits light of a specific wavelength when cAMP binds. In its unbound conformation, the sensor emits light at 520 nm (Venus). When cAMP binds, the sensor emits light at 480 nm (CFP) upon excitation at 420 nm (Figure 6). The GPR84 cell line is stably transfected with the GPR84 receptor, whereas the wild-type EPAC cell line does not express the receptor endogenously. Thus, the wild-type EPAC cell line can be used as a control.

GPR84 is a Gi-coupled receptor. Therefore, an agonistic ligand leads to the inactivation of adenylate cyclase (Figure 5). Consequently, the conversion of ATP to cAMP decreases, and more light at a wavelength of 520 nm is emitted by the sensor.
However, an antagonistic ligand leads to less inactivation of adenylate cyclase, resulting in more cAMP formation from ATP and more light emission at a wavelength of 480 nm.

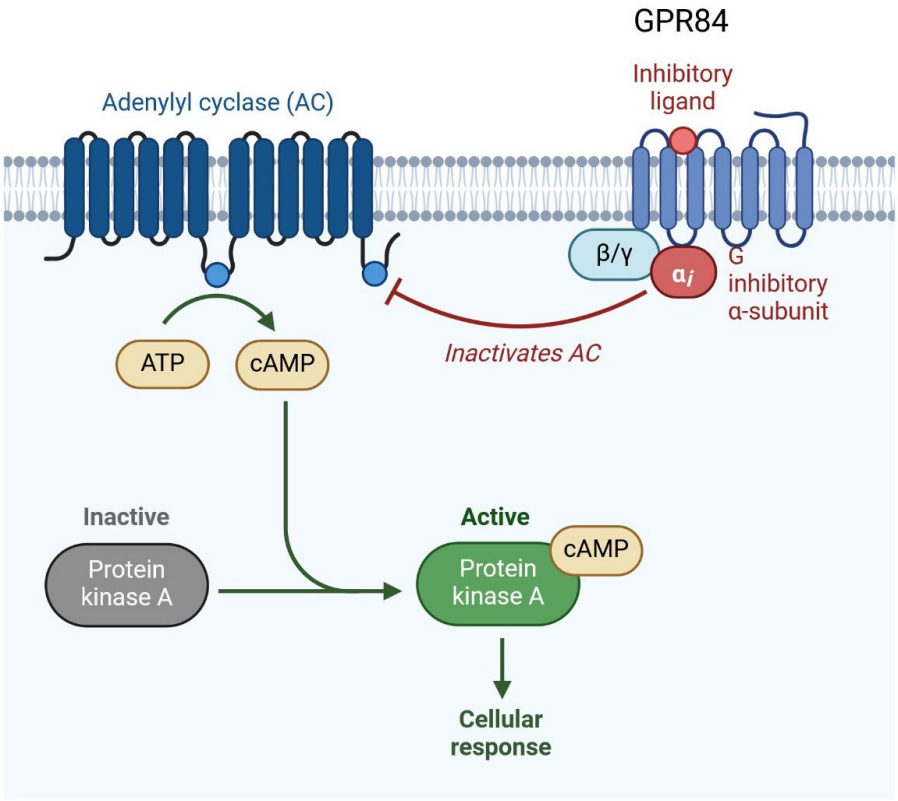

Figure 5: Principle of the EPAC assay. An agonistic ligand binds to the GPR84 receptor, activating the α-subunit. This leads to the inactivation of adenylyl cyclase (AC), which results in reduced conversion of ATP to cAMP. Consequently, less protein kinase A is activated, and the cellular response declines. The amount of free cAMP is crucial for the outcome of the EPAC assay. Created in https://BioRender.com

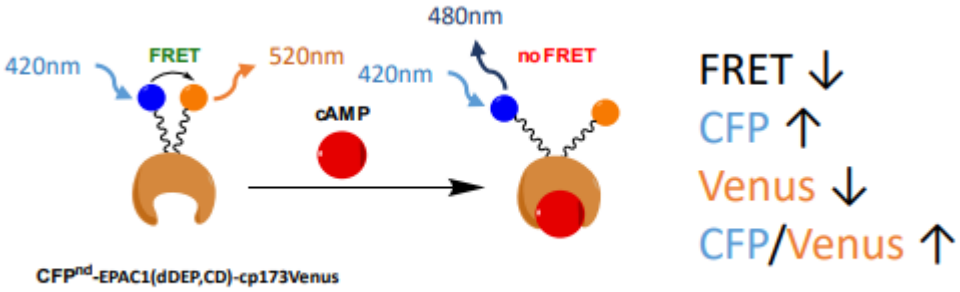

Figure 6: Principle of the EPAC biosensor. An EPAC-based FRET sensor stably transfected in HEK cells emits light at a wavelength of 520 nm when unbound and excited at 420 nm. When cAMP binds to the sensor, FRET (fluorescence resonance energy transfer) is absent, and the emission changes to a wavelength of 480 nm. The higher the intracellular cAMP levels, the more emission at 480 nm can be detected and the less emission at 520 nm. The ratio of CFP (480 nm) to Venus (520 nm) was used to evaluate intracellular cAMP levels.[37]

A TECAN Spark photometer detected the emitted light. The photometer scanned the emission at multiple wavelengths and calculated the ratio of CFP (480 nm) to Venus (520 nm), indicating the amount of cAMP in the cells.
In simple terms, the amount of cAMP in the cells was measured photometrically in this assay.

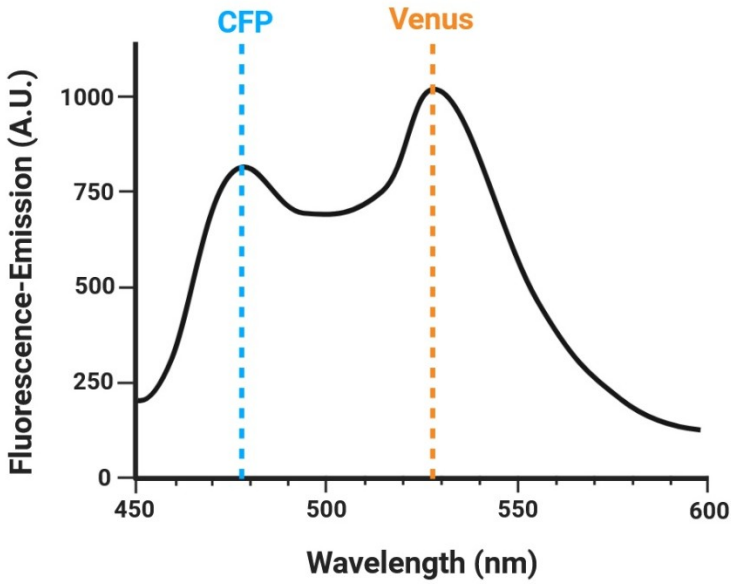

Figure 7: Example for an emission curve in the EPAC assay. This curve shows that a higher emission was detected at 520 nm (Venus) than at 480 nm (CFP). Therefore, the CFP-to-Venus ratio was below 1, indicating agonistic activity in the agonistic mode of the EPAC assay. Created in https://BioRender.com

The TECAN Spark computer program showed emission curves, such as those in Figure 7. In this case, the figure shows spectra of low cAMP levels because the Venus curve is higher than the CFP curve, indicating a low CFP/Venus ratio. This suggests that the substance likely has an agonistic effect on the GPR84 receptor. Conversely, if the CFP emission is higher than the Venus curve, the compound does not have agonistic effects.
To enhance the basal level of cAMP in cells, forskolin was used because it regulates cAMP production by activating adenylate cyclase.
Embelin, a known GPR84 agonist, was chosen as a comparison substance.

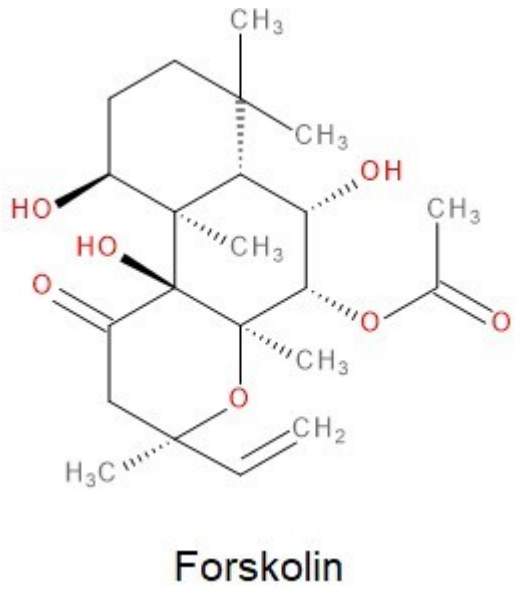

Figure 8: Chemical structure of Forskolin. Created in BIOVIA Draw 2019.

The assay for testing antagonistic activity on the GPR84 receptor works almost the same, but the curves need to be read in reverse. Therefore, Embelin acts as a proven agonist, and antagonistic substances possibly lower its effect, leading to increased cAMP levels. This means that a substance of interest shows higher Venus levels and lower CFP levels; therefore, the quotient is higher.

To evaluate the data, we took the measured CFP and Venus emission values and calculated the quotients. These quotients were then plotted in a bar chart using Prism GraphPad software (version 9.4.1, GraphPad Software, Inc.) and compared to the positive and negative controls (DMSO and forskolin only).

3.5.2 Workflow of the EPAC Assay

The EPAC Assay workflow has been divided into tasks for "Day 1" and "Day 2". Day 1 includes the previously described cell culture work involving splitting and seeding. Day 2 is a continuation of Day 1 and is always performed the following day to ensure comparable results. The following table shows what a typical week of the EPAC Assay looks like:

Table 3: Typical week plan of the EPAC assay.

Mon	Tue	Wen	Thu	Fri	Sat	Sun
Day 1	Day 2	Day 1	Day 2	Splitting	-	-

3.5.2.1 Cell seeding for the EPAC Assay (Day 1)

The first step of every EPAC assay was seeding the cells, which was done during the cell splitting process described above. For this step, the remaining cell suspension from the cell splitting was used, so the initial cell concentration count was crucial. For this experiment, a concentration of 0.75 x 10^6 cells per mL was chosen, so each well (200 µL) of a 96-well plate was filled with around 0.15 x 10^6 cells. Only 72 of the 96 wells were seeded with cells; rows D and H were left empty to serve as negative controls (substance dilution only, no cells), as shown in Figure 9. The seeded plates were incubated overnight to allow the cells to adhere and form a layer on the bottom of the wells. For screening the DNTI compounds, only GPR84 cells were used. For substances that appeared promising in the screening, concentration-response testing was performed with the GPR84 cell line, and the EPAC cell line was used as a control. The seeding of the cells depended on the planned treatments for Day 2.

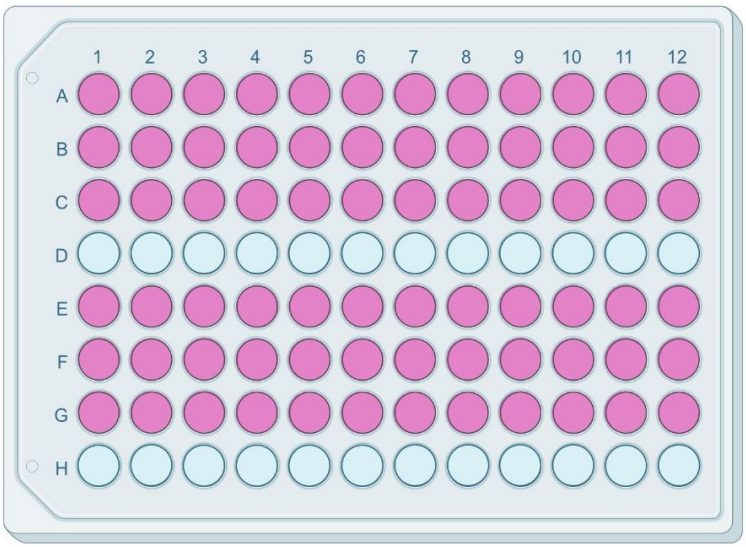

Figure 9: Seeding scheme of GPR84 and EPAC cells on a 96-well plate. The cell suspension was pipetted into the wells, but the rows D and H were left empty. Created in https://BioRender.com

3.5.2.2 Substance treatment and measurement (Day 2)

Day 1 consisted of preparatory steps, including planning the treatment, preparing 1X FURA buffer, and making a 10 mM forskolin stock solution. Day 2 involved the treatment and actual measurement.

First, a mixture of Complete Induction Buffer (CIB) containing 10 µM forskolin (a direct adenylate cyclase activator) was prepared and diluted in 1X FURA buffer. For one 96-well plate, 23 mL of CIB was sufficient; therefore, 23 mL of 1X FURA buffer was mixed with 23 µL of a 10 mM stock solution of forskolin.
In a tube rack, 24 Eppendorf tubes (1.5 ml) were prepared (tubes 1–12 for rows A–D and tubes 13–24 for rows E–H), as shown in Figure 10.

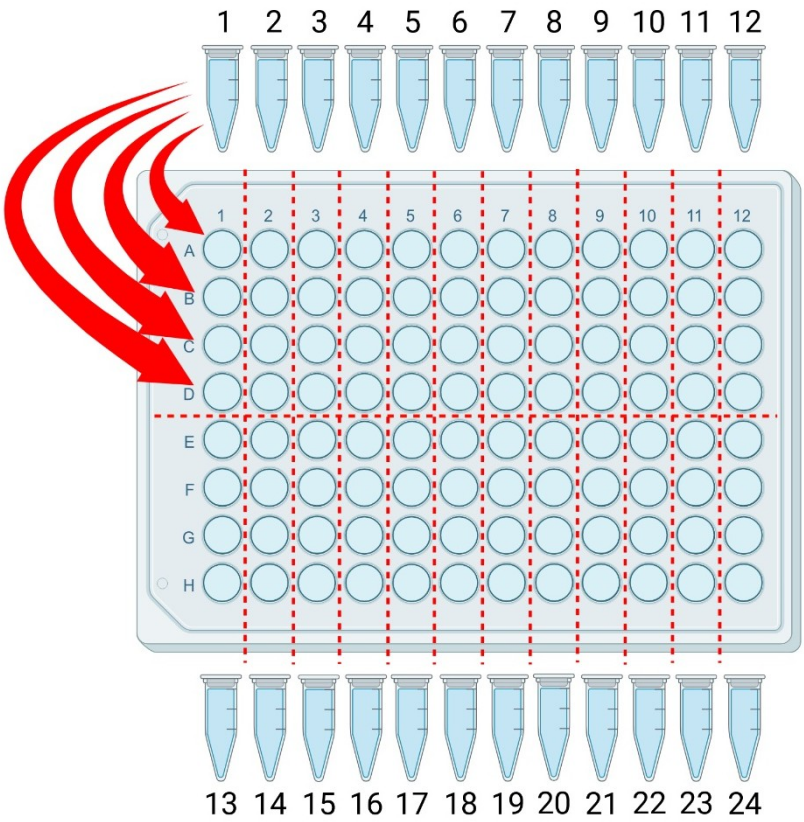

Figure 10: Pipetting scheme for the EPAC assay. Substance dilutions were prepared in 24 Eppendorf tubes (tubes 1–12 for rows A–D and tubes 13–24 for rows E–H). Each Eppendorf tube contained 1,000 µL of the substance dilution, divided into four wells (250 µL each). Created in https://BioRender.com

3.5.2.2.1 Agonistic testing:

Eppendorf tube 1 (Eppi 1) was filled with 998 µL of 1X Fura buffer and 2 µL of DMSO, which served as the DMSO control.
Eppi 2 was filled with 999 µL of CIB and 1 µL of DMSO for the negative control (Forskolin only).
The remaining Eppis (3–12) were filled with 999 µL of CIB and 1 µL of the test compound.

3.5.2.2.2 Antagonistic testing:

Eppendorf tube 13 was filled with 997 µL of 1X Fura buffer and 3 µL of DMSO, which served as the DMSO control.
Eppi 14 was filled with 998 µL of CIB and 2 µL of DMSO for the positive control (Forskolin only).
The remaining Eppis (15-24) were filled with 998 µL of CIB, 1 µL of the test compound, and 1 µL of Embelin mM (a known GPR84 agonist).

To ensure homogenous compound and control dilutions, all the Eppis needed to be thoroughly vortexed. To simplify and accelerate the process, the solutions were pipetted into non-sterile 96-well plates (sterility is not necessary and these plates are much cheaper). The contents of one Eppendorf tube (1 mL) were pipetted into four wells (250 µL each) in one column, as shown in Figure 10. Alternatively, 0.5-ml dilutions could have been made and divided into four 125-µl wells because only 100 µl were needed for treatment (to save compound and FURA buffer). However, we decided to make 1-ml dilutions because 1-µl compound stock can be pipetted more precisely than 0.5-µl stock, and exact concentrations are important for reliable, comparable results.

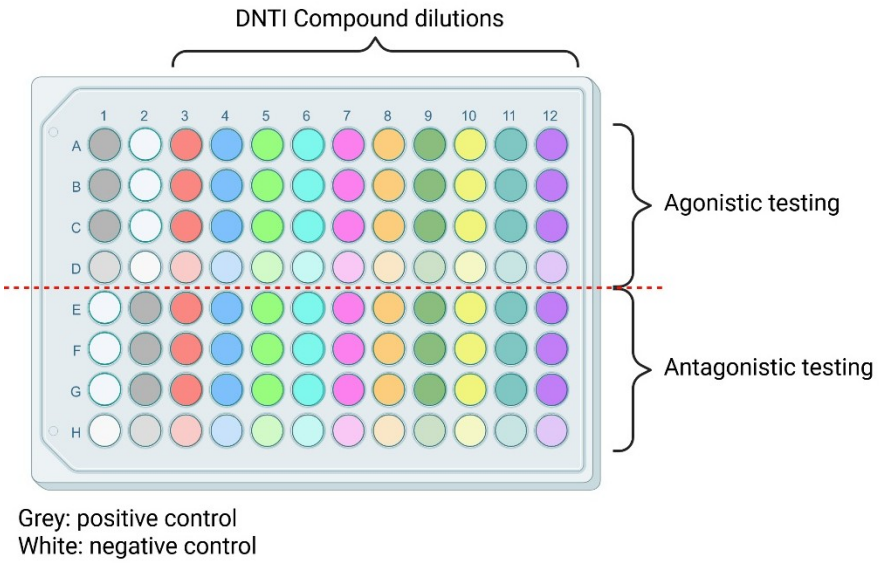

Figure 11: Pipetting scheme of substance dilutions for the EPAC assay in the screening. The upper half of the plate was used for agonistic screening and the lower half for antagonistic screening. Column 1 was used for the DMSO control, and column 2 was used for the forskolin control. The other columns (shown in colors) were filled with the prepared test solutions. The last two rows (D and H) were left empty and served as controls (shown in transparent colors). Created in https://BioRender.com

After transferring all treatment dilutions to the well plate, the 96-well plate prepared on Day 1 was removed from the incubator, and the medium was carefully removed using a multichannel pipette. Then, the wells were rinsed with 150 µL of 1X FURA buffer to wash away the remaining medium. Then, 100 µL of the prepared treatment solutions were pipetted from the non-sterile 96-well plate to the plate containing the cells using a multi-channel pipette. Measurements were taken immediately with the TECAN Spark photometer to minimize the time that the cells were exposed to unfavorable conditions (incorrect temperature and CO_2 concentration) and to ensure consistent substance treatment in every experiment.
After the measurement, the cells and well plates were discarded.

3.5.3 Evaluation of the data

After the measurement was taken, the data was saved as an Excel file on the connected computer and transferred to the office computer via USB. Using a previously created Excel template, the imported data was quickly and easily evaluated to create data sets (CFP/Venus ratio standardized to the DMSO control) that could be imported into GraphPad Prism software.

The template picked out only the values measured at wavelengths of 480 and 520 nm from the spectra and subtracted the associated blank values. As shown in Figure 11, only the first three rows of each quadruplicate contained cells. The fourth row contained only the compound dilution for subtracting the autofluorescence of each substance. Then, the emission values at 480 nm were divided by the corresponding emissions at 520 nm to obtain the CFP/Venus ratio. Since each substance was tested in technical triplicates, three ratios of each compound dilution were obtained. Each ratio was then divided by the mean of the three values of the DMSO control (in the agonistic assay) or the negative control (in the antagonistic assay) to obtain normalized data.
Finally, these standardized triplets were imported into GraphPad Prism to create bar charts for all the substances tested, to determine whether they were closer to the positive or negative control.

3.6 Neutrophil Migration Assay

3.6.1 Principle of the Assay

This assay tests whether substances of interest can stimulate fresh neutrophils extracted from human blood to migrate through a cell layer. In the case of an antagonistic substance, the assay tests whether the substance can inhibit the migration of neutrophils induced by Embelin, a known agonist. Therefore, a monolayer of Calu-3 cells is grown on the outer side of Transwell inserts with a semipermeable membrane containing 3-µm pores. If the compound dilution outside the insert has a chemotactic effect, the neutrophils inside the insert will be activated and migrate through the monolayer. They can then be quantified in the well (Figure 12).

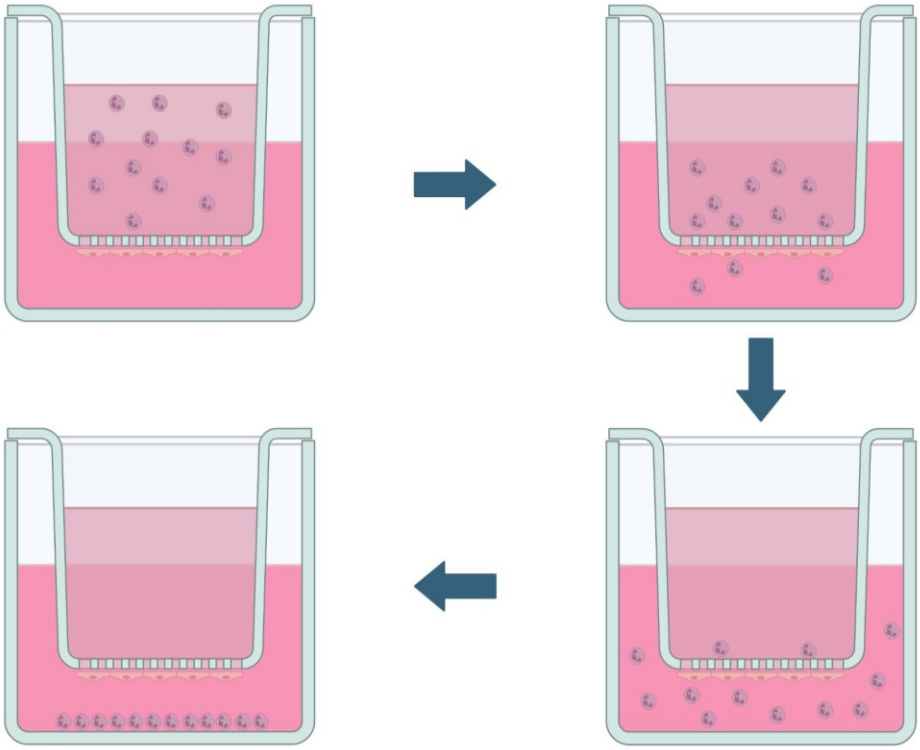

Figure 12: Principle of the migration assay. The well (apical) is filled with a substance dilution and the insert (basolateral) is filled with a neutrophil cell suspension. When stimulated by the test substance, the neutrophils migrate through the Calu-3 cell monolayer from the basolateral side to the apical side and settle at the bottom of the wells. The migrated cells can then be quantified in the wells. Created in https://BioRender.com

3.6.2 Cultivation of Calu-3 cells

Because of the disadvantages of Calu-3 cells, preparing the migration assay is complicated and time-consuming. First, they grow slowly, so it takes one to two weeks (depending on the number of seeded cells) to obtain enough cells for seeding the inserts and further cultivation. Second, these cells attach strongly to the bottom of the flask, resulting in significant cell loss during splitting. To improve the yield, the trypsinization time was extended to 15-20 minutes. A 1:1 mixture of DMEM complete and Ham's F12 complete medium (DMEM/F12) was used as a growth medium. At the beginning of the practical work, two cell culture flasks were prepared: one with two to three million cells and one with six million cells. This allows for the parallel cultivation of the cells, enabling the performance of one migration assay every week.

The growth progress was checked under the microscope and the medium was renewed every Monday, Wednesday, and Friday. Once the cell layer reached the appropriate density (as

determined by microscopy), cell splitting was performed on one flask while the other was incubated with the new medium.

3.6.3 Cell passaging and seeding on inserts

The cell splitting process was the same as that used for the HEK-EPAC cell line, but it included 15-20 minutes of trypsinization to detach as many cells as possible from the bottom of the flask. After cell counting, the cell suspension was centrifuged, and the supernatant was removed. The cell pellet was resuspended in enough medium to reach a concentration of 2.86 million cells/mL (0.2 million cells per insert in 70 µL of medium).
Under sterile conditions, 12 inserts were placed upside down on the bottom of an empty culture dish. Using a pipette, 70 µL of the concentrated cell suspension was pipetted onto the semi-permeable membrane of the inserts, as shown in Figure 13. Using ~2 mL of the remaining cell suspension (~6 million cells), a new cell culture flask was prepared and incubated. The remaining suspension was discarded.

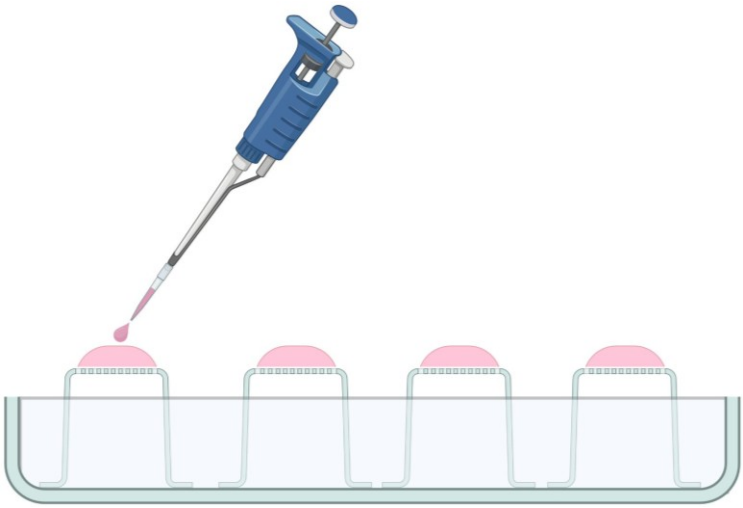

Figure 13: Preparation of the inserts with a Calu-3 cell suspension. The previously diluted cell suspension (with a concentration of 2.86 million cells/mL) is pipetted onto the inserts, which are placed upside down, under sterile conditions (70 µL per insert). This allows a Calu-3 monolayer to grow on the membrane of the inserts. Created in https://BioRender.com

After that, another dish bottom was placed on top of the dish bottom (because the height of the dish lid did not leave enough space for the inserts), and the dish was incubated until the next day.

The next day (Tuesday or Thursday), the cells had enough time to settle and adhere to the semi-permeable membranes of the inserts. They were then ready to be placed in a 24-well plate. Therefore, a sterile 24-well plate was taken under the laminar airflow, and the first 12 wells were filled with 800 µL of complete DMEM/F12 medium. The inserts were carefully flipped with sterile tweezers and placed in the medium-filled wells. Then, 400 µL of complete DMEM/F12 was gently pipetted into the basolateral compartment of the inserts, as the cells primarily absorb nutrients through their basolateral side (Figure 14). It was important to fill the inserts slowly to avoid damaging the cell monolayer.

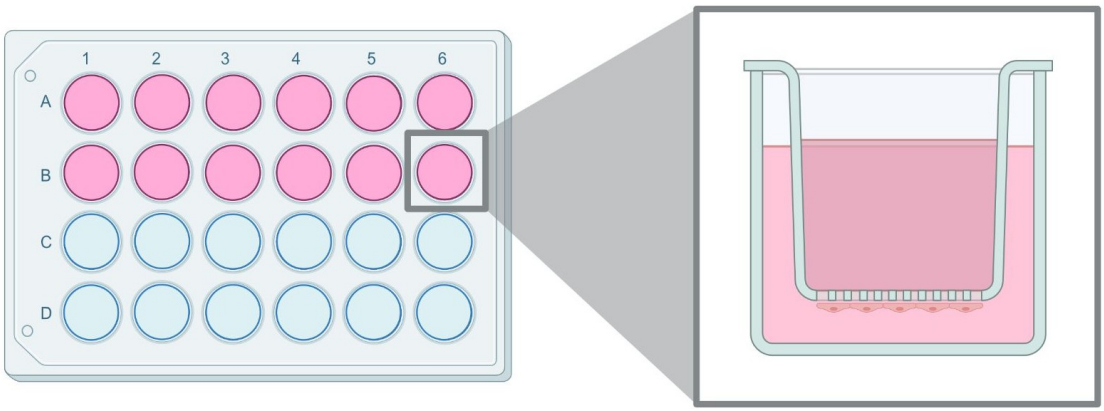

Figure 14: Migration assay setup. Twenty-four-well plates were used for the migration assay. Once the Calu-3 cell layer on the inserts was dense enough, 800 µL of DMEM/F12 complete was added to a corresponding number of wells, and the inserts were flipped and placed in the wells. Then, the inserts were filled with 400 µL of complete DMEM/F12 so that the Calu-3 cells could absorb nutrients from their basolateral side. Created in https://BioRender.com

The 24-well plate and the two dish bottoms were incubated again. The dish bottoms can be reused after being thoroughly disinfected with 60% ethanol.

On every subsequent Monday, Wednesday, and Friday, the medium needed to be changed on the apical and basolateral sides, and the TEER values were measured (Figure 15). The inserts were considered ready for the migration assay when they reached a TEER value greater than 300 Ω·cm².

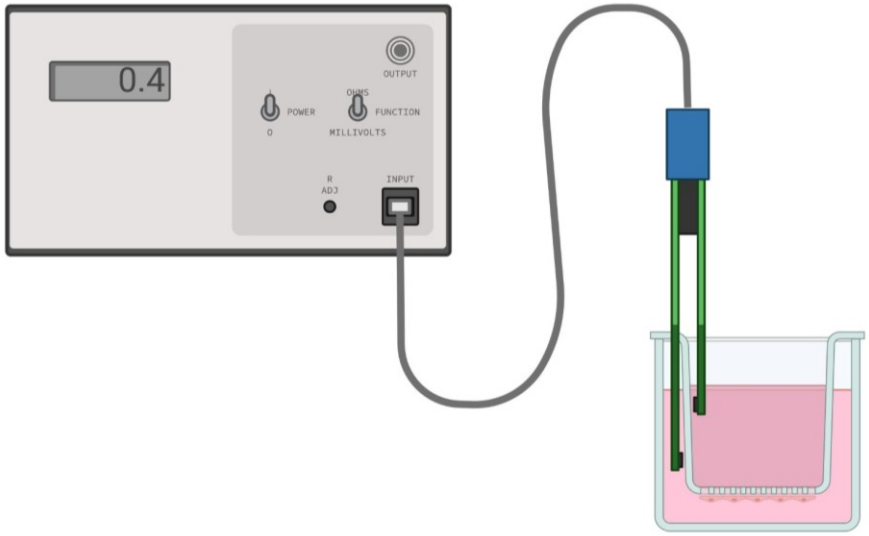

Figure 15: Measurement of TEER values with the EVOM2 VoltOhmmeter. The device contains a diode that measures resistance between the apical and basolateral sides of the Calu-3 monolayer to evaluate its density. A resistance of at least 300 ohms per square centimeter per insert is necessary to ensure that the cell monolayer is dense enough to begin the migration assay. Created in https://BioRender.com

Once the inserts were ready, or at least most of them were, the actual migration assay was scheduled for one of the following days.

3.6.4 Process of the neutrophil migration assay

3.6.4.1 Isolation of neutrophil granulocytes from whole blood

For the neutrophil migration assay freshly isolated neutrophil granulocytes from healthy donors were necessary. Therefore, 40-50 ml whole blood was provided by the Austrian Red Cross. The blood was collected in tubes that contained EDTA as an anticoagulant.

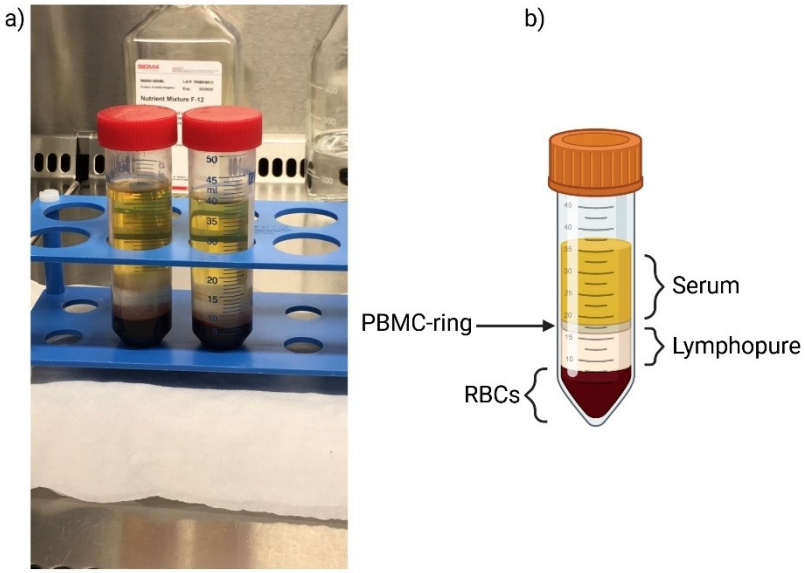

Figure 16: Separated blood components. Serum (yellow), PBMCs (cloudy light grey), Lymphopure (clear), RBCs (red). Picture a) was made by Marvin Csar; Picture b) created in https://BioRender.com

F For isolation purposes, the laminar airflow was thoroughly disinfected with 1% Hexaquart and 70% ethanol. Then, tissues were placed to soak up any spilled blood. The blood was diluted 1:1 with PBS. After gently inverting the bottle, the correct amount of Lymphopure was transferred into a new falcon tube (0.5 mL of Lymphopure per 1 mL of diluted blood). The blood dilution was carefully layered on top of the Lymphopure without mixing the two resulting phases. After centrifuging the falcon tubes for 30 minutes at 800 g (without brake) at room temperature, four phases formed, as shown in Figure 16. The upper layer (yellow) is plasma and the middle layer (transparent) is the density gradient medium. A thin, cloudy film of PBMCs (peripheral blood mononuclear cells) formed between the yellow and transparent layers. For the migration assay, only the neutrophils among the red blood cells (in the bottom red layer) were relevant.

Figure 17: Centrifuged white blood cells in RPMI + HEPES. This figure shows the clear white cell pellet of isolated neutrophils. Picture made by Marvin Csar

The serum and Lymphopure layer were carefully removed to avoid wasting blood cells. The cell pellet was resuspended and brought up to the 50 mL mark in each tube with 1X RBC lysis buffer.
The tubes were then centrifuged for five minutes at 500 g and 18-22 °C. Since not all of the neutrophils were pelleted by centrifugation, additional lysis steps were performed to prevent

the loss of useful cells. Therefore, the supernatant was divided into one or two additional falcon tubes per tube, and the volume was topped up to 50 mL with 1X RBC lysis buffer. To improve lysis, all the falcon tubes (four or six, depending on how they were divided) were gently shaken by hand for five minutes. The tubes were then centrifuged again at 500 g for five minutes at 18-22 °C. At this point, the neutrophils were stacked on the RBC (red blood cell) pellet, and the supernatant had to be carefully removed.
The pellets were resuspended in one milliliter of 1x RBC lysis buffer and collected in a Falcon tube. The tube was filled with lysis buffer once again, shaken by hand for five minutes, and then centrifuged at 500 g for five minutes.
If the cell pellet appeared clear white, as shown in Figure 17, then lysis was successful and the neutrophils were properly isolated. If the pellet remained red, additional lysis steps were necessary to remove the remaining erythrocytes.
Next, the supernatant was aspirated and the cells were resuspended in 15 mL of PBS to wash them. One milliliter of the cell suspension in PBS was taken to count the cell concentration with the ViCell counter. The remaining 14 mL were centrifuged for 5 minutes at 500 g, after which the supernatant was removed and the pellet was resuspended in an amount of RPMI stripped + HEPES medium to yield a suspension of $5x10^6$ cells/mL. Typically, 50 mL of whole blood yields 50 to 200 million neutrophils, though this number varies depending on the donor and other factors.

3.6.4.2 Preparation of compound dilutions

To ensure the same conditions as in the cell suspension, the compound dilutions were freshly prepared in RPMI stripped + HEPES medium. This was done under a laminar airflow hood so that the migration step could occur under sterile conditions. Therefore, Eppendorf tubes have been filled with 999 µL of RPMI stripped + HEPES medium and 1 µL of each stock solution. The negative control was 0.1% DMSO, and the positive controls were fMLP at 10nM and IL-8 at 100 ng/ml. An intermediate dilution step was necessary for the final fMLP dilution because only a 10 mM stock solution was available. One microliter of the 10 mM stock solution was mixed with 999 microliters of medium, and one microliter of this dilution was mixed again with 999 microliters of medium. All of these dilutions were thoroughly vortexed and pipetted into a sterile 24-well plate under the laminar airflow.

Next, the prepared inserts were removed from the incubator and the growth medium inside the Transwell inserts was discarded. Then, the inserts were placed in wells containing compound dilutions. To initiate migration, the inserts were filled with 400 µL of the previously

prepared neutrophil suspension. The 24-well plate was then incubated at 37°C for two hours to allow for the migration process to occur.

3.6.4.3 Detection of the migrated neutrophils

After two hours of incubation, the neutrophils had migrated through the Calu-3 cell layer on the inserts. First, the inserts were removed, and pictures were taken of the migrated cells in the 24-well plate. Then, the well plate was carefully moved from the incubator to the TECAN SPARK machine, which has a photography function. It was important not to shake the well plate because only the cells that had settled could be seen in the photographs. While the photos did not allow for serious quantification, they provided a good initial indication of how well the migration worked. After the photos were taken, the cells were carefully resuspended with a pipette, and 500 µL aliquots were transferred into labeled Eppendorf tubes for later quantification by FACS analysis.

The next analysis was the luminol oxidation assay. Two injection solutions were prepared for this assay.

Solution A: A 55 mM stock solution of luminol (400 µL) was diluted to 4,000 µL with RPMI + HEPES in a Falcon tube. Only 10 µL of this solution was injected, but at least 4,000 µL were needed to prime the TECAN SPARK injector. Thus, the final concentration of luminol after injection was 55 µM.

Solution B: One microliter of 10 mM fMLP was added to 4,000 µL of RPMI + HEPES in a Falcon tube. Then, 10 µL were injected, resulting in a final concentration of 100nM fMLP.

Next, the 24-well plate containing the remaining cell suspensions (500 µL each) was taken, and 500 µL of RPMI stripped + HEPES was added to each well, bringing the volume to 1 mL per well. The plate was placed in the TECAN Spark for the luminol oxidation assay. For the measurement, solutions A and B were injected into each well. The fMLP in solution B caused the degranulation of the migrated neutrophils. The released mediators then oxidized the luminol in solution A, causing light emission, which was measured by the TECAN Spark.

The Eppis previously labeled with 500 µl aliquots were taken to the cell culture lab to perform a cell count using the ViCell. Therefore, 100 µL of the aliquots were pipetted into ViCell tubes and topped off with 1000 µL of RPMI stripped + HEPES. The cells were counted with an

adjusted dilution factor of 10 in the system. Another aliquot of the original, unmigrated suspension was counted in the same way. Four hundred microliters of the original suspension were taken for the FACS preparation.

The remaining 400-µL aliquots have been mixed with a staining solution for FACS quantification.
This staining solution was made by mixing 135 µL of P/F/E buffer (PBS/FBS/EDTA) with 1 µL of each of the following antibody solutions:

- CD45 (Vio Blue) for leukocytes
- CD14 (APC) as a negative marker, mostly macrophages
- CD16 (PE Vio770) for natural killer cells, neutrophils, monocytes, T-cells, macrophages
- CD11b (APC Vio770) for natural killer cells, monocytes, granulocytes, macrophages
- CD66b (FITC) specific for neutrophils

The cell suspension in the Eppendorf tube (not yet stained) was centrifuged at 5,000 g for five minutes. The neutrophils formed a pellet at the bottom, and the supernatant was carefully removed. The pellet was resuspended in 10 µL of staining solution and incubated for 30 minutes in the dark. Then, the samples were filled to 200 µL with PFE buffer. Shortly before analysis, one drop of propidium iodide was added to each sample, which was then thoroughly vortexed. Then, all 200 µL of each Eppendorf tube was pipetted into a row of a 96-well plate. A volume of 150 µL was analyzed by the FACS machine for the measurement.
To count only the neutrophils the following FACS-gating was used: granulocytes/single cells/alive/CD45+/CD11b+/CD66b+.

4 Results

4.1 Characterization of a stably transfected GPR84 HEK EPAC cell clone

At the beginning of the project, some substances described as GPR84 agonists in the literature were tested at different concentrations in stable GPR84 EPAC HEK cells (clone 11) and EPAC HEK cells (clone 5). This was done to verify GPR84 receptor expression and the assay conditions in the EPAC assay. The stable cell lines were provided by Dr. Alexander Perhal. Each experiment was performed in triplicate.

The following figures show the fluorescence emission ratio between CFP and Venus as a bar chart for each substance solution/concentration. For the agonistic assay, the first bar is always the DMSO control, and the second bar is the forskolin control. In other words, the lower the bar, the greater the agonistic effect of the substance/concentration.

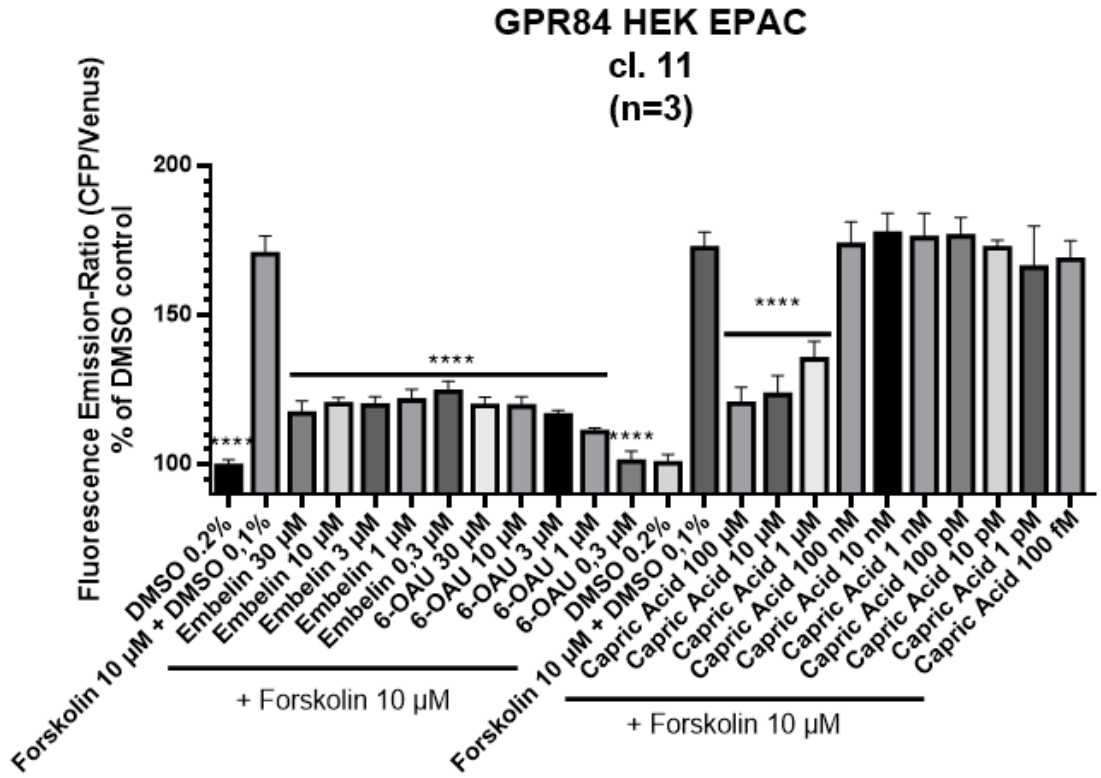

Figure 18: Quotients of emissions of several measured concentrations of reported GPR84 agonists with GPR84 cells. Embelin, 6-OAU, and capric acid (decanoic acid) were tested at various concentrations in the EPAC

assay. DMSO was used as the vehicle control, and DMSO plus forskolin was used as the negative control. The tests were performed in GPR84 cells. The measured fluorescence emission ratios (CFP/Venus) were normalized to the DMSO vehicle control. The bar charts represent the mean ± SD of three biological replicates (n = 3), which were measured in technical duplicates. A one-way ANOVA and Dunnett's post hoc test were used for statistical analysis (**** $p \leq 0.0001$, *** $p \leq 0.001$, ** $p \leq 0.01$, * $p \leq 0.05$, ns $p > 0.05$). Embelin and capric acid (decanoic acid) exhibited slight concentration-dependent agonistic effects, but only at concentrations higher than 100nM. However, 6-OAU's effect was rather inverse to its concentration. Figure made with GraphPad Prism.

The clone characterization experiment results showed detectable agonistic effects of all three tested substances at the GPR84 receptor (Figure 18). Capric acid, a natural ligand of the receptor, only produced an effect at higher concentrations. Unlike 6-OAU (6-(octylamino)-2,4(1H,3H)-pyrimidinedione), embelin exhibited a concentration-response correlation. Therefore, embelin was chosen as the reference substance in the agonistic assay and as the validated GPR84 agonist in the antagonistic assay. No effects were visible for the non-GPR84 expressing EPAC cell line (Figure 19). Due to this outcome, the cell clone was deemed suitable for ongoing substance testing.

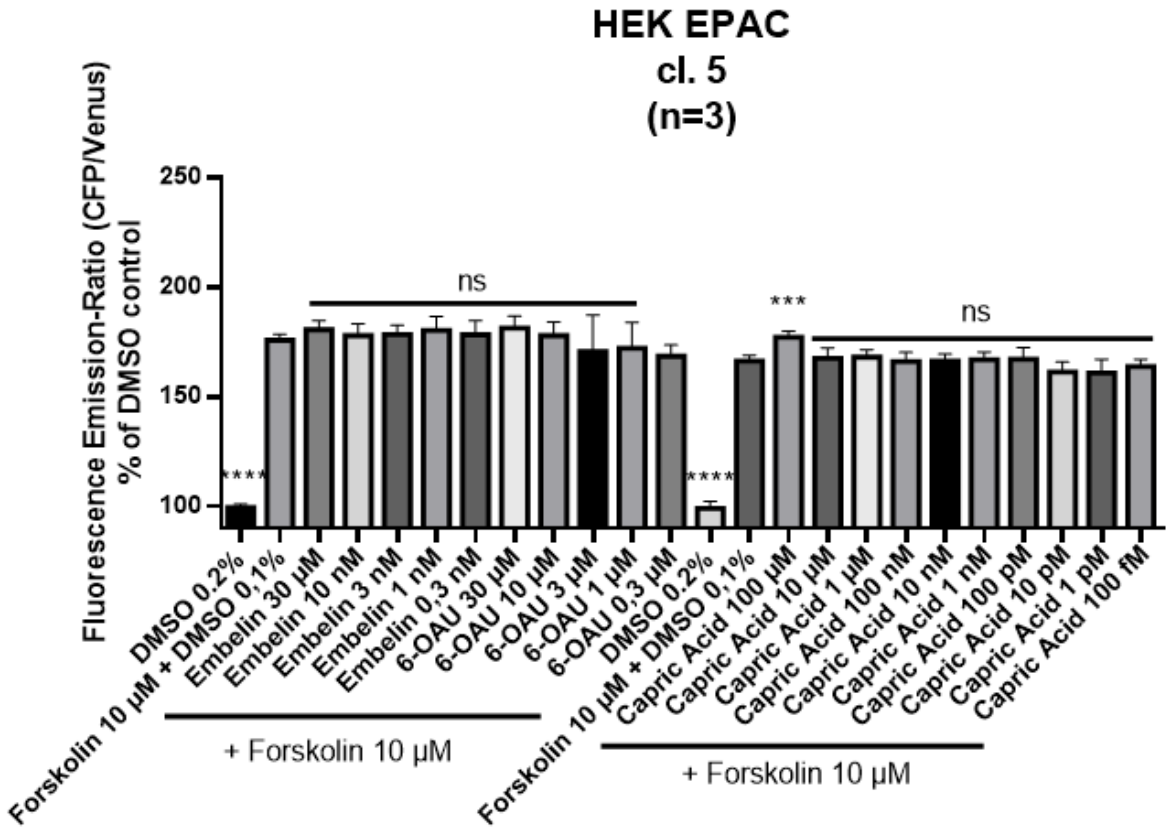

Figure 19 Quotients of emissions of several measured concentrations of reported GPR84 agonists with EPAC cells. Several concentrations of embelin, 6-OAU, and capric acid (decanoic acid) were tested in an EPAC assay against a DMSO vehicle control and a DMSO + forskolin negative control in EPAC cells. The measured

fluorescence emission ratios (CFP/Venus) were normalized to the DMSO vehicle control. The bar charts represent the mean ± SD of three biological replicates (n = 3), which were measured in technical duplicates. A one-way ANOVA and Dunnett's post hoc test were used for statistical analysis (**** p ≤ 0.0001, *** p ≤ 0.001, ** p ≤ 0.01, * p ≤ 0.05, ns p > 0.05). Reported GPR84 agonists had no effect on non-transfected EPAC-HEK cells. This was used as a control. Figure made with GraphPad Prism.

To further validate the effect of Embelin, additional experiments were conducted with this compound at various concentrations in GPR84 HEK EPAC cells (Figure 20a). Additionally, a concentration-response curve was created, yielding an EC_{50} of 116nM (Figure 20b).

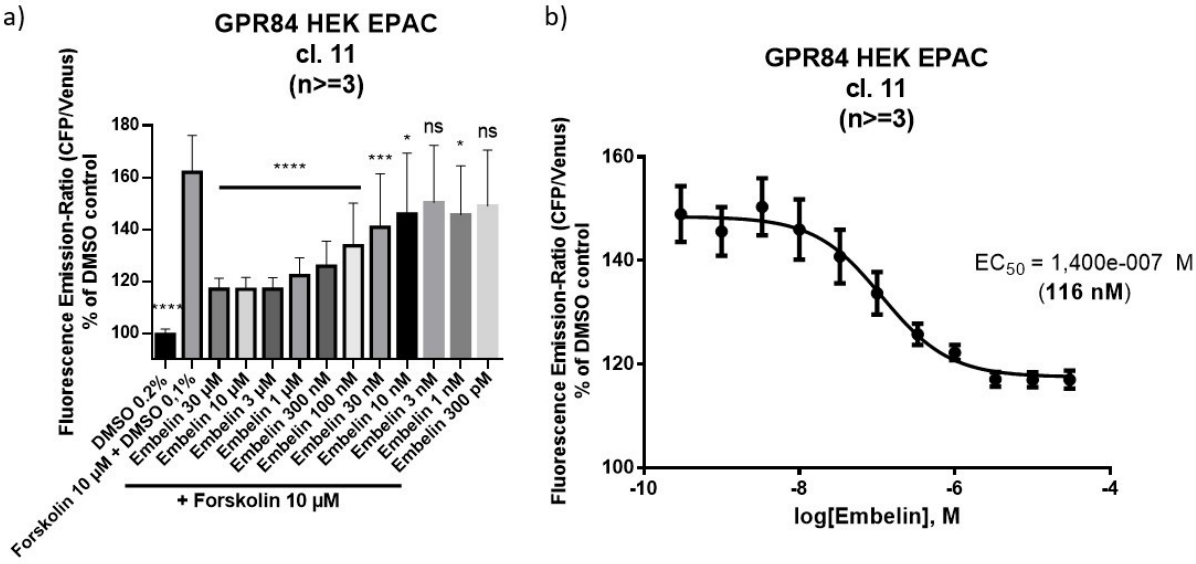

Figure 20: Quotients of emissions of several measured concentrations of Embelin in GPR84 cells (a) and related concentration response curve (b). (a) Embelin was tested at various concentrations to confirm its suitability as a control substance for potential antagonists in an antagonistic EPAC assay. The fluorescence emission ratios (CFP/Venus) were normalized using DMSO as the vehicle control. DMSO and forskolin were used in combination as a negative control. The bar charts represent the mean ± SD of at least three biological replicates (n ≥ 3), which were measured in technical duplicates. A one-way ANOVA and Dunnett's post hoc test were used for statistical analysis (**** p ≤ 0.0001, *** p ≤ 0.001, ** p ≤ 0.01, * p ≤ 0.05, and ns p > 0.05). (b) A concentration-response curve of Embelin's agonistic activity in GPR84 cells was created, yielding a calculated IC_{50} value of 116nM. Figures made with GraphPad Prism.

During the project, it was found that the first value of each triplet often differed greatly from the other two values. Therefore, many trials were conducted to improve the assay conditions, but without success. Consequently, the decision was made to exclude the first value of each triplet (see Figure 21) to obtain more reliable results (i.e., the results are biological duplicates).

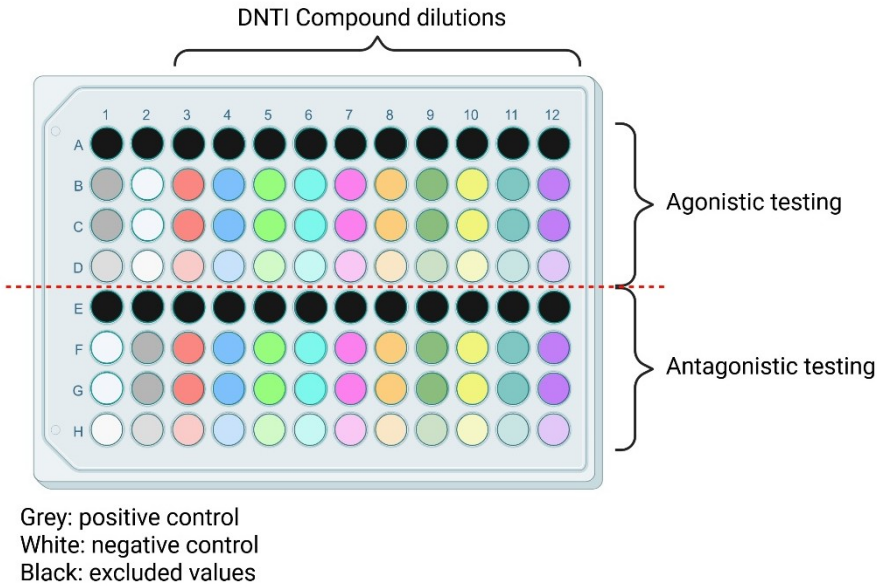

Figure 21: Evaluation scheme illustrated as 96-well plate. The first rows (A and E) were excluded to reduce the standard deviation, which is shown in black. The last rows (D and H) were filled with substance dilutions without cells to serve as a control (shown in transparent colors). The gray and white wells served as positive and negative controls. Created in https://BioRender.com

4.2 Results of the most promising DNTI substances in the EPAC assay

4.2.1 Potential GPR84 agonists

4.2.1.1 DNTI compound 1045

The substance DNTI 1045 was identified as the polyyne 8-acetoxy-hexadeca-1,9-diene-4,6-diyn-3-ol. Using the BIOVIA Draw 2019 software, the IUPAC name, [(E)-1-(5-hydroxyhept-6-en-1,3-diynyl)non-2-enyl] acetate, was created, and the compound was listed in the attachment. The compound was tested multiple times at different concentrations in both the GPR84 and EPAC cell lines, showing positive results as a potential GPR84 agonist. More than four replicates were performed for this compound in the GPR84 cell line because additional dilutions were added after the initial experiments to obtain more data. A

concentration-response correlation was visible in the EPAC assay, as shown in Figure 23 below.

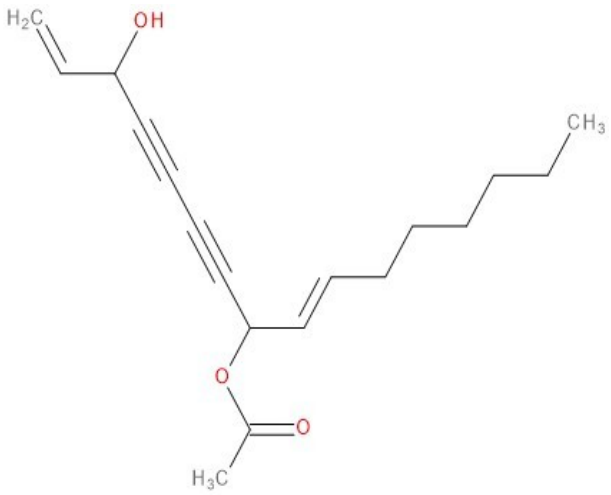

8-acetoxy-hexadeca-1,9-diene-4,6-diyn-3-ol

Figure 22: Chemical structure of DNTI 1045. Created in BIOVIA Draw 2019.

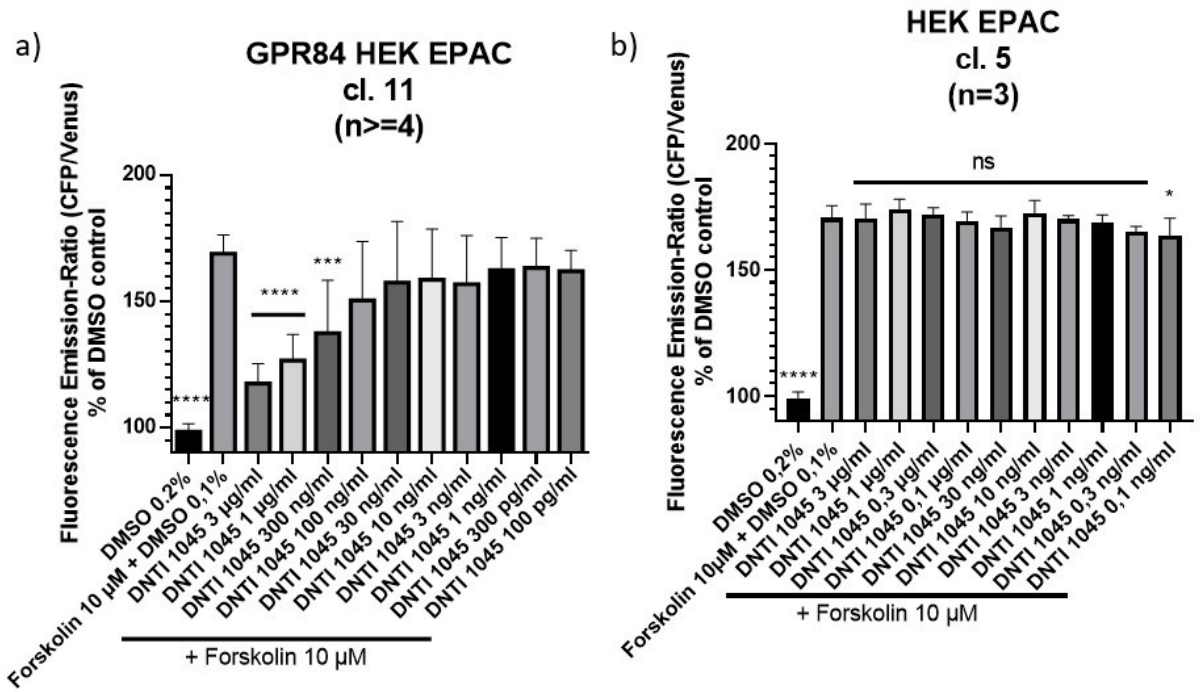

Figure 23: Quotients of emissions of several measured concentrations of DNTI 1045 in GPR84 (a) and EPAC (b) cells. Substance 1045 was tested at various concentrations in the EPAC assay, using DMSO as the vehicle control and DMSO + forskolin as the negative control. The measured fluorescence emission ratios (CFP/Venus) were normalized to the DMSO control. The bar charts represent the mean ± SD of at least three biological replicates ($n \geq 4$, $n = 3$), which were measured in technical duplicates. A one-way ANOVA and Dunnett's post hoc test were used for statistical analysis (**** $p \leq 0.0001$, *** $p \leq 0.001$, ** $p \leq 0.01$, * $p \leq 0.05$, and ns $p > 0.05$). In GPR84 cells, 1045 exhibited a promising, concentration-dependent agonistic effect (a). No agonistic effect was visible in non-transfected EPAC cells (b). Figures made with GraphPad Prism.

4.2.1.2 DNTI compound 1099

DNTI 1099 (an NF-κB inhibitor sent by Hermann Stuppner's group from the University of Innsbruck) was tested three times in both cell lines after showing promise in substance screening. Using BONVIA Draw 2019, the IUPAC name, 3-[(E)-(4-ethoxyphenyl)iminomethyl]benzene-1,2-diol, was generated. The results showed a concentration-response correlation, but the observed effect was low and only present at the highest concentrations of the compound (Figure 25). Because of the low efficacy, the substance was not chosen for further testing in the migration assay.

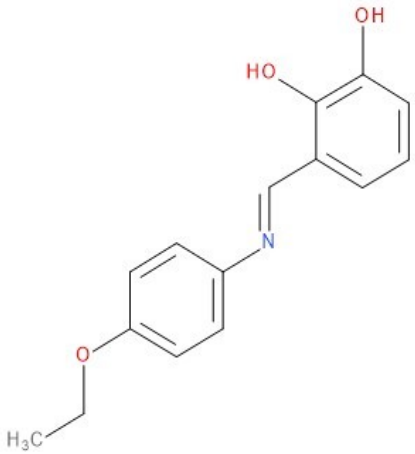

3-[(E)-(4-ethoxyphenyl)iminomethyl]benzene-1,2-diol

Figure 24: Chemical structure of DNTI 1099. Created in BIOVIA Draw 2019.

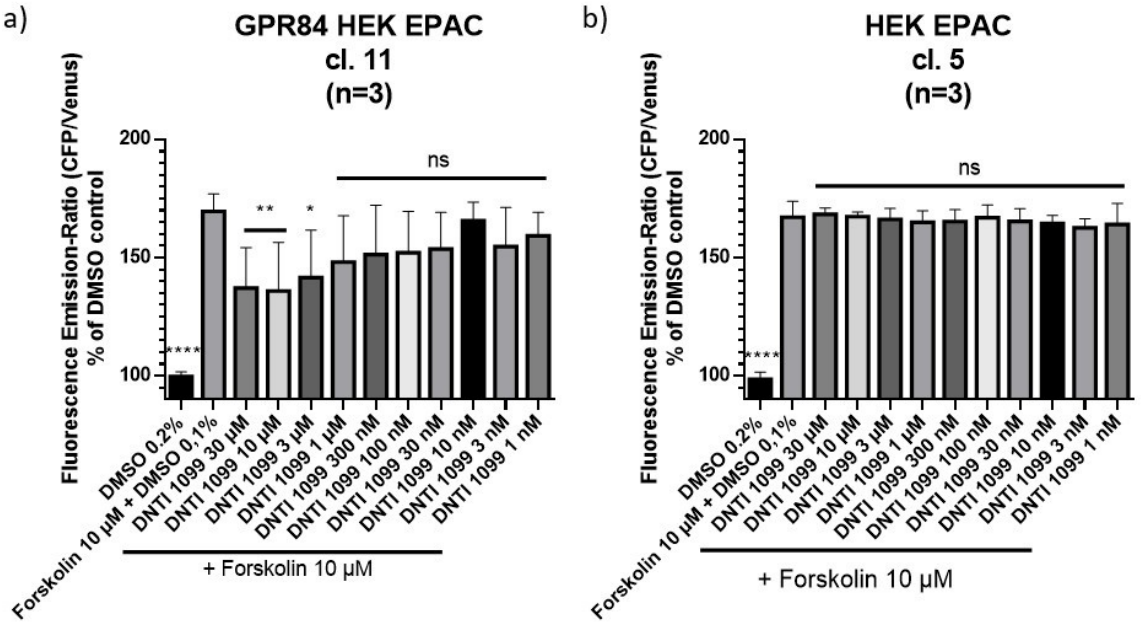

Figure 25: Quotients of emissions of several measured concentrations of DNTI 1099 in GPR84 (a) and EPAC (b) cells. Substance 1099 was tested at various concentrations in the EPAC assay, using DMSO as the vehicle

control and DMSO + forskolin as the negative control. The measured fluorescence emission ratios (CFP/Venus) were normalized to the DMSO control. The bar charts show the mean ± SD of three biological replicates (n = 3), which were measured in technical duplicates. A one-way ANOVA and Dunnett's post hoc test were used for statistical analysis (**** $p \leq 0.0001$, *** $p \leq 0.001$, ** $p \leq 0.01$, * $p \leq 0.05$, and ns $p > 0.05$). In GPR84 cells, Substance 1099 exhibited a slight, concentration-dependent agonistic effect (a), while no visible effect was observed in non-transfected EPAC cells (b). Figures made with GraphPad Prism.

4.2.1.3 DNTI compound 1742

The substance DNTI 1742 was identified as (10E,12Z)-9-oxooctadeca-10,12-dienoic acid, also known as 9-oxo-ODE. It was extracted from *Clematis armandii* (Ranunculaceae) by Rudolf Bauer's group from the University of Graz. After the compound showed promising results in the EPAC screening assay, it was tested three to four times at multiple concentrations to fit a concentration-response curve (Figure 27). Due to the results obtained, this substance was considered the most interesting in the agonistic screening. Next, the compound was tested in a neutrophil migration assay.

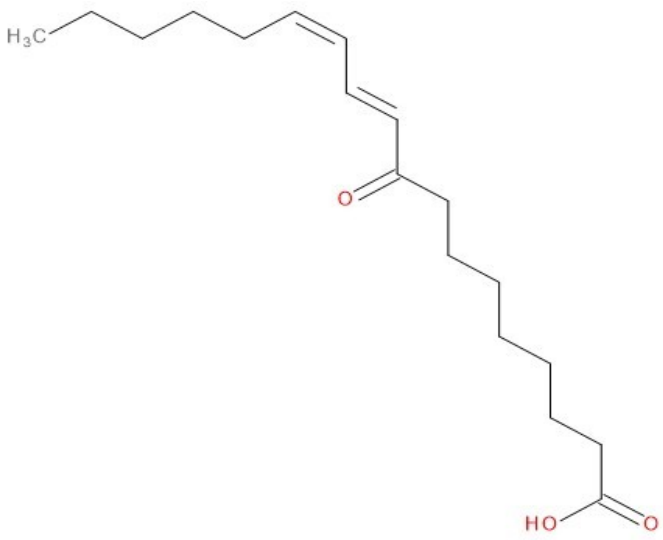

(10E,12Z)-9-oxooctadeca-10,12-dienoic acid

Figure 26: Chemical structure of DNTI 1742. Created in BIOVIA Draw 2019.

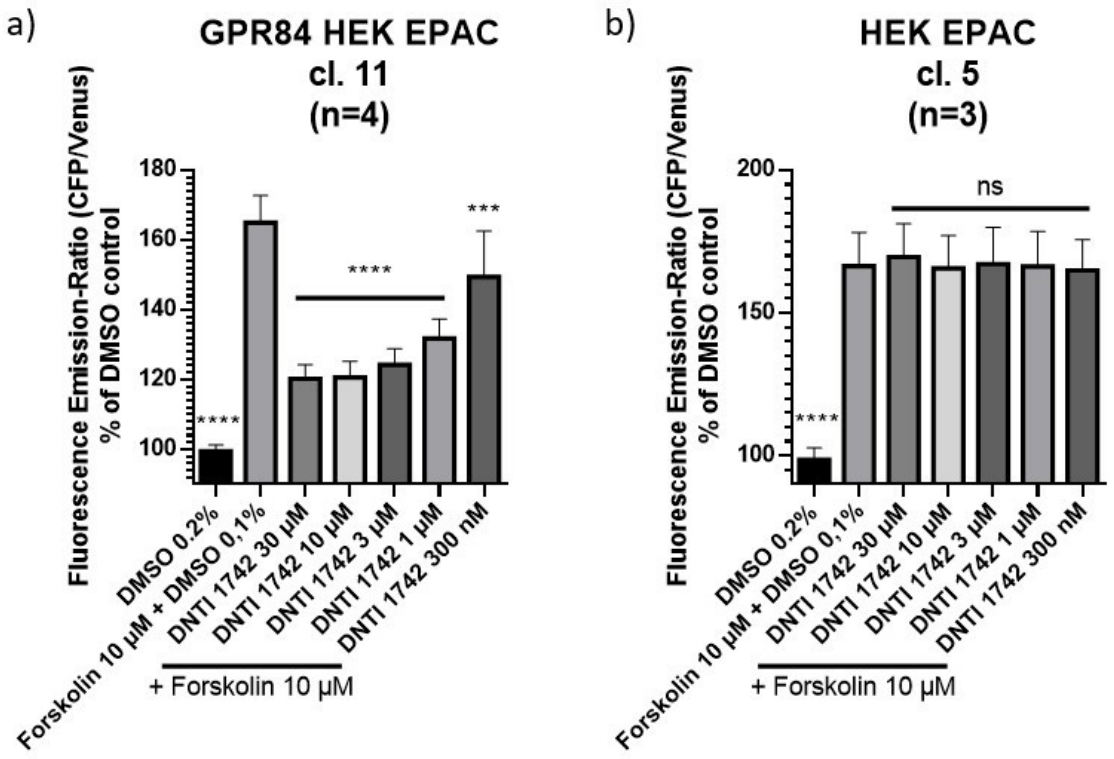

Figure 27: Quotients of emissions of several measured concentrations of DNTI 1742 in GPR84 (a) and EPAC (b) cells. Substance 1742 was tested at various concentrations in the EPAC assay, with DMSO serving as the vehicle control and DMSO + forskolin serving as the negative control. The measured fluorescence emission ratios (CFP/Venus) were normalized to the DMSO control. The bar charts represent the mean ± SD of at least three biological replicates (n = 4 or 3) measured in technical duplicates. A one-way ANOVA and Dunnett's post hoc test were used for statistical analysis (**** $p \leq 0.0001$, *** $p \leq 0.001$, ** $p \leq 0.01$, * $p \leq 0.05$, ns $p > 0.05$). Substance 1742 exhibited a concentration-dependent agonistic effect in GPR84 cells (a) and no effect in non-transfected EPAC cells (b). Figure made with GraphPad Prism.

4.2.1.4 DNTI compound 1743

DNTI 1743 is a substance similar to DNTI 1742, except it has a hydroxyl group instead of a keto group in position C9. It was extracted from *Clematis armandii* (Ranunculaceae) by Rudolf Bauer's group at the University of Graz. The IUPAC name, (10E,12Z)-9-hydroxyoctadeca-10,12-dienoic acid, was then assigned, and the compound was identified as 9-HODE. Due to its similarity to 9-oxo-ODE, the compound was tested at several concentrations to determine if a concentration-response correlation existed, which was confirmed (Figure 29). However, the observed effect was lower than that of 9-oxo-ODE. This substance was also tested in a neutrophil migration assay, and the results will be shown in the next chapter.

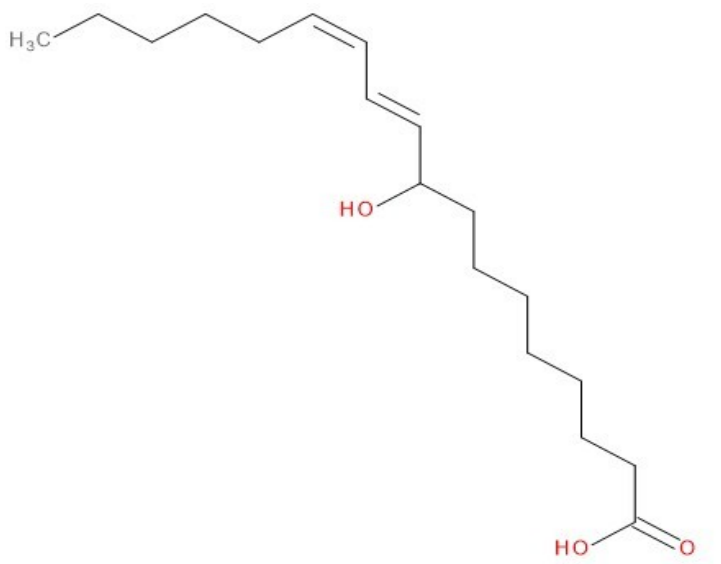

(10E,12Z)-9-hydroxyoctadeca-10,12-dienoic acid

Figure 28: Chemical structure of DNTI 1099. Created in BIOVIA Draw 2019.

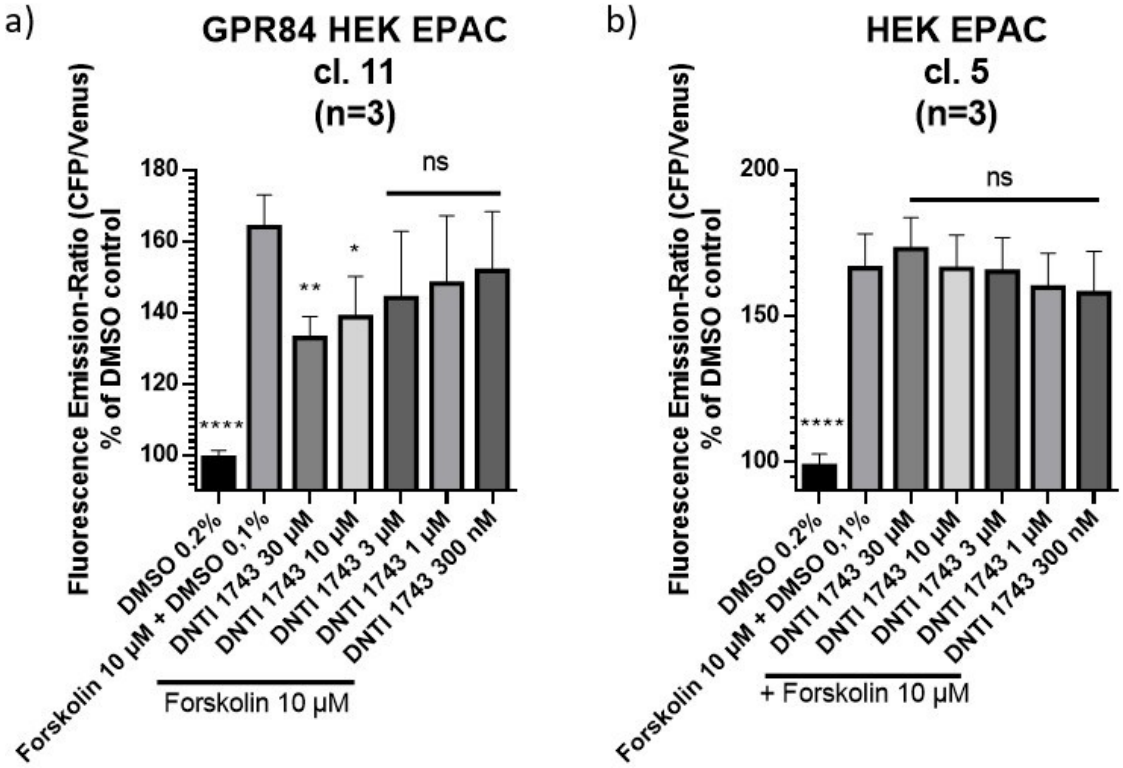

Figure 29: Quotients of emissions of several measured concentrations of DNTI 1743 in GPR84 (a) and EPAC (b) cells. Substance 1743 was tested at various concentrations in the EPAC assay, using DMSO as the vehicle control and DMSO + forskolin as the negative control. The measured fluorescence emission ratios (CFP/Venus) were normalized to the DMSO control. The bar charts show the mean ± SD of three biological replicates (n = 3), which were measured in technical duplicates. A one-way ANOVA and Dunnett's post hoc test were used for statistical analysis (**** $p \leq 0.0001$, *** $p \leq 0.001$, ** $p \leq 0.01$, * $p \leq 0.05$, and ns $p > 0.05$). Substance 1743 exhibited a weaker agonistic effect than Substance 1742 in GPR84 cells, though concentration dependency was evident (a). No agonistic effect was visible in non-transfected EPAC cells (b). Figure made with GraphPad Prism.

4.2.1.5 Related compounds to DNTI 1742 and 1743

Due to the promising results of 9-HODE and, in particular, 9-oxo-ODE in the EPAC assay, literature research was conducted to learn more about the underlying measured effect. Both substances are part of the linoleic acid metabolic pathway and belong to the OXLAM (oxidized linoleic acid metabolite) group. Thus, linoleic acid (LA), alpha-linolenic acid (ALA), arachidonic acid (AA), eicosapentaenoic acid (EPA), and docosahexaenoic acid (DHA) were also tested.

4.2.1.5.1 Linoleic acid

Linoleic acid, a precursor of 9-oxo-ODE and 9-HODE, was one of the interesting substances in the further screening. The EPAC assay results showed effects similar to those of 9-oxo-ODE. Additionally, a concentration-response correlation was evident except at a concentration of 30 µM (Figure 31). It was unclear why this concentration diverged so much from the others, especially since the dilution series was made repeatedly. The absence of effects in the cell line without the transfected GRP84 receptor led to the assumption that the receptor was related to the outcome. To learn more about these connections, linoleic acid (LA) was chosen for testing in a migration assay. The results can be found in the associated chapter.

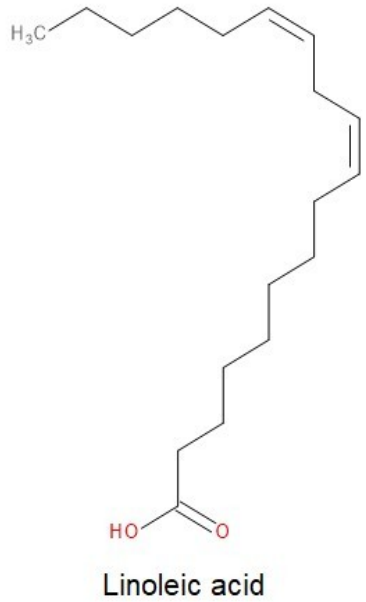

Figure 30: Chemical structure of linoleic acid. Created in BIOVIA Draw 2019.

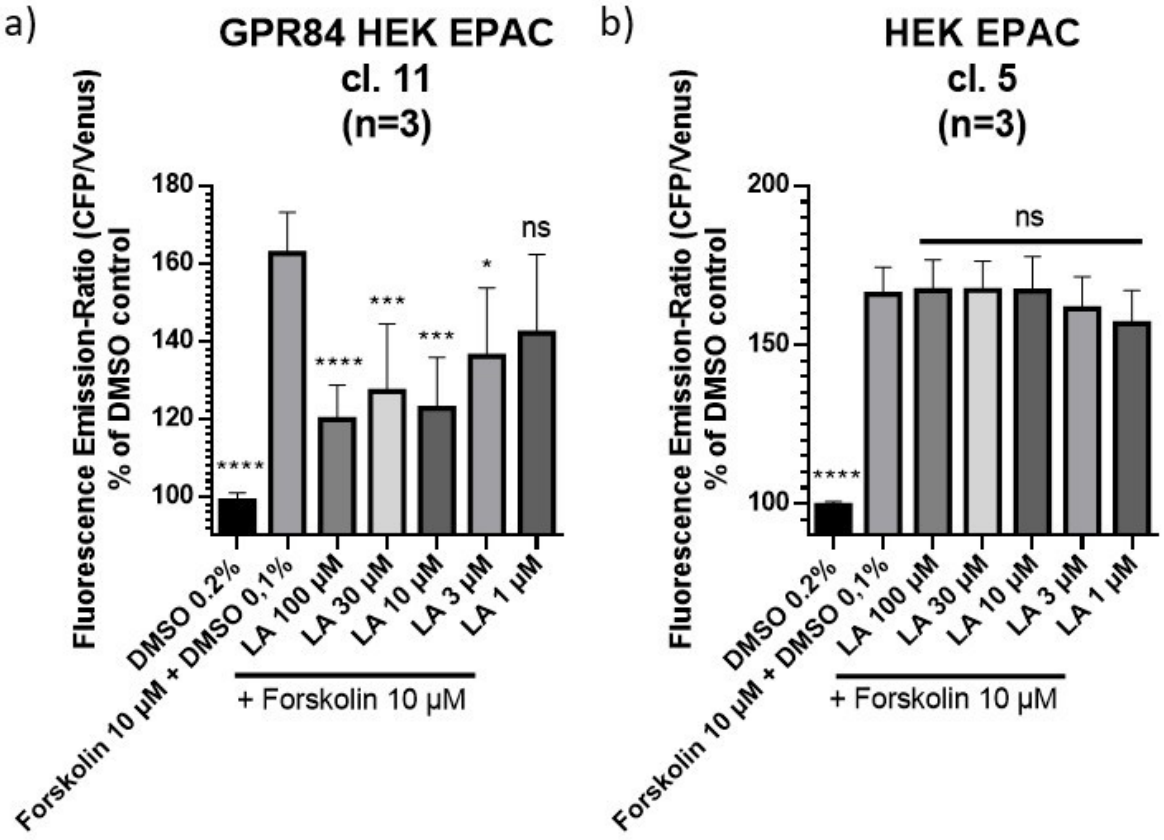

Figure 31: Quotients of emissions of several measured concentrations of linoleic acid in GPR84 (a) and EPAC (b) cells. Several concentrations of linoleic acid were tested in the EPAC assay against a DMSO vehicle control and a DMSO + forskolin negative control. The measured fluorescence emission ratios (CFP/Venus) were normalized to the DMSO control. The bar charts represent the mean ± SD of three biological replicates (n = 3), which were measured in technical duplicates. A one-way ANOVA and Dunnett's post hoc test were used for statistical analysis (**** $p \leq 0.0001$, *** $p \leq 0.001$, ** $p \leq 0.01$, * $p \leq 0.05$, and ns $p > 0.05$). Linoleic acid exhibited an almost concentration-dependent agonistic effect in GPR84 cells (a). No agonistic effect was visible in non-transfected EPAC cells (b). Figure made with GraphPad Prism.

4.2.1.5.2 Alpha linolenic acid (ALA)

Alpha-linolenic acid (ALA) is structurally similar to linoleic acid, except ALA has an additional double bond, making it an omega-3 fatty acid. Because of its structural similarity to LA, this substance was also tested at different concentrations (Figure 33). The results were quite similar to those of LA. Therefore, ALA was chosen for testing in the migration assay as well.

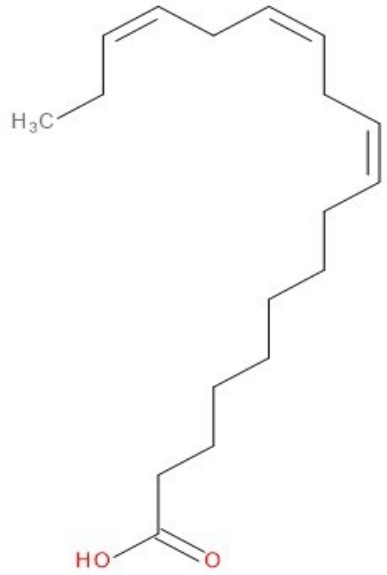

Figure 32: Chemical structure of alpha linolenic acid. Created in BIOVIA Draw 2019.

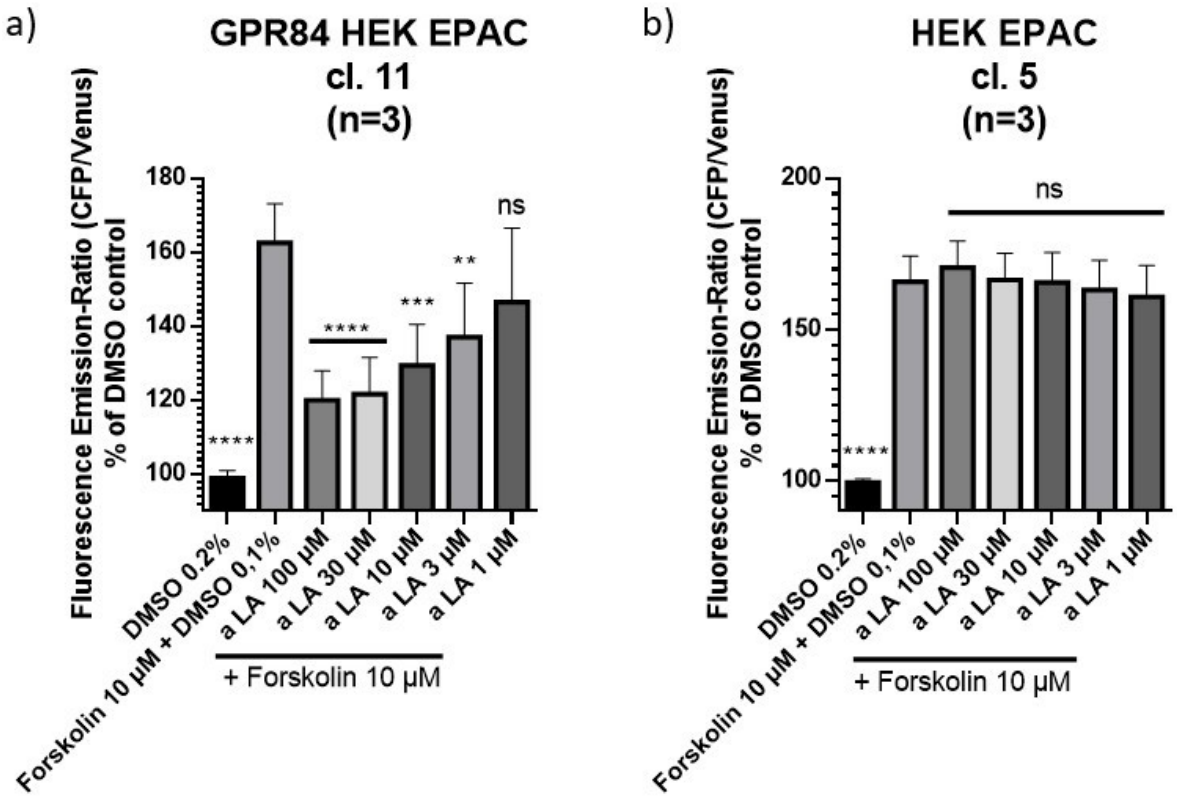

Figure 33: Quotients of emissions of several measured concentrations of alpha linolenic acid in GPR84 (a) and EPAC (b) cells. Several concentrations of alpha-linolenic acid were tested in the EPAC assay against a DMSO vehicle control and a DMSO + forskolin negative control. The measured fluorescence emission ratios (CFP/Venus) were normalized to the DMSO control. The bar charts represent the mean ± SD of three biological replicates (n = 3), which were measured in technical duplicates. A one-way ANOVA and Dunnett's post hoc test were used for

statistical analysis (**** $p \leq 0.0001$, *** $p \leq 0.001$, ** $p \leq 0.01$, * $p \leq 0.05$, and ns $p > 0.05$). In GPR84 cells, alpha-linolenic acid clearly exhibited a concentration-dependent agonistic effect (a), whereas no effect was visible in non-transfected EPAC cells (b). Figure made with GraphPad Prism.

4.2.1.5.3 Arachidonic acid

Arachidonic acid is another metabolite of linoleic acid. It is also known to be a relevant mediator in pro-inflammatory pathways. Therefore, it was assumed that arachidonic acid could affect the GPR84 receptor as well. However, no agonistic effects were visible in the EPAC assay (Figure 35). Conversely, higher concentrations appeared to lead to lower agonistic effects, suggesting an indirect correlation between concentration and agonistic effect. Nevertheless, the substance was chosen for the neutrophil migration assay to exclude methodical errors.

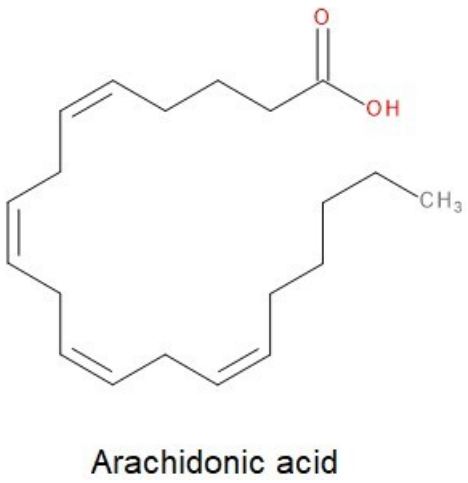

Figure 34: Chemical structure of arachidonic acid. Created in BIOVIA Draw 2019.

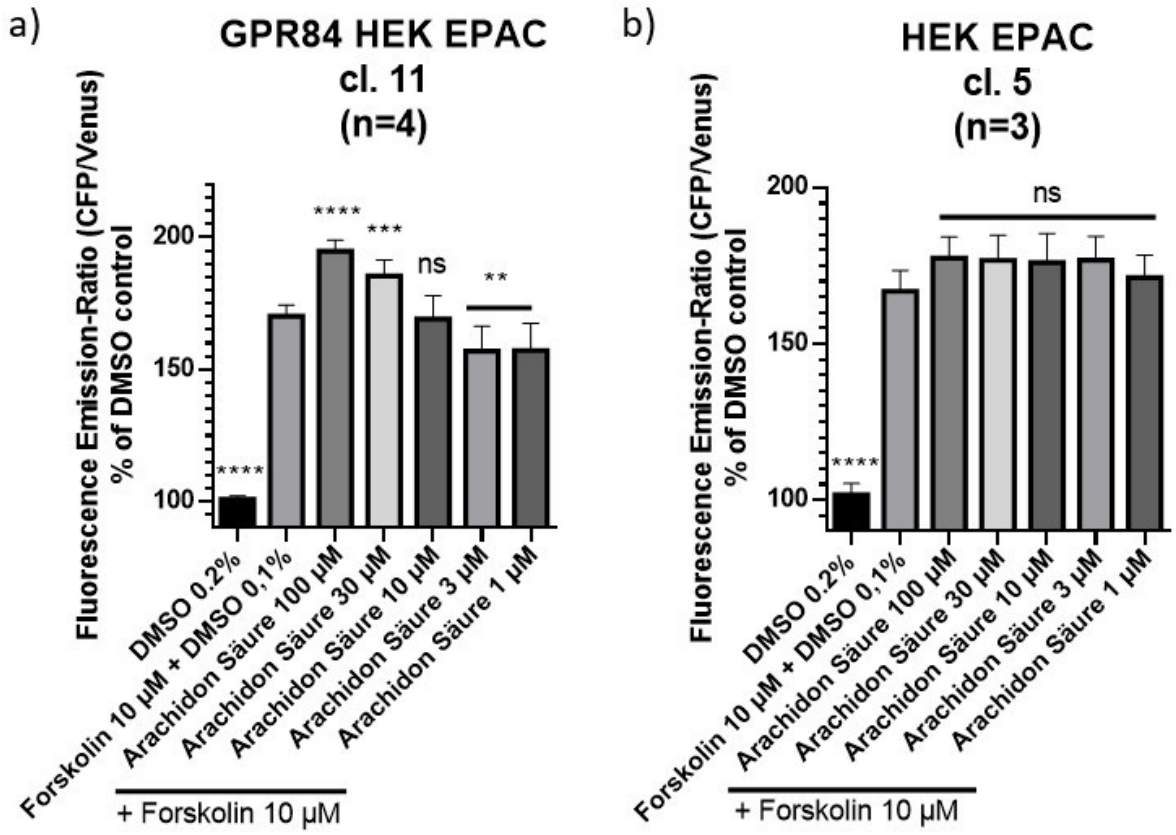

Figure 35: Quotients of emissions of several measured concentrations of arachidonic acid in GPR84 (a) and EPAC (b) cells. Several concentrations of arachidonic acid were tested in the EPAC assay against a DMSO vehicle control and a DMSO + forskolin negative control. The measured fluorescence emission ratios (CFP/Venus) were normalized to the DMSO control. The bar charts represent the mean ± SD of at least three biological replicates (n = 4, n = 3) measured in technical duplicates. A one-way ANOVA and Dunnett's post hoc test were used for statistical analysis (**** $p \leq 0.0001$, *** $p \leq 0.001$, ** $p \leq 0.01$, * $p \leq 0.05$, and ns $p > 0.05$). In GPR84 cells, arachidonic acid showed no agonistic effect, though an inverted concentration dependency was visible (a). No effect was visible in non-transfected EPAC cells (b). Figure made with GraphPad Prism.

4.2.1.5.4 Eicosapentaenoic acid (EPA)

Eicosapentaenoic acid (EPA) is structurally similar to arachidonic acid and can be naturally synthesized from alpha-linolenic acid. It is an important metabolic factor in anti-inflammatory processes[38,39]. Although the effects observed in the EPAC assay were minimal, the results from non-transfected EPAC cells (Figure 37 b) showed patterns similar to those from GPR84-transfected cells treated with arachidonic acid (Figure 35 a). This could indicate cAMP induction by the substance.

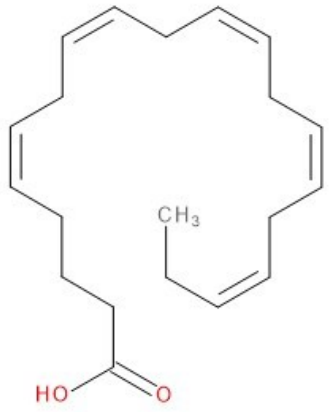

Eicosapentaenoic acid

Figure 36: Chemical structure of eicosapentaenoic acid (EPA). Created in BIOVIA Draw 2019.

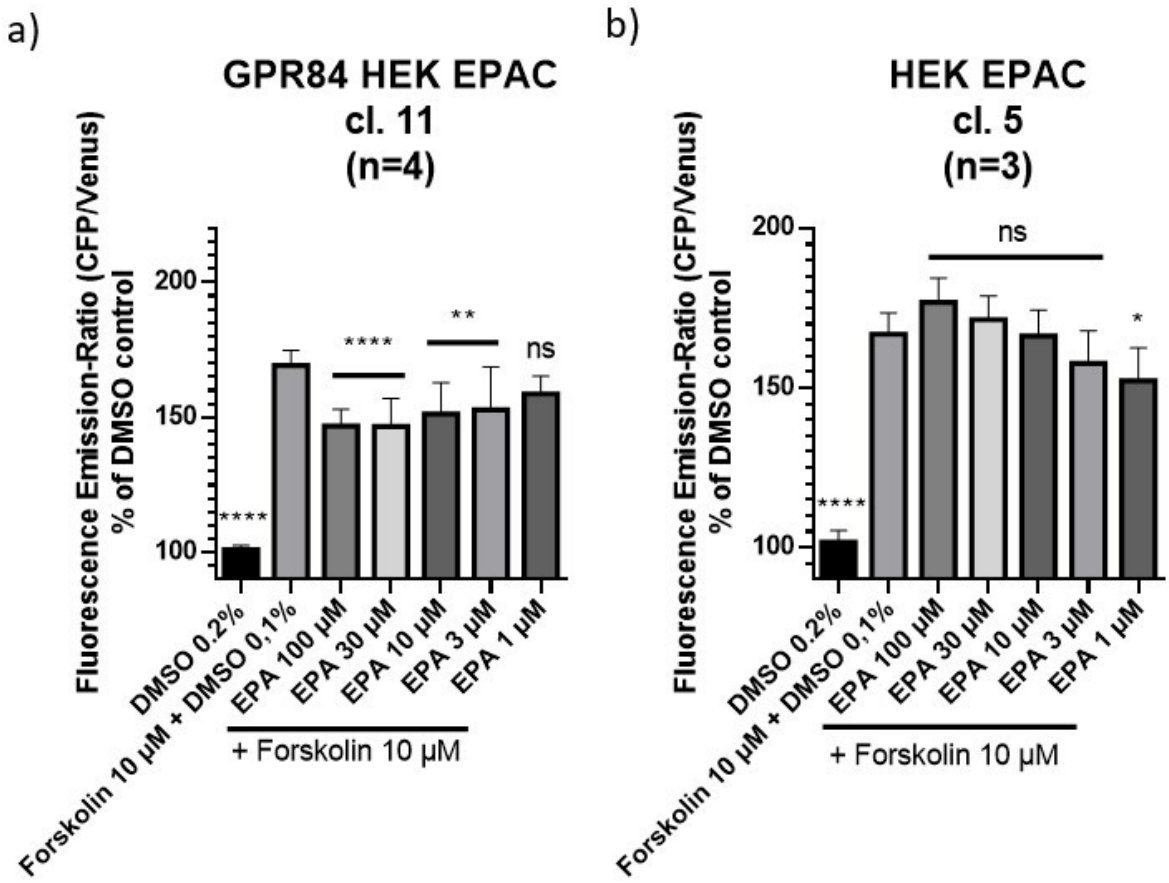

Figure 37: Quotients of emissions of several measured concentrations of eicosapentaenoic acid in GPR84 (a) and EPAC (b) cells. Several concentrations of eicosapentaenoic acid were tested in the EPAC assay against a DMSO vehicle control and a DMSO + forskolin negative control. The measured fluorescence emission ratios (CFP/Venus) were normalized to the DMSO control. The bar charts represent the mean ± SD of at least three

biological replicates (n = 4, n = 3) measured in technical duplicates. A one-way ANOVA and Dunnett's post hoc test were used for statistical analysis (**** $p \leq 0.0001$, *** $p \leq 0.001$, ** $p \leq 0.01$, * $p \leq 0.05$, and ns $p > 0.05$). In GPR84 cells, EPA exhibited a minimal, albeit slightly concentration-dependent, agonistic effect (a). However, in non-transfected EPAC cells, an inverted concentration dependency was observed (b). Figure made with GraphPad Prism.

4.2.1.5.5 Docosahexaenoic acid (DHA)

Like EPA, DHA is naturally produced from alpha-linolenic acid and has anti-inflammatory properties[38,39]. The results of the EPAC assay showed that the compound had no concentration-dependent effect on GPR84 cells, though a slight agonistic effect was visible. There was no visible effect in non-transfected EPAC cells.

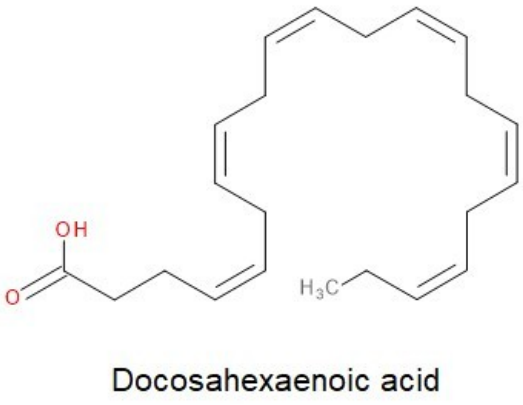

Docosahexaenoic acid

Figure 38: Chemical structure of docosahexaenoic acid. Created in BIOVIA Draw 2019.

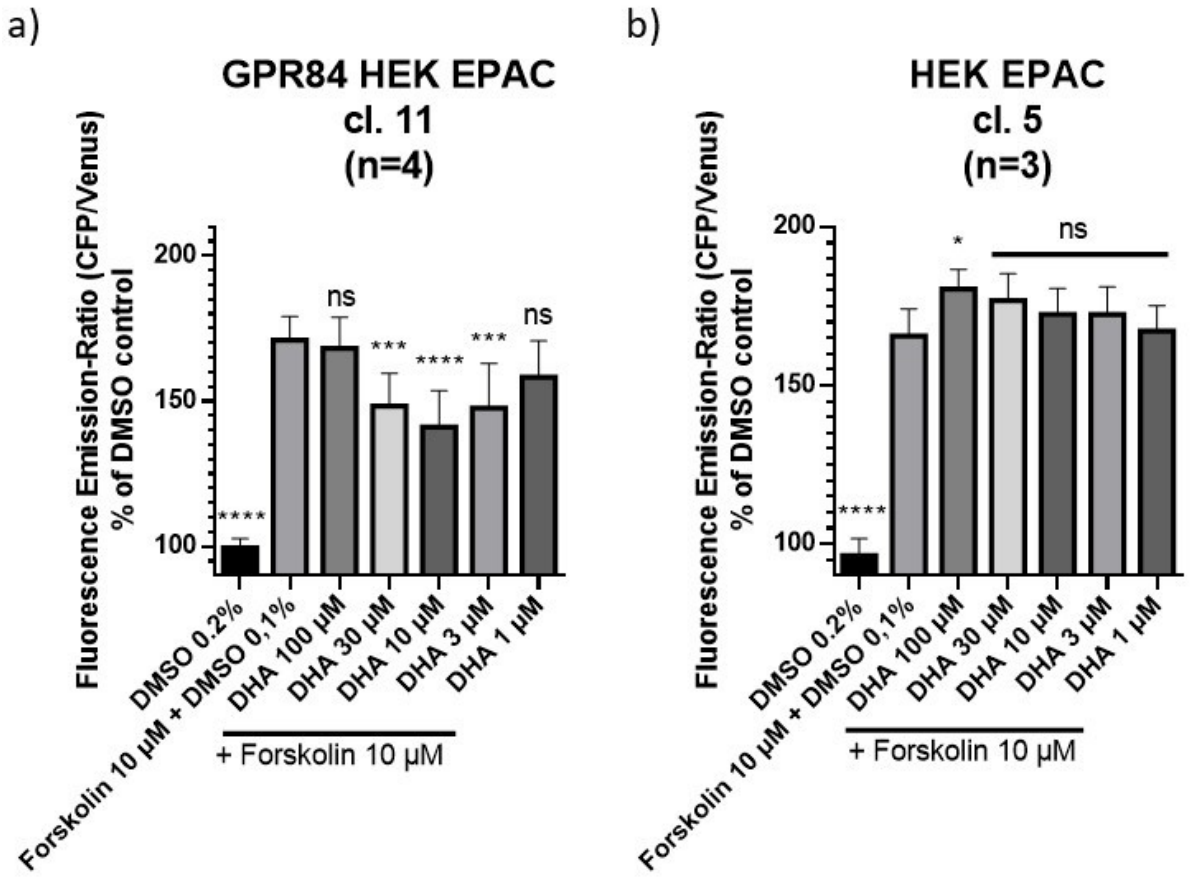

Figure 39: Quotients of emissions of several measured concentrations of docosahexaenoic acid in GPR84 (a) and EPAC (b) cells. Several concentrations of docosahexaenoic acid were tested in the EPAC assay against a DMSO vehicle control and a DMSO + forskolin negative control. The measured fluorescence emission ratios (CFP/Venus) were normalized to the DMSO control. The bar charts represent the mean ± SD of at least three biological replicates (n = 4, n = 3) measured in technical duplicates. A one-way ANOVA and Dunnett's post hoc test were used for statistical analysis (**** $p \leq 0.0001$, *** $p \leq 0.001$, ** $p \leq 0.01$, * $p \leq 0.05$, ns $p > 0.05$). In GPR84 cells, DHA exhibited low agonistic effects independent of concentration (a), whereas no effect was visible in non-transfected EPAC cells (b). Figure made with GraphPad Prism.

4.2.1.6 9-Oxo-ODE & 9-HODE

One disadvantage of the DNTI substance collection is that the compounds were isolated 10 to 15 years before this project began, making it difficult to determine whether the substances have remained stable over time and whether the concentrations of the stock solutions are the same as before. To confirm the measured effects of 9-Oxo-ODE (DNTI 1742) and 9-HODE (DNTI 1743), the compounds were ordered for retesting. However, the new substances had two major issues. First, they were very low in concentration. Second, they were dissolved in ethanol instead of DMSO, like the DNTI substances. Therefore, testing a concentration of 30

µM was not possible because there was insufficient substance for three biological replicates, and the ethanol concentration in the finished test solutions would be too high, which could damage the HEK cells and bias the results. The highest concentration tested in these trials was 10 µM, with a final ethanol concentration of 3%. To appropriately standardize, 3% ethanol was also added to the controls.

The results showed a definite agonistic effect and concentration dependency (Figure 40). The high cAMP value measured in GPR84 cells with 9-HODE at 10 µM was curious, though a similar effect was observed in the control group of non-transfected EPAC cells.

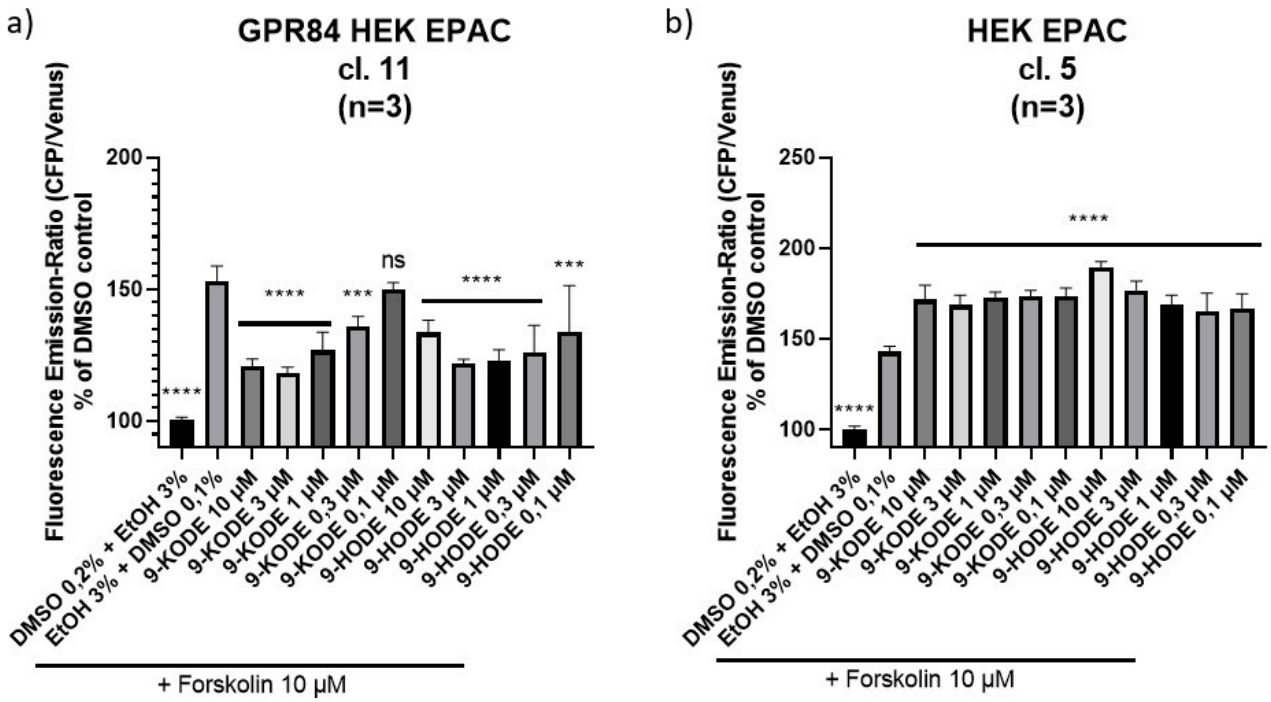

Figure 40: Quotients of emissions of several measured concentrations of freshly ordered 9-KODE (=9-Oxo-ODE) and 9-HODE in GPR84 (a) and EPAC (b) cells. Several concentrations of 9-KODE and 9-HODE were tested in the EPAC assay against the vehicle controls of DMSO and 3% EtOH, as well as the negative control of DMSO, 3% EtOH, and forskolin. The measured fluorescence emission ratios (CFP/Venus) were normalized to the DMSO control. The bar charts represent the mean ± SD of three biological replicates (n = 3), which were measured in technical duplicates. A one-way ANOVA and Dunnett's post hoc test were used for statistical analysis (**** $p \leq 0.0001$, *** $p \leq 0.001$, ** $p \leq 0.01$, * $p \leq 0.05$, and ns $p > 0.05$). In GPR84 cells, both substances exhibited concentration-dependent agonistic effects (a), whereas no agonistic effects were observed in non-transfected EPAC cells (b). The high cAMP concentration at 9-HODE 10 µM could not be clarified, but it was measured in both the test and control cell clones. Figure made with GraphPad Prism.

4.2.2 Potential GPR84 antagonists

During the screening process, the potential antagonistic activity of all substances on the GPR84 receptor was also tested. The method was similar to agonistic testing, except Embelin (1 μM) was added to each substance dilution to allow an antagonistic substance to counteract Embelin's agonistic effect. To understand the following figures (emission figures 41-53), note that in antagonistic screening, the first bar is always the negative control (Forskolin + Embelin), and the second bar is the positive control (Forskolin only). Since the reduction of the Embelin-induced effect by a compound is evaluated, the higher the bar (i.e., closer to the Forskolin-only control), the greater the compound's potential antagonistic effect.

4.2.2.1 Retest of promising potential antagonists from the screening

For the sake of simplicity, only the results of retesting promising potential antagonists are presented in this thesis. Due to time constraints, it was not possible to test every substance of interest at different concentrations in order to establish a concentration-response curve. Therefore, a large-scale retesting of only the positively screened antagonistic substances was performed in biological triplicates to confirm activity. In the first round, substances ranging from 697 to 1715 (Figure 41) and from 1716 to 2544 (Figure 43) were tested in GPR84 cells. Controls in normal EPAC cells were performed later for comparison (Figures 42 and 44). A negative control of 10 μM forskolin, 1 μM embelin, and 0.1% dimethyl sulfoxide (DMSO) in 1X FURA buffer was used when the retest in GPR84 cells was performed. When the control in EPAC cells was performed, it was decided that the same negative control would not be appropriate for these cells because embelin would have no effect without the GPR84 receptor. Therefore, a negative control of 0.3% DMSO was used for this cell line. For the final round of retesting (substances 2545–2784), experiments were conducted simultaneously in both GPR84 and EPAC cells, and the same controls were employed: 0.3% DMSO as the negative

control and a solution of 10 µM Forskolin and 0.2% DMSO as the positive control, as illustrated in Figure 45.

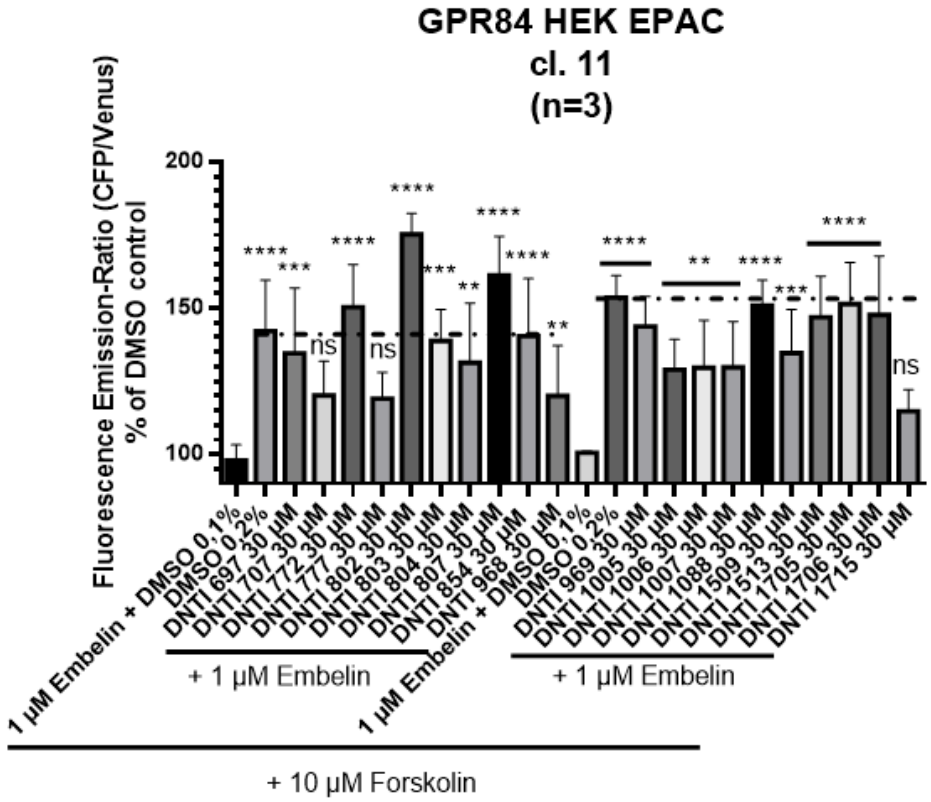

Figure 41: Quotients of emissions of positively screened potential antagonists in GPR84 HEK EPAC cells. Several substances that showed positive antagonistic activity in the initial screening were retested using the EPAC antagonism mode in GPR84 cells to confirm their activity. A solution of Embelin, Forskolin, and DMSO was used as the negative control, and a solution of DMSO and Forskolin was used as the positive control. The fluorescence emission ratios (CFP/Venus) were normalized to the negative control. The bar charts represent the mean ± SD of three biological replicates (n = 3), which were measured in technical duplicates. A one-way ANOVA and Dunnett's post hoc test were used for statistical analysis (**** $p \leq 0.0001$, *** $p \leq 0.001$, ** $p \leq 0.01$, * $p \leq 0.05$, ns $p > 0.05$). Substances with bars above the dashed line were assessed as potential antagonists of the GPR84 receptor. Figure made with GraphPad Prism.

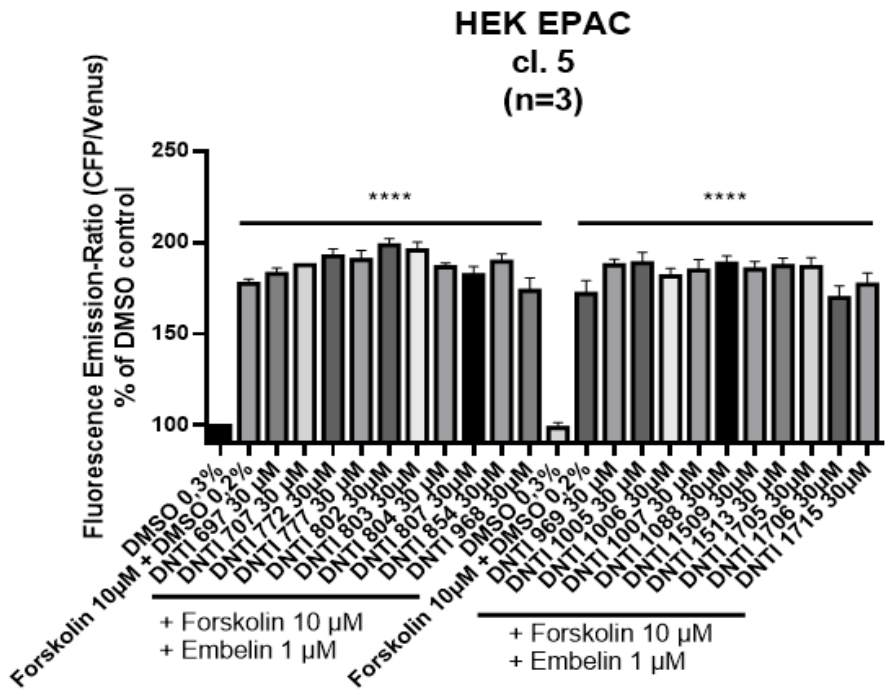

Figure 42: Quotients of emissions of several measured concentrations of positively screened potential antagonists with non-transfected HEK EPAC cells. Several substances that showed positive antagonistic activity in the initial screening were retested using the EPAC assay's antagonistic mode to confirm their activity. Testing in EPAC cells served as a control for the results of testing in GPR84 cells. DMSO was used as the negative control and a solution of DMSO and forskolin was used as the positive control. The fluorescence emission ratios (CFP/Venus) were normalized to the negative control. The bar charts represent the mean ± SD of three biological replicates (n = 3), which were measured in technical duplicates. A one-way ANOVA and Dunnett's post hoc test were used for statistical analysis (**** $p \leq 0.0001$, *** $p \leq 0.001$, ** $p \leq 0.01$, * $p \leq 0.05$, ns $p > 0.05$). Figure made with GraphPad Prism.

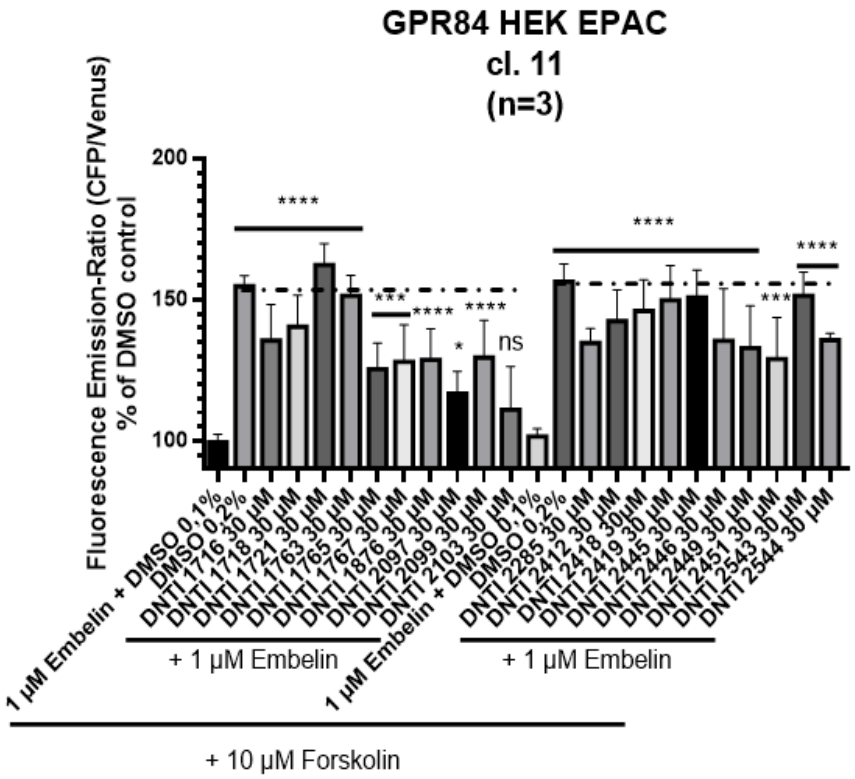

Figure 43: Quotients of emissions of several measured concentrations of positively screened potential antagonists in GPR84 HEK EPAC cells. Several substances that showed positive antagonistic activity in the initial screening were retested using the EPAC antagonism mode in GPR84 cells to confirm their activity. A solution of Embelin, Forskolin, and DMSO was used as the negative control, and a solution of DMSO and Forskolin was used as the positive control. The fluorescence emission ratios (CFP/Venus) were normalized to the negative control. The bar charts represent the mean ± SD of three biological replicates (n = 3), which were measured in technical duplicates. A one-way ANOVA and Dunnett's post hoc test were used for statistical analysis (**** $p \leq 0.0001$, *** $p \leq 0.001$, ** $p \leq 0.01$, * $p \leq 0.05$, and ns $p > 0.05$). Substances with bars above the dashed line were assessed as potential antagonists of the GPR84 receptor. Figure made with GraphPad Prism.

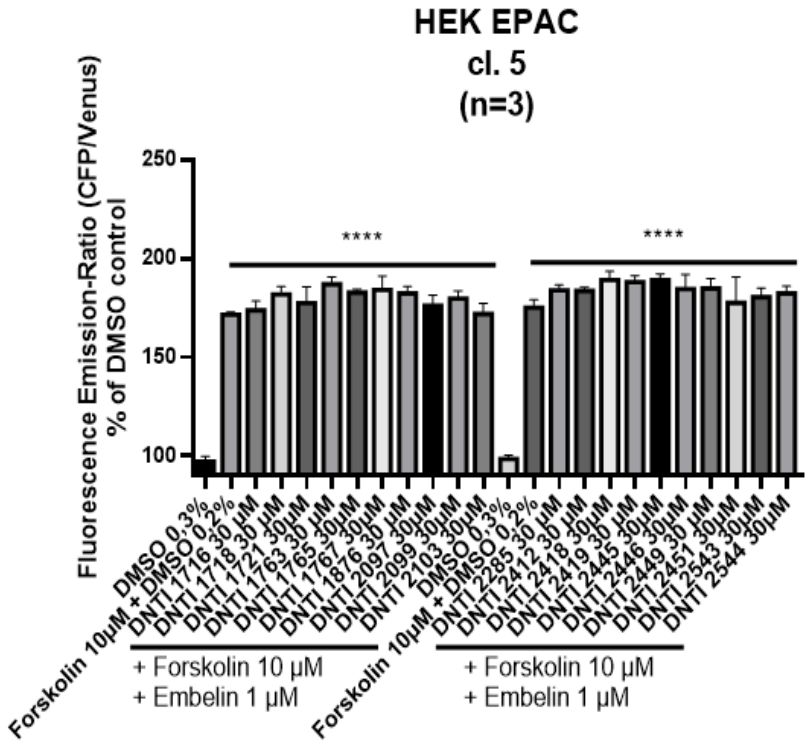

Figure 44: Quotients of emissions of several measured concentrations of positively screened potential antagonists in non-transfected HEK EPAC cells. Several substances that showed positive antagonistic activity in the initial screening were retested using the EPAC assay's antagonistic mode to confirm their activity. Testing in EPAC cells served as a control for the results of testing in GPR84 cells. DMSO was used as the negative control and a solution of DMSO and forskolin was used as the positive control. The fluorescence emission ratios (CFP/Venus) were normalized to the negative control. The bar charts represent the mean ± SD of three biological replicates (n = 3), which were measured in technical duplicates. A one-way ANOVA and Dunnett's post hoc test were used for statistical analysis (**** $p \leq 0.0001$, *** $p \leq 0.001$, ** $p \leq 0.01$, * $p \leq 0.05$, ns $p > 0.05$). Figure made with GraphPad Prism.

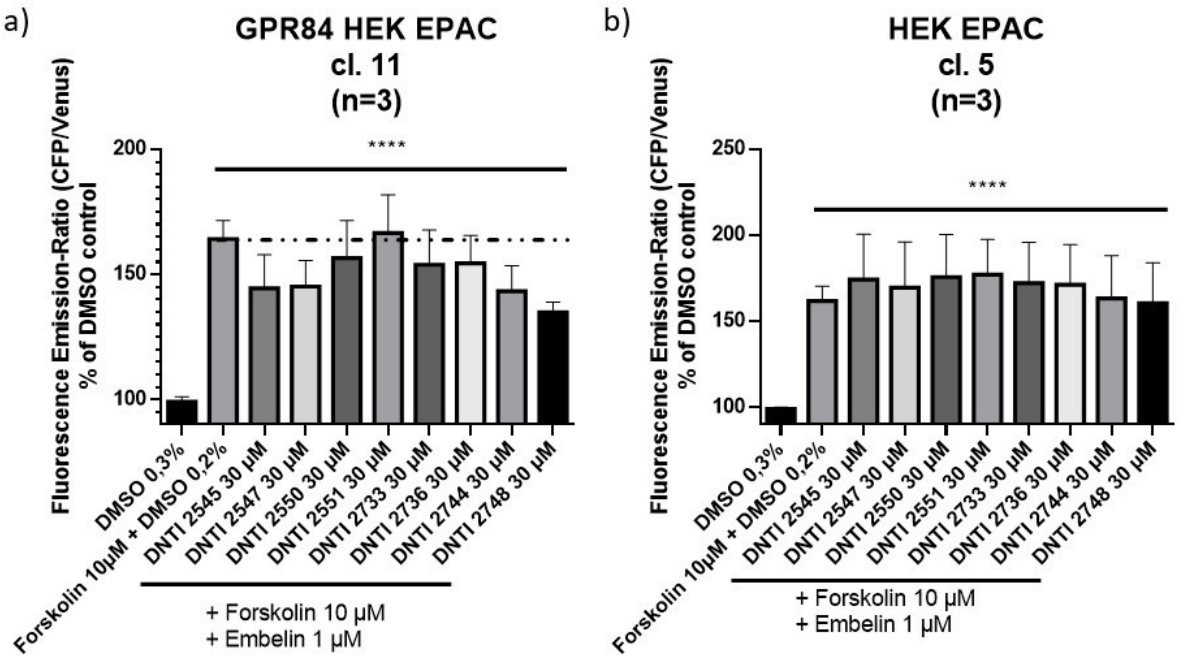

Figure 45: Quotients of emissions of several measured concentrations of possible antagonists with GPR84 (a) and EPAC (b) cells. Several substances that showed positive antagonistic activity in the initial screening were retested using the EPAC assay's antagonistic mode in GPR84 cells to confirm their activity. Testing in EPAC cells was done as a control (b). DMSO was used as the negative control and a solution of DMSO and forskolin was used as the positive control. The fluorescence emission ratios (CFP/Venus) were normalized to the negative control. The bar charts represent the mean ± SD of three biological replicates (n = 3), which were measured in technical duplicates. A one-way ANOVA and Dunnett's post hoc test were used for statistical analysis (**** $p \leq 0.0001$, *** $p \leq 0.001$, ** $p \leq 0.01$, * $p \leq 0.05$, and ns $p > 0.05$). Substances with bars above the dashed line in the results of testing with the GPR84 cell line were assessed as potential antagonists of the GPR84 receptor. Figure made with GraphPad Prism.

Many of those compounds showed potential antagonistic results after retesting. Due to time constraints, only four interesting compounds (DNTI 1721, 1763, 2412, and 2543) were tested at different concentrations to confirm concentration dependency. The other substances that screened positively (697, 772, 854, 1088, 1513, 1705, 1706, 2418, 2419, 2445, 2545, 2547, 2550, 2551, 2733, 2736, and 2744) still need to be tested at more concentrations.

4.2.2.2 DNTI compound 1721

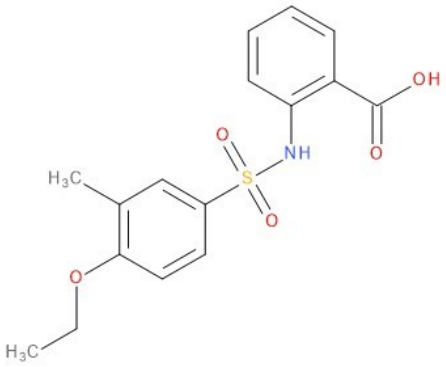

2-{[(4-Ethoxy-3-methylphenyl)sulfonyl]amino}benzoic acid

Figure 46: Chemical structure of DNTI 1721. Created in BIOVIA Draw 2019.

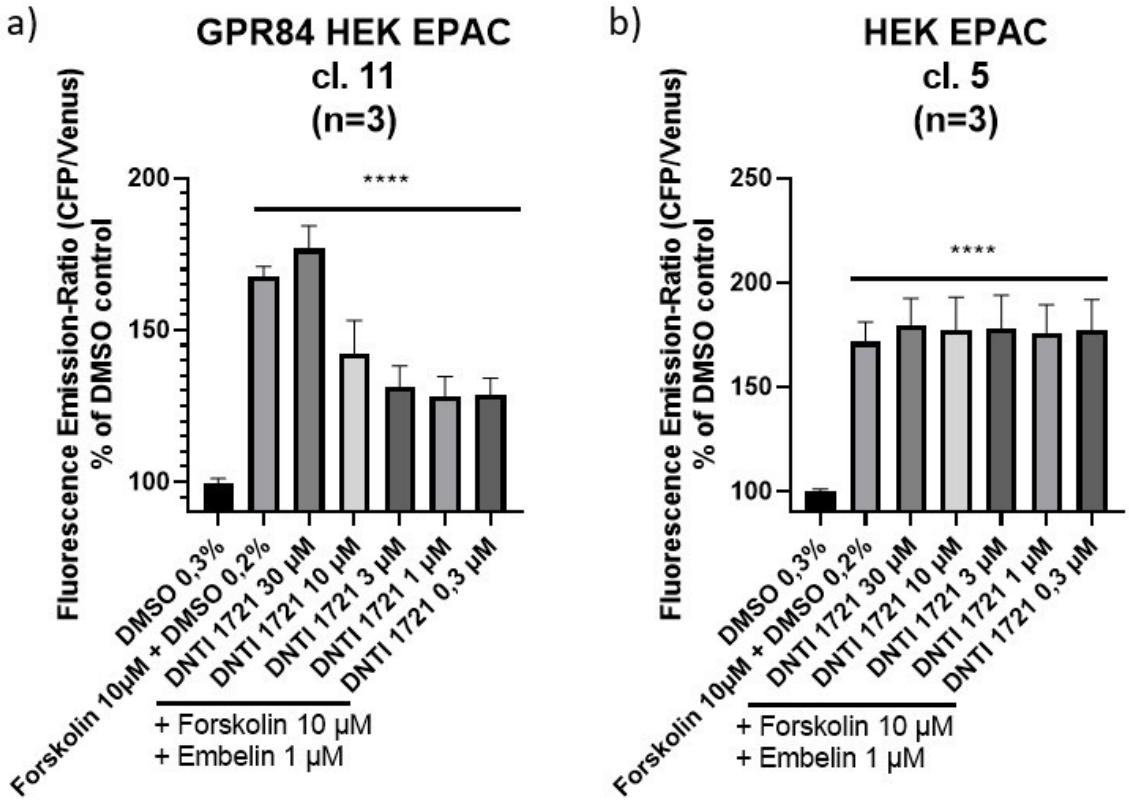

Figure 47: Quotients of emissions of several measured concentrations of DNTI 1721 in GPR84 (a) and EPAC (b) cells. Substance 1721 was tested at five different concentrations in an antagonistic EPAC assay using GPR84 cells (a) and normal EPAC cells (b). DMSO was used as the negative control and a solution of forskolin and DMSO was used as the positive control. The bar charts represent the mean ± SD of three biological replicates (n = 3), which were measured in technical duplicates. A one-way ANOVA and Dunnett's post hoc test were used for statistical analysis (**** $p \leq 0.0001$, *** $p \leq 0.001$, ** $p \leq 0.01$, * $p \leq 0.05$, ns $p > 0.05$). 1721 showed an exponential concentration-dependent antagonistic effect against Embelin as reported agonist in GPR84 cells (a). No effect was visible in non-transfected EPAC cells (b). Figure made with GraphPad Prism.

The DNTI compound 1721 is a predicted NF-κB inhibitor named according to the IUPAC nomenclature: 2-{[(4-ethoxy-3-methylphenyl)sulfonyl]amino}benzoic acid. Different concentrations were tested against Embelin as reported agonist and showed antagonistic results. An exponential concentration-dependent activity was visible in GPR84 cells, but no effect was visible in non-transfected EPAC cells (Figure 47).

4.2.2.3 DNTI compound 1763

The DNTI compound 1763 was identified as Pinoresinol, which was isolated from sesame seeds by the University of Innsbruck. Its IUPAC name is 4-[(3S,3aR,6S,6aR)-6-(4-hydroxy-3-methoxy-phenyl)-1,3,3a,4,6,6a-hexahydrofuro[3,4-c]furan-3-yl]-2-methoxy-phenol. An antagonistic effect and a linear concentration-response relationship were observed when 1763 was tested at different concentrations in GPR84 cells. No antagonistic effect was visible in non-transfected EPAC cells (Figure 49).

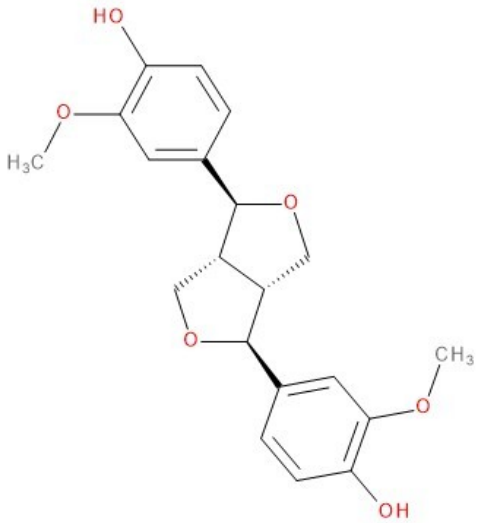

Pinoresinol

Figure 48: Chemical structure of DNTI 1763. Created in BIOVIA Draw 2019.

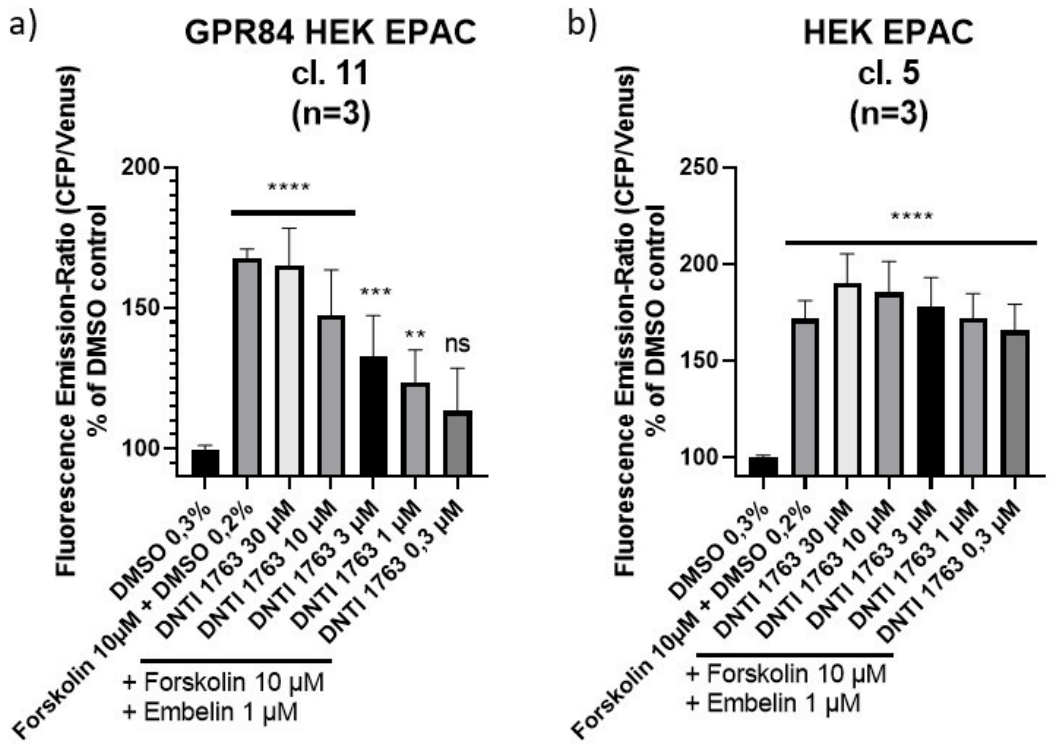

Figure 49: Quotients of emissions of several measured concentrations of DNTI 1763 in GPR84 (a) and EPAC (b) cells. Substance 1763 was tested at five different concentrations in an antagonistic EPAC assay using GPR84 cells (a) and normal EPAC cells (b). DMSO was used as the negative control and a solution of forskolin and DMSO was used as the positive control. The bar charts represent the mean ± SD of three biological replicates (n = 3), which were measured in technical duplicates. A one-way ANOVA and Dunnett's post hoc test were used for statistical analysis (**** $p \leq 0.0001$, *** $p \leq 0.001$, ** $p \leq 0.01$, * $p \leq 0.05$, and ns $p > 0.05$). In GPR84 cells, 1763 exhibited a linear, concentration-dependent antagonistic effect against the reported agonist, Embelin (a). No effect was observed in non-transfected EPAC cells (b). Figure made with GraphPad Prism.

4.2.2.4 DNTI compound 2412

The DNTI compound 2412 was identified as imbricaric acid, which was isolated from *Cetrelia monachorum* by the University of Innsbruck. Its IUPAC name is 2-hydroxy-4-(2-hydroxy-4-methoxy-6-pentylbenzoyl)oxy-6-propylbenzoic acid, and it was generated using BIOVIA Draw 2019. The substance was tested at five different concentrations and exhibited potent antagonistic activity at a concentration of 30 µM in GPR84 cells. This activity decreased quickly at concentrations of 10 µM and lower (Figure 51). Nevertheless, due to its effectiveness, the substance was tested in a neutrophil migration assay. No antagonistic effect was visible in non-transfected EPAC cells.

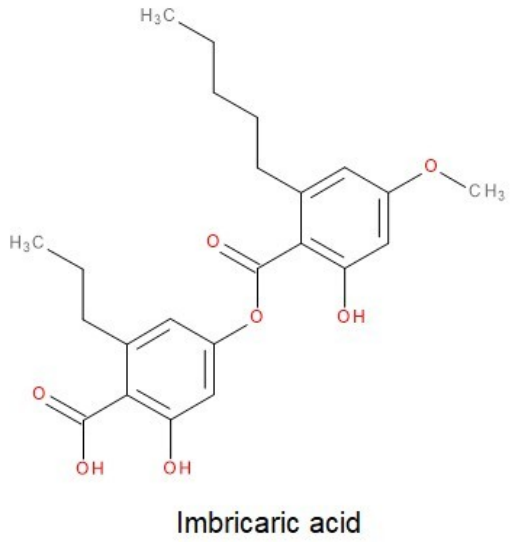

Figure 51: Chemical structure of DNTI 2412. Created in BIOVIA Draw 2019.

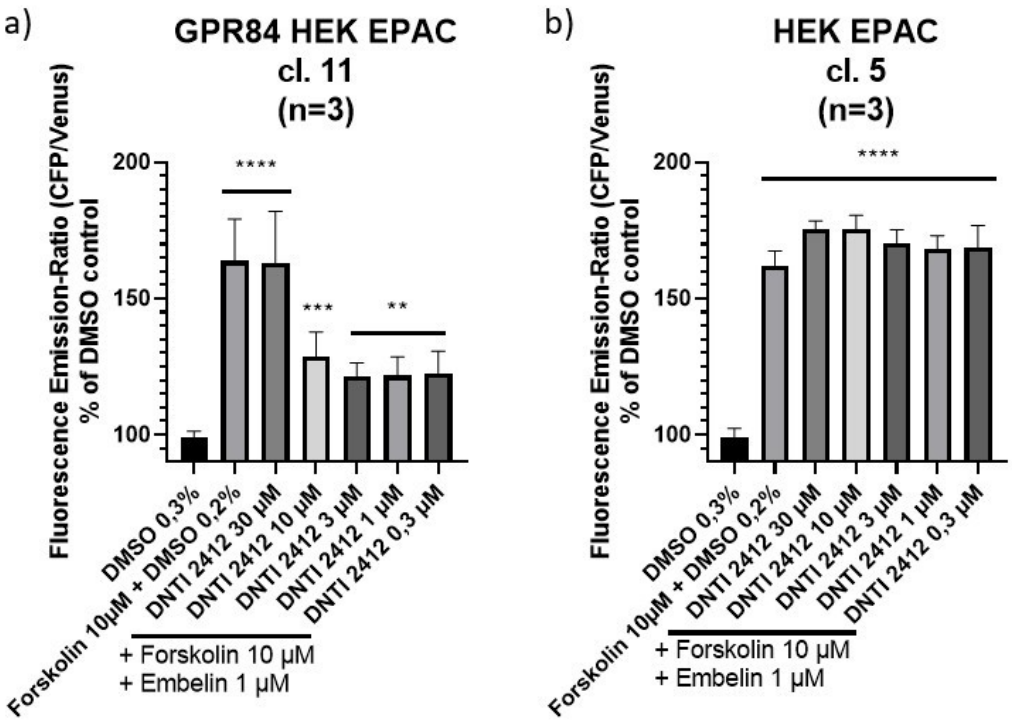

Figure 50: Quotients of emissions of several measured concentrations of DNTI 2412 in GPR84 (a) and EPAC (b) cells. Substance 2412 was tested at five different concentrations in an antagonistic EPAC assay using GPR84 cells (a) and normal EPAC cells (b). DMSO was used as the negative control and a solution of forskolin and DMSO was used as the positive control. The bar charts represent the mean ± SD of three biological replicates (n = 3), which were measured in technical duplicates. A one-way ANOVA and Dunnett's post hoc test were used for statistical analysis (**** $p \leq 0.0001$, *** $p \leq 0.001$, ** $p \leq 0.01$, * $p \leq 0.05$, and ns $p > 0.05$). The substance showed potent antagonistic activity at a concentration of 30 µM in GPR84 cells. This activity decreased rapidly at concentrations of 10 µM and below (a). No antagonistic effect was visible in non-transfected EPAC cells (b). Figure made with GraphPad Prism.

4.2.2.5 DNTI compound 2543

The DNTI compound 2543 is a synthetic Leoligin derivative. It was named according to the IUPAC nomenclature as: (2S,3R,4R)-2-(3,4-dimethoxyphenyl)-4-[(3,4-dimethoxyphenyl)methyl]tetrahydrofuran-3-yl methyl cyclopropanecarboxylate. The compound was tested at five different concentrations (see Figure 53) and exhibited a linear concentration-response correlation similar to 1763 (see Figure 49) when tested in GPR84 cells. Due to its promising antagonistic activity in the EPAC assay, the compound was also tested in a neutrophil migration assay. No effect was observed in non-transfected EPAC cells.

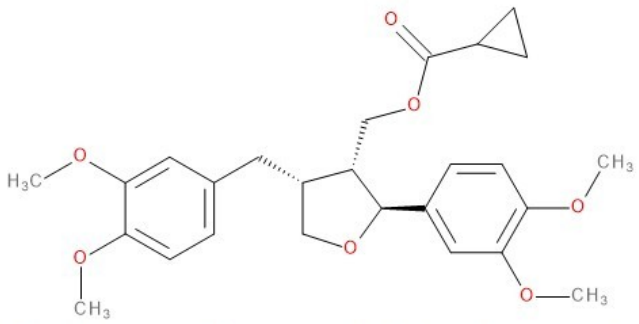

[(2*S*,3*R*,4*R*)-2-(3,4-dimethoxyphenyl)-4-[(3,4-dimethoxyphenyl)methyl] tetrahydrofuran-3-yl]methyl cyclopropanecarboxylate

52: Figure Chemical structure of DNTI 2412. Created in BIOVIA Draw 2019.

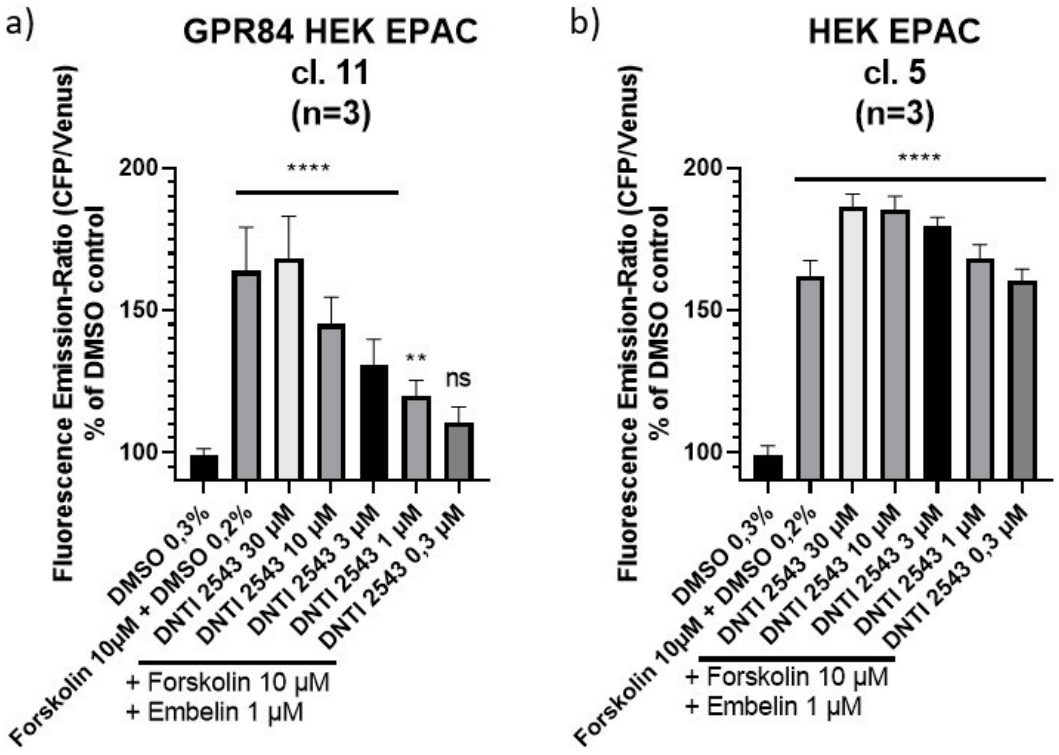

Figure 53: Quotients of emissions of several measured concentrations of DNTI 2543 in GPR84 (a) and EPAC (b) cells. Substance 2543 was tested at five different concentrations in an antagonistic EPAC assay using GPR84 cells (a) and normal EPAC cells (b). DMSO was used as the negative control and a solution of forskolin and DMSO was used as the positive control. The bar charts represent the mean ± SD of three biological replicates (n = 3), which were measured in technical duplicates. A one-way ANOVA and Dunnett's post hoc test were used for statistical analysis (**** $p \leq 0.0001$, *** $p \leq 0.001$, ** $p \leq 0.01$, * $p \leq 0.05$, and ns $p > 0.05$). When tested in GPR84 cells, 2543 exhibited an antagonistic effect and a linear concentration-response correlation (a). No effect was observed in non-transfected EPAC cells (b). Figure made with GraphPad Prism.

4.3 Neutrophil Migration assay

The quantification method using the ViCell counter described in the Methods section was not considered for this thesis. While this counting method is simple, it is not reliable and can only provide an initial idea of how well the migration assay worked. The ViCell counter requires a minimum cell concentration to provide reliable results. However, the concentrations of migrated PMNs were mostly too low for the machine to count reliably; therefore, the values could hardly be considered accurate. For this reason, the results of this method are not presented in this paper. Pictures were taken directly after the migration process in the TECAN Spark photometer to provide an initial semiquantitative impression of the results. Pictures were also taken for documentation, even if quantification was not possible.

4.3.1 Migration assay performed on 01.12.2023

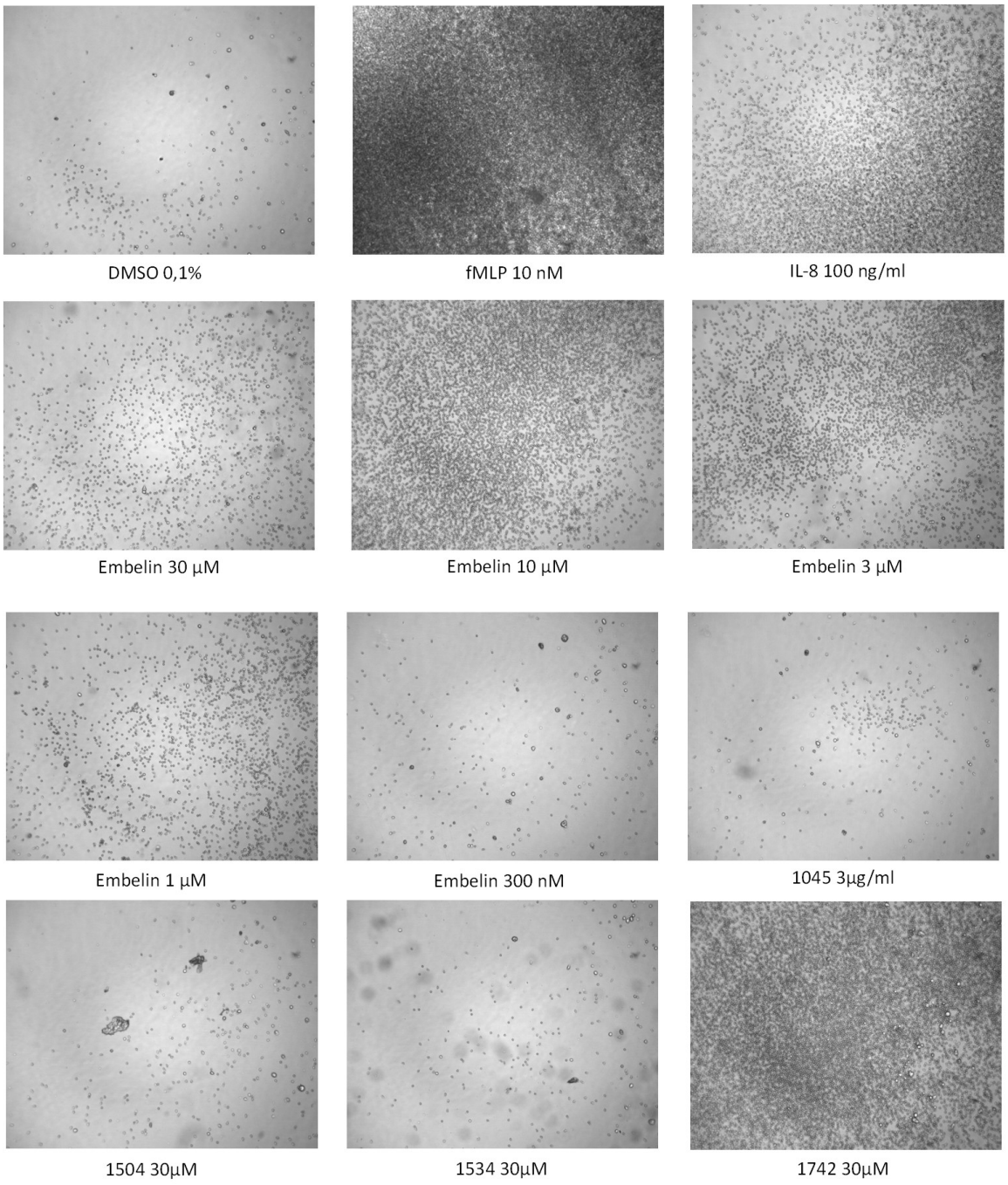

Figure 54: Pictures of the well bottoms of the migration assay from the 01.12.2023. Pictures show neutrophils that have successfully migrated and settled in the wells of the 24-well plate. DMSO served as the negative control, while fMLP and IL-8 served as the positive controls. Embelin exhibited concentration-dependent cell migration, except at a concentration of 30 µM. Test substances 1045, 1504, and 1534 showed almost no chemotactic effect, whereas substance 1742 showed promising results. Pictures were taken with the TECAN Spark by Dr. Alexander Perhal.

For the first migration assay, Embelin was evaluated at different concentrations. fMLP (10nM) and IL-8 (100ng/ml) were used as positive controls, and DMSO (0.1%) was used as a negative control. This became the standard for all subsequent experiments. After the migration process, pictures of the wells were taken with the TECAN Spark (Figure 54), and the luminol oxidation assay (Figure 55) and FACS counting (Figure 56) were performed.

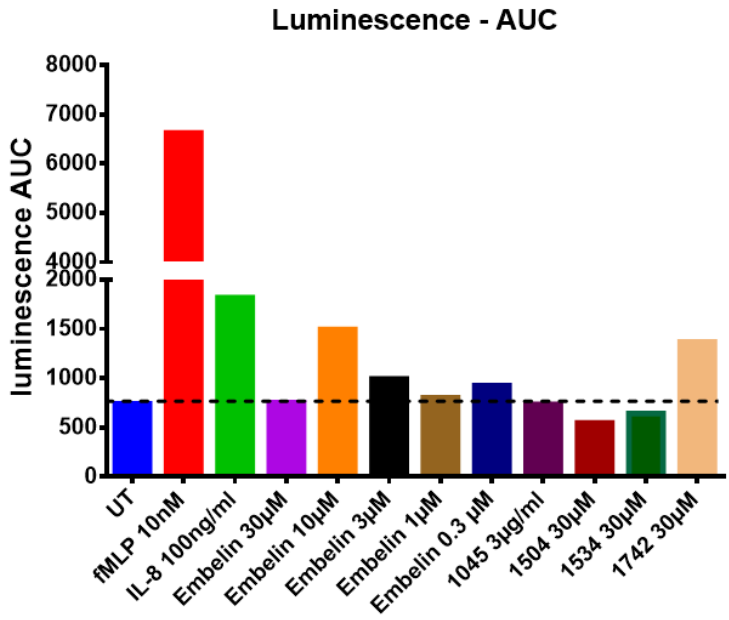

Figure 55: Results of the luminol oxidation assay from the 01.12.2023. After the neutrophil migration assay, an aliquot of migrated cells was treated with luminol and fMLP to induce neutrophil degranulation. The released mediators oxidized the luminol, and the emitted light was measured. The x-axis shows the name of each tested well, and the y-axis shows the corresponding luminescence area under the curve (AUC). FMLP and IL-8 were used as positive controls. Embelin was tested at different concentrations and exhibited a concentration-dependent effect, except at concentrations of 30 µM and 0.3 µM. Of the tested substances, only 1742 exhibited positive activity. Figure was made in GraphPad Prism

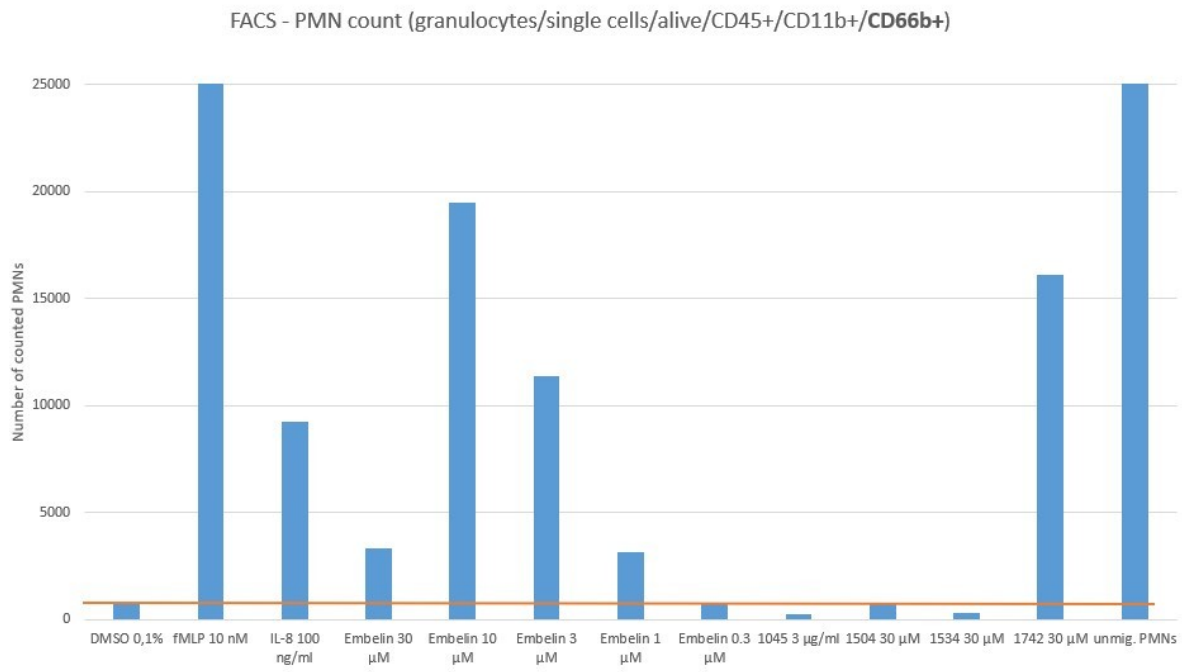

Figure 56: Results of the FACS counting - PMN measurement from the 01.12.2023. The migrated cells were counted with the FACS-gating: granulocytes/single cells/alive/CD45+/CD11b+/CD66b+. The x-axis shows the names of the tested wells, and the y-axis shows the corresponding FACS counts. The bars are limited to 25,000 counted cells to make them more comparable in the figure. fMLP and IL-8 were used as positive controls. Embelin was tested at different concentrations and exhibited a concentration-dependent effect, except at a concentration of 30 µM. Of the tested substances, only 1742 exhibited positive activity. Figure was made in Excel

For the first migration assay, the results of the FACS counting analysis and the luminescence oxidation assay were comparable. A concentration-dependent effect of Embelin was visible, except at a concentration of 30 µM. A probably cytotoxic effect was suspected as the reason. The pictures taken by the TECAN Spark photometer also showed a dose-response relationship for Embelin, except at a concentration of 30 µM. Of the tested substances, 1742 (9-Oxo-ODE) at 30 µM was the only one that exhibited a chemotactic effect, though the number of migrated cells was nearly equivalent to that of Embelin at 10 µM. The other tested substances (1045, 1504, and 1534) showed almost no effect, so they were excluded from further experiments.

4.3.2 Migration assay performed on 14.12.2023

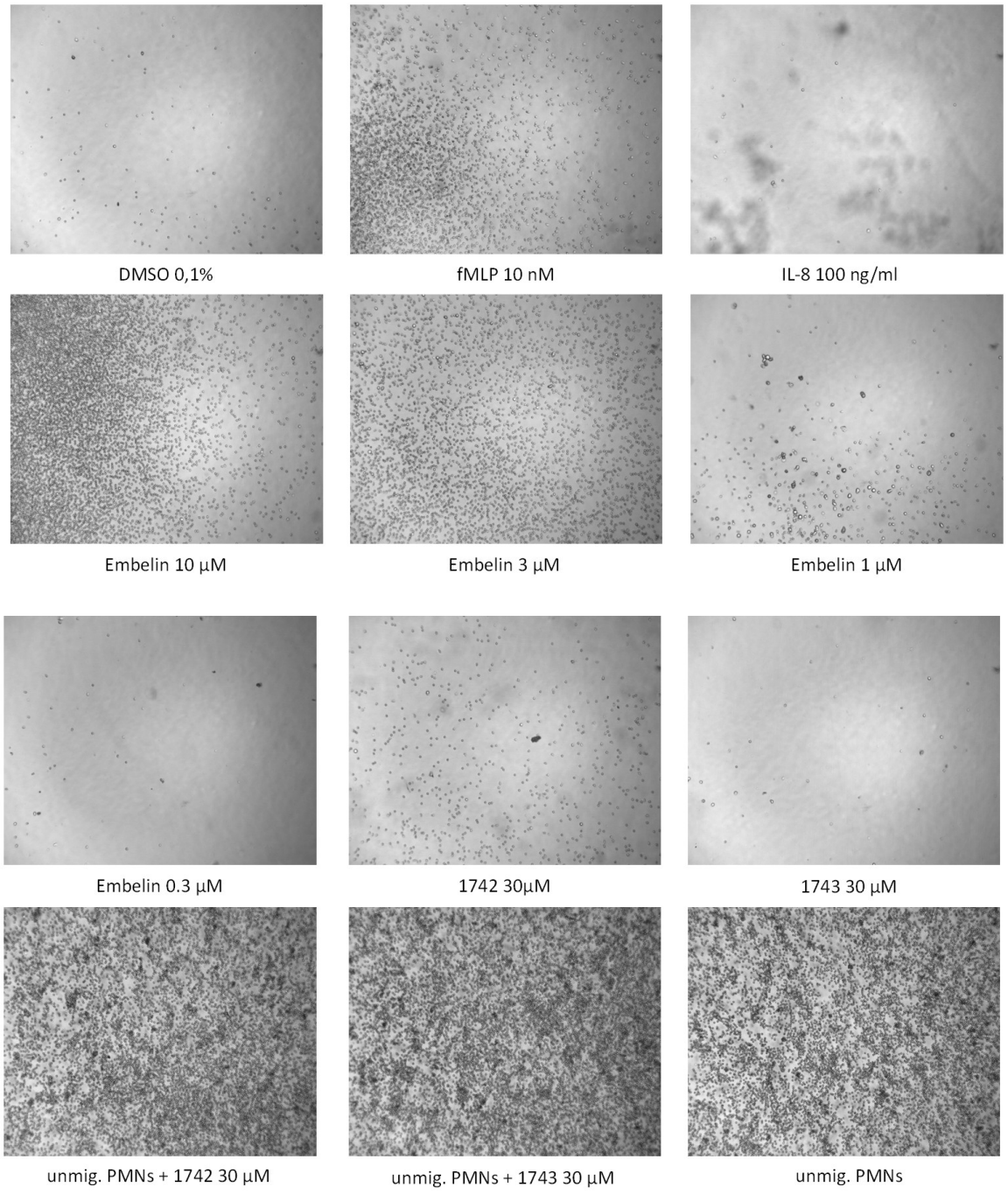

Figure 57: Pictures of the well bottoms of the migration assay from the 14.12.2023. Pictures show the neutrophils that successfully migrated. DMSO served as the negative control. The negative controls, fMLP and IL-8, were not as effective in this experiment. However, embelin again demonstrated concentration-dependent chemotaxis induction. Substance 1742 only had a slight effect; 1743 had almost no effect. Both substances were also combined with unmigrated PMNs, but no differences were visible in the pictures. Pictures were taken with the TECAN Spark by Dr. Alexander Perhal.

DMSO 0.1% was used as the negative control, while fMLP at 10nM and IL-8 at 100 ng/ml were used as the positive controls. Several Embelin concentrations were tested again to achieve three biological replicates, this time excluding the 30 µM concentration. Only nine inserts met the prerequisites for the assay, so the last three wells were filled with the originally isolated cell suspension ("unmig. PMNs"), one with an addition of 30 µM 1742 and another with 30 µM 1743, to see if anything would happen and to avoid wasting well plate slots. However, no differences could be seen in the pictures (Figure 57) of the last three wells.

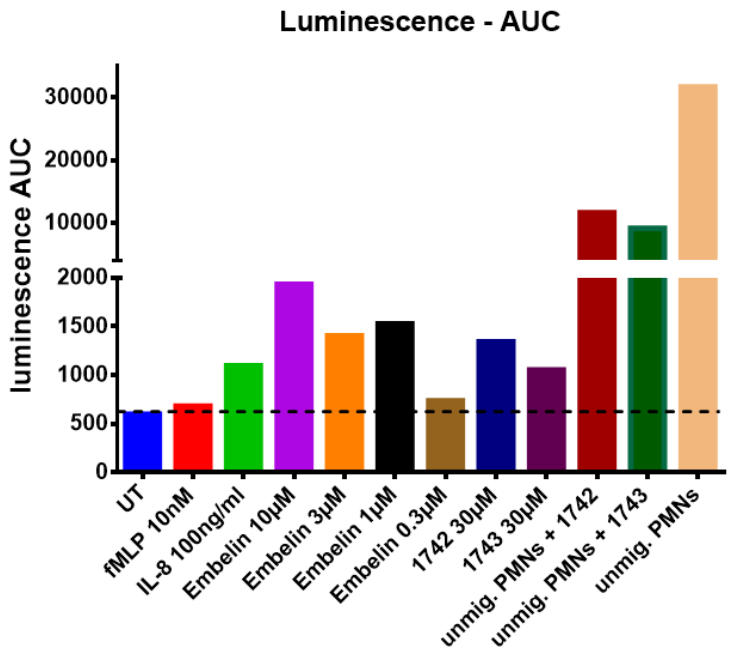

Figure 58: Results of the luminol oxidation assay from the 14.12.2023. After the neutrophil migration assay, an aliquot of migrated cells was treated with luminol and fMLP to induce neutrophil degranulation. The released mediators oxidized the luminol, and the emitted light was measured. The x-axis shows the name of each tested well, and the y-axis shows the corresponding luminescence area under the curve (AUC). In this experiment, the positive controls fMLP and IL-8 showed little effect. The activity of different concentrations of Embelin was less visible, and Embelin's effect was higher than that of the positive controls. Both 1742 and 1743 showed activity, reducing the number of unmigrated PMNs when treated. Figure was made in GraphPad Prism

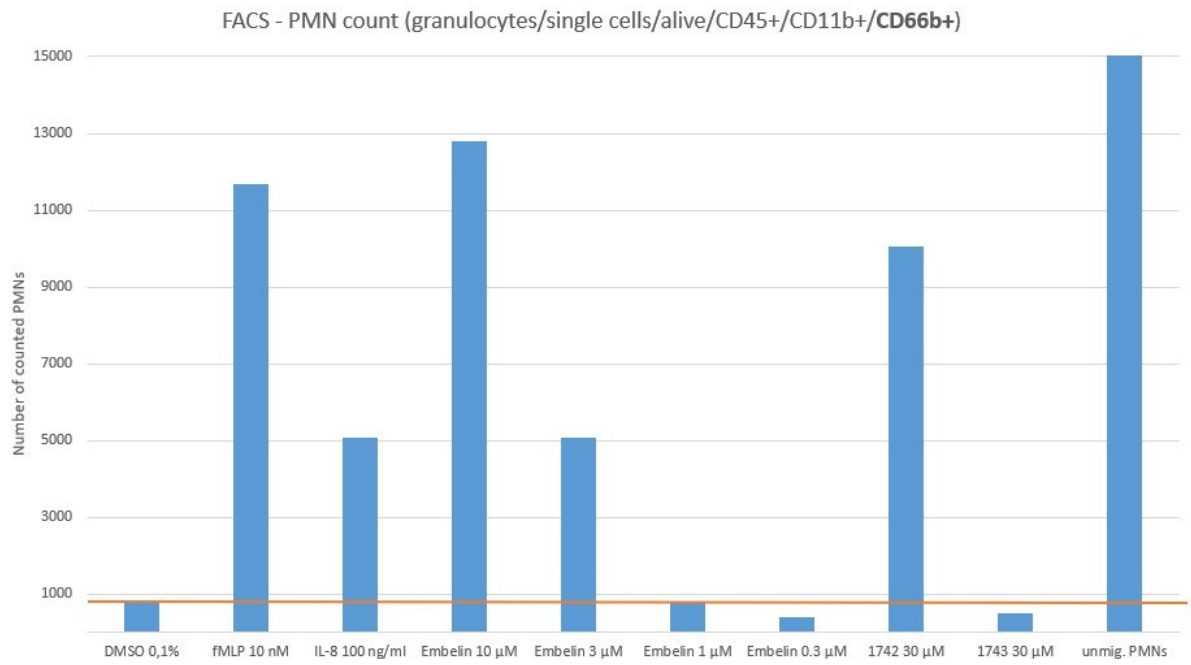

Figure 59: Results of the FACS - PMN measurement from the 14.12.2023. The migrated cells were counted with the FACS-gating: granulocytes/single cells/alive/CD45+/CD11b+/CD66b+. The x-axis shows the names of the tested wells, and the y-axis shows the corresponding FACS counts. The bars are limited to 15,000 counted cells to make them more comparable in the figure. In this experiment, the positive controls fMLP and IL-8 were much less effective than usual. In contrast to the luminol oxidation assay, a concentration-dependent activity of different Embelin concentrations was visible here. According to the results of the FACS counting, only 1742 showed activity. Figure was made in Excel

In the second migration assay, several Embelin concentrations were tested repeatedly, revealing a concentration-dependent effect. Testing substance 1742 (30 µM) was almost as effective as Embelin (10 µM) and the positive control, fMLP. However, the positive controls (fMLP and IL-8) did not work as well this time, though the results were still considered acceptable. Substance 1743 (9-HODE) at 30 µM showed almost no effect. This clearly shows that the luminescence oxidation assay is not always reliable (Figure 58). The results of the luminescence oxidation assay showed no concentration-dependent effect of Embelin, and the positive controls (fMLP and IL-8) barely worked. However, the FACS counting results showed a concentration-dependent activity of Embelin (Figure 59). FACS results are generally more reliable, which is why they are preferred for analysis.

4.3.3 Migration assay performed on 20.12.2023

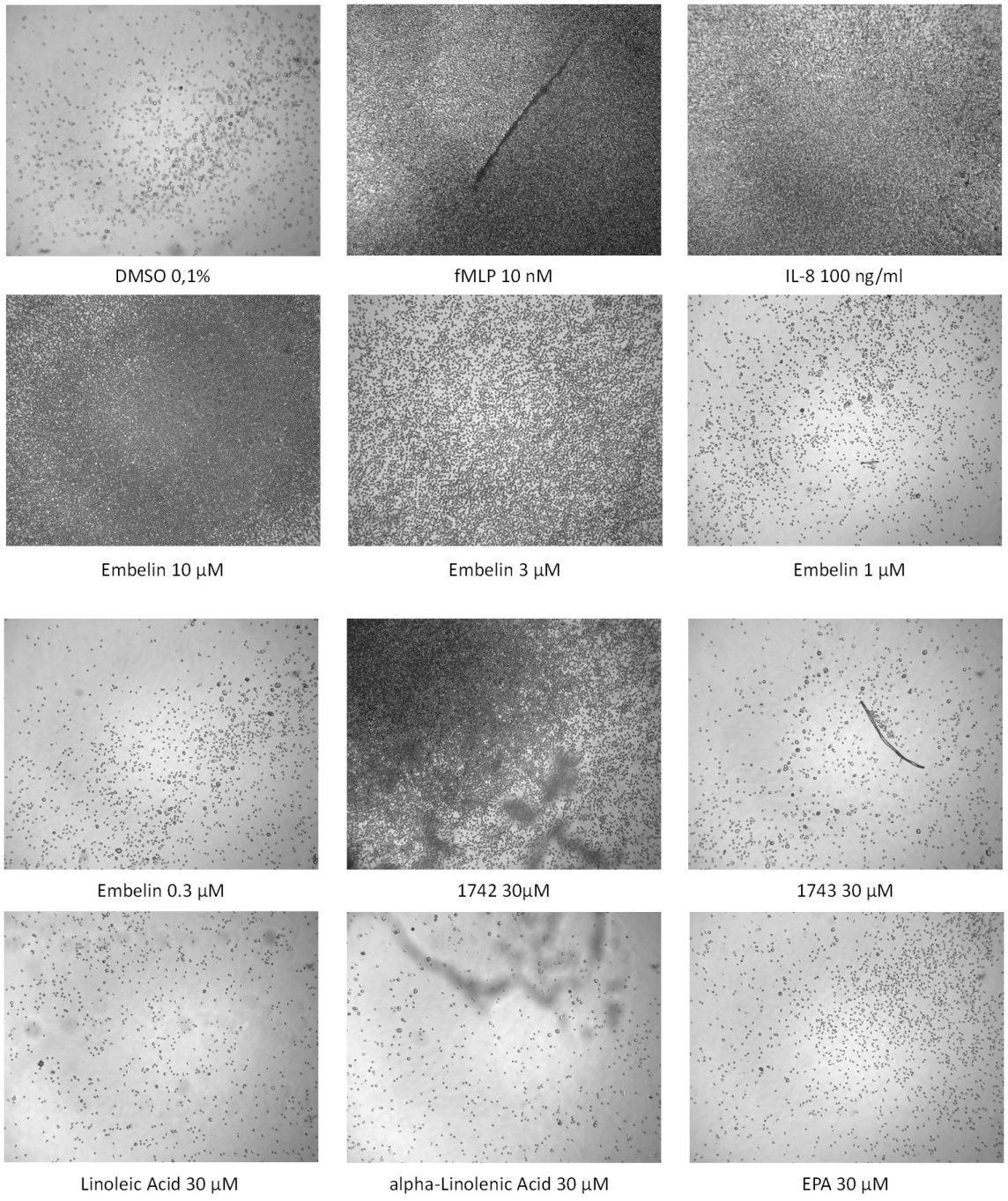

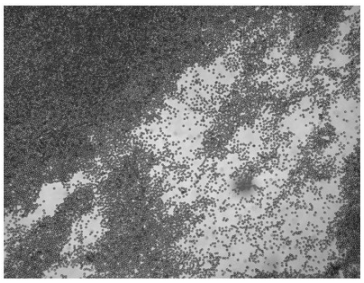

Figure 60: Pictures of the well bottoms of the migration assay from the 20.12.2023. Pictures show the successful migration of neutrophils. In this experiment, the negative control (DMSO) and the positive controls (fMLP and IL-8) performed well, and Embelin exhibited concentration-dependent activity. Substance 1742 exhibited a promising chemotactic effect, whereas the other test substances (1743, LA, ALA, and EPA) exhibited no visible activity. Pictures were taken with the TECAN Spark by Dr. Alexander Perhal.

The migration worked especially well this time. Embelin was tested at several concentrations for the third time to obtain three biological replicates. DMSO again served as the negative control, and fMLP and IL-8 served as the positive controls.

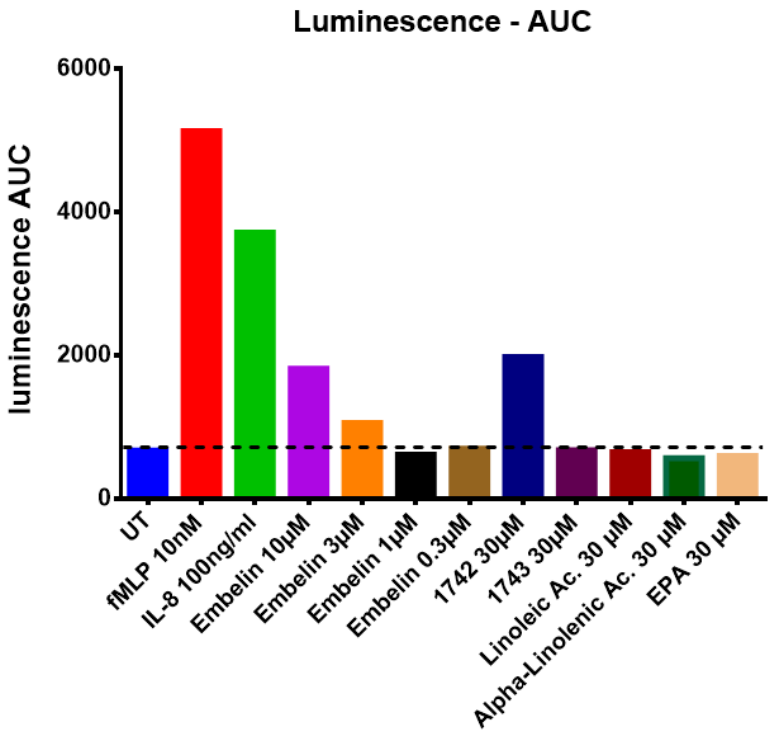

Figure 61: Results of the luminol oxidation assay from the 20.12.2023. After the neutrophil migration assay, an aliquot of migrated cells was treated with luminol and fMLP to induce neutrophil degranulation. The released mediators oxidized the luminol, and the emitted light was measured. The x-axis shows the name of the tested well, and the y-axis shows the corresponding luminescence area under the curve (AUC). For embelin, a relatively good concentration-dependent effect was visible. Of the tested substances, only 1742 exhibited activity with an AUC greater than that of the negative control (DMSO). Figure was made in GraphPad Prism

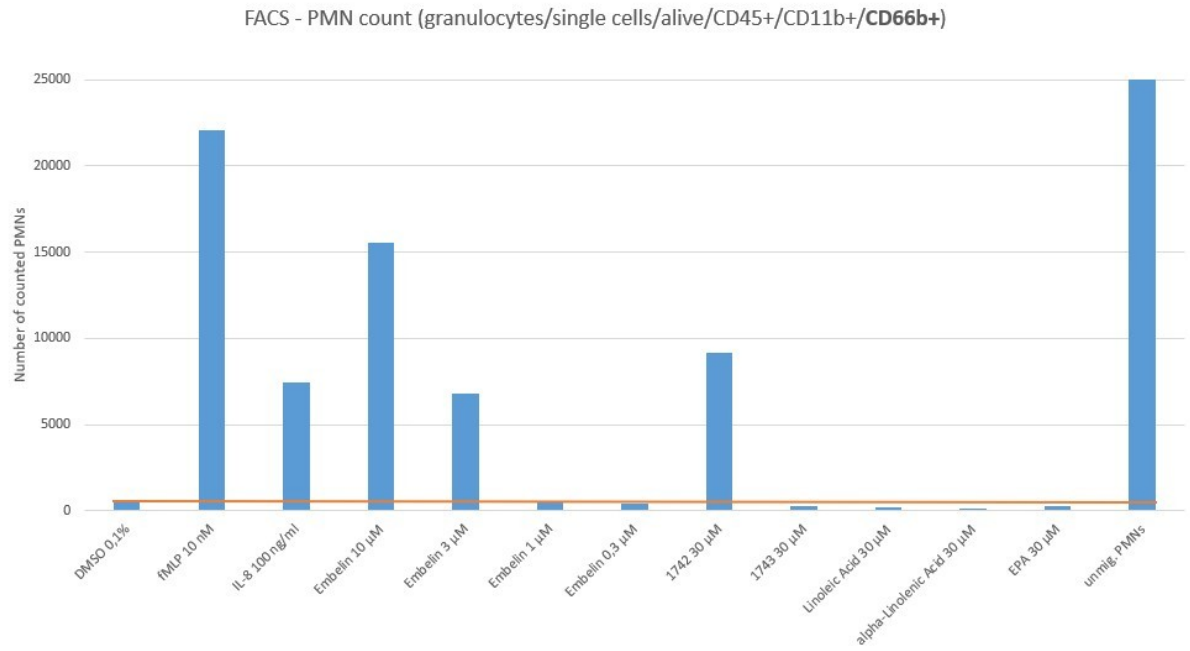

Figure 62: Results of the FACS - PMN measurement from the 20.12.2023. The migrated cells were counted with the FACS-gating: granulocytes/single cells/alive/CD45+/CD11b+/CD66b+. The x-axis shows the names of the tested wells, and the y-axis shows the corresponding FACS counts. The bars are limited to 25,000 counted cells to make them more comparable in the figure. Embelin exhibited a concentration-dependent effect, with Embelin at 10 µM demonstrating higher activity than the second positive control (IL-8). Of all the substances tested, only 1,742 showed positive activity (higher than Embelin at 3 µM). Figure was made in Excel

Both analysis methods produced comparable results this time, except for IL-8, which was much more effective according to the luminescence oxidation assay (Figure 61) than the FACS count (Figure 62). The pictures taken matched the results of the FACS count and the luminescence oxidation assay (Figure 60). The results again showed good chemotactic effects for substance 1742, while almost no effect was visible for the other tested substances (1743, LA, ALA, and EPA). Embelin again demonstrated a concentration-dependent effect.

4.3.4 Migration assay performed on 17.01.2024

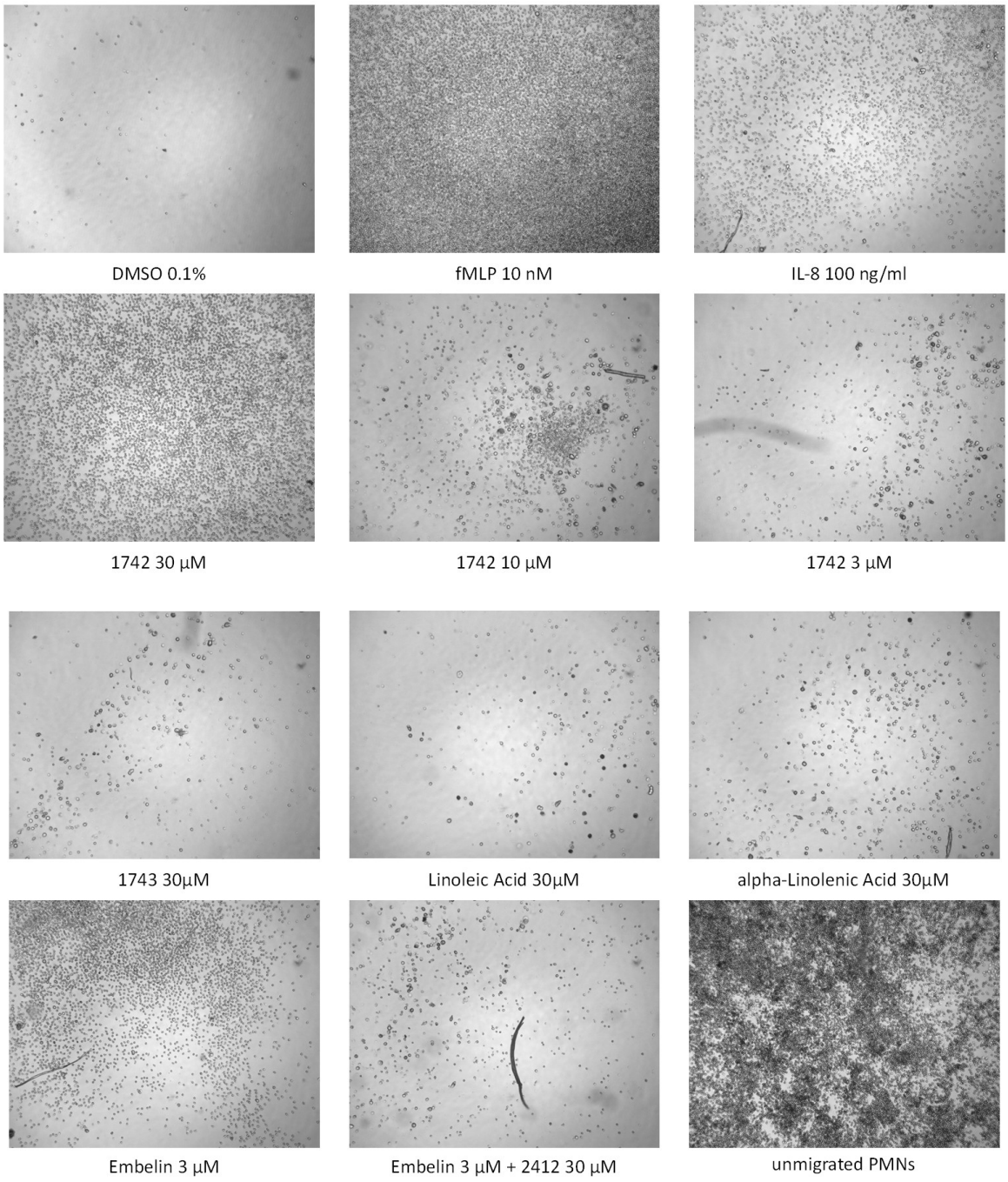

Figure 63: Pictures of the well bottoms of the migration assay from the 17.01.2024. Pictures show migrated neutrophils. DMSO served as the negative control, and fMLP and IL-8 served as the positive controls. Substance 1742 was tested at different concentrations, showing concentration-dependent activity. Substances 1743, LA, and ALA showed almost no activity. Embelin at 3 µM was compared to Embelin at 3 µM co-treated with 2412 as a potential antagonist. The number of migrated neutrophils was reduced by substance 2412, confirming its antagonistic activity. Pictures were taken with the TECAN Spark by Dr. Alexander Perhal.

Since three replicates of several Embelin concentrations were already available, different 1742 concentrations were tested instead this time. This experiment involved the first test of a potential antagonist in the neutrophil migration assay. Therefore, the agonistic effect of Embelin 3 µM was compared to Embelin in combination with compound 2412 (imbricaric acid). As can be seen in the pictures, Embelin co-treated with 2412 had fewer migrated neutrophils than Embelin alone (Figure 63, wells 10 and 11). This suggests that the antagonization of Embelin by 2412 may have worked in this assay.

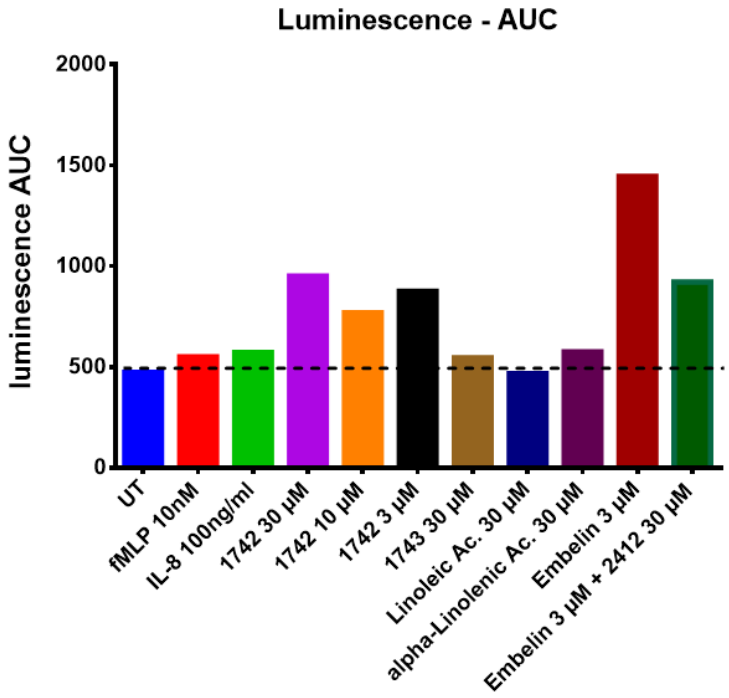

Figure 64: Results of the luminol oxidation assay from the 17.01.2024. After the neutrophil migration assay, an aliquot of migrated cells was treated with luminol and fMLP to induce neutrophil degranulation. The released mediators oxidized the luminol, and the emitted light was measured. The x-axis shows the name of each tested well, and the y-axis shows the corresponding luminescence area under the curve (AUC). In the luminol oxidation assay, the positive controls (fMLP and IL-8) exhibited minimal activity. Several concentrations of 1742 were tested, but concentration-dependent activity was barely visible. Embelin at 3 µM was compared to Embelin at 3 µM co-treated with 2412 as a potential antagonist. The number of migrated neutrophils was reduced by substance 2412, confirming its antagonistic activity. Figure was made in GraphPad Prism

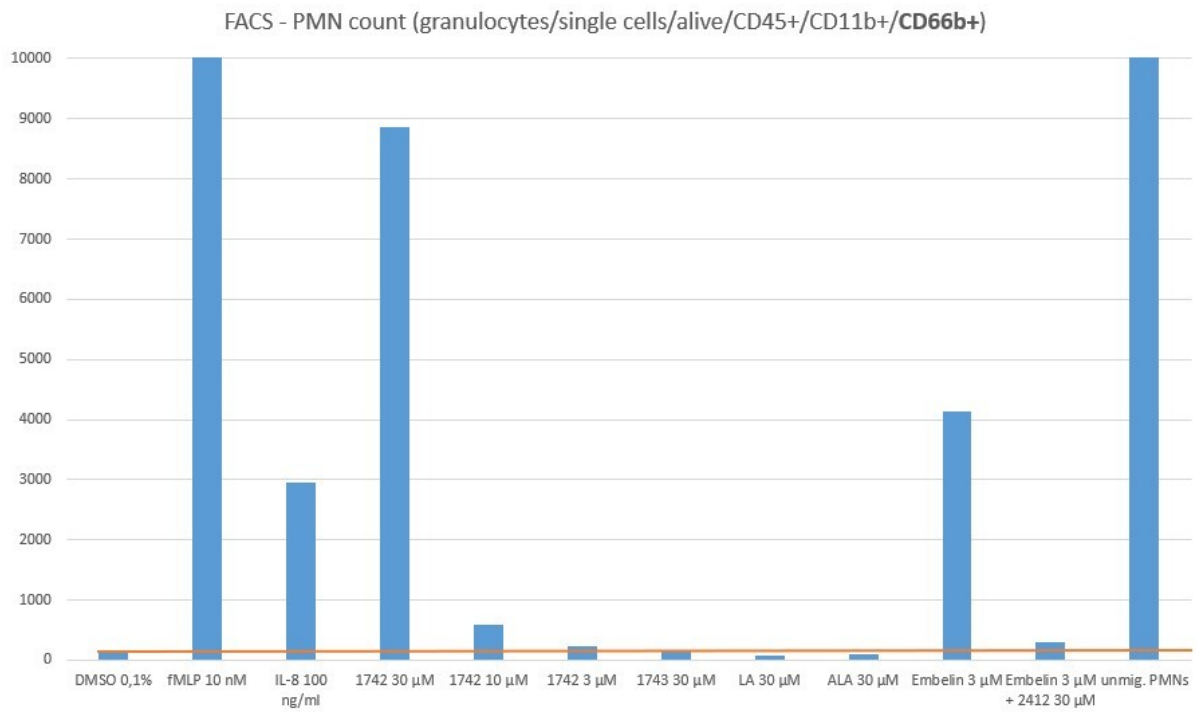

Figure 65: Results of the FACS - PMN measurement from the 17.01.2024 The migrated cells were counted with the FACS-gating: granulocytes/single cells/alive/CD45+/CD11b+/CD66b+. The x-axis shows the names of the tested wells, and the y-axis shows the corresponding FACS counts. The bars are limited to 10,000 counted cells to make them more comparable in the figure. Several concentrations of 1742 were tested, but concentrations lower than 30 µM exhibited significantly reduced activity. Embelin at a concentration of 3 µM was compared to Embelin at a concentration of 3 µM co-treated with 2412 as a potential antagonist. The number of migrated neutrophils was reduced by substance 2412, confirming its antagonistic activity. Figure was made in Excel

This time, the positive controls (fMLP and IL-8) did not work at all in the luminol oxidation assay, which calls its significance into question (Figure 64). The different concentrations of 1742 also hardly showed a concentration-dependent effect. The other substances (1743, LA, and ALA) exhibited no chemotactic activity. However, antagonization by 2412 of Embelin was visible in both the luminol oxidation assay and the FACS results (Figure 65). FACS counting showed that the positive control, fMLP, worked normally; only IL-8 was less effective. The concentration dependency of 1742 was more apparent than in the luminol oxidation assay, but the other substances (1743, LA, and ALA) showed no effect.

4.3.5 Migration assay performed on 26.01.2024

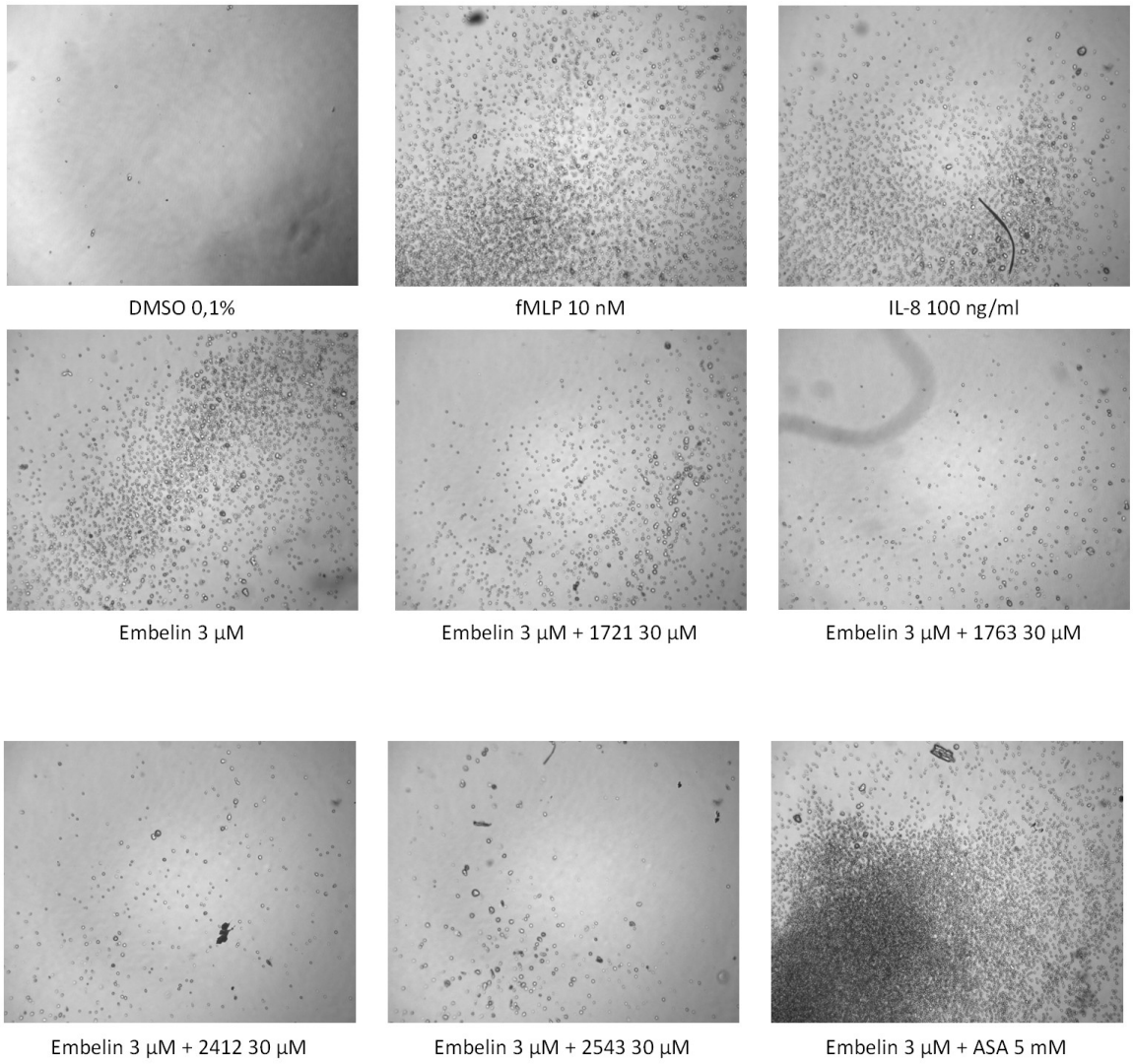

Figure 66: Pictures of the well bottoms of the migration assay from the 26.01.2024. Pictures show migrated neutrophils. DMSO served as the negative control, while fMLP and IL-8 served as the positive controls. Embelin at a concentration of 3 µM was co-treated with potential antagonists (substances 1721, 1763, 2412, and 2543), as well as with acetylsalicylic acid. Compared to Embelin alone, all four potential antagonists showed reduced numbers of migrated neutrophils in their co-treatment. ASA increased the number of migrated neutrophils. Pictures were taken with the TECAN Spark by Dr. Alexander Perhal.

In the most recent migration assay, the four most promising antagonistic candidates identified in the EPAC assay were tested alongside other interesting compounds, such as 5 mM acetyl salicylic acid in combination with 3 µM Embelin. Of the four antagonists tested (1721, 1763, 2412, and 2543), those co-treated with Embelin exhibited reduced migrated neutrophils compared to Embelin (3 µM) alone, as observed in Figure 66. This led us to assume that all four substances antagonized Embelin's chemotactic effect. However, ASA (5 mM) in

combination with Embelin exhibited a high number of migrated cells. Due to technical issues, quantification by luminol oxidation assay or FACS counting was not possible. Only pictures were taken as semi-quantitative results of this migration assay.

4.3.6 Summarized results of relevant substances

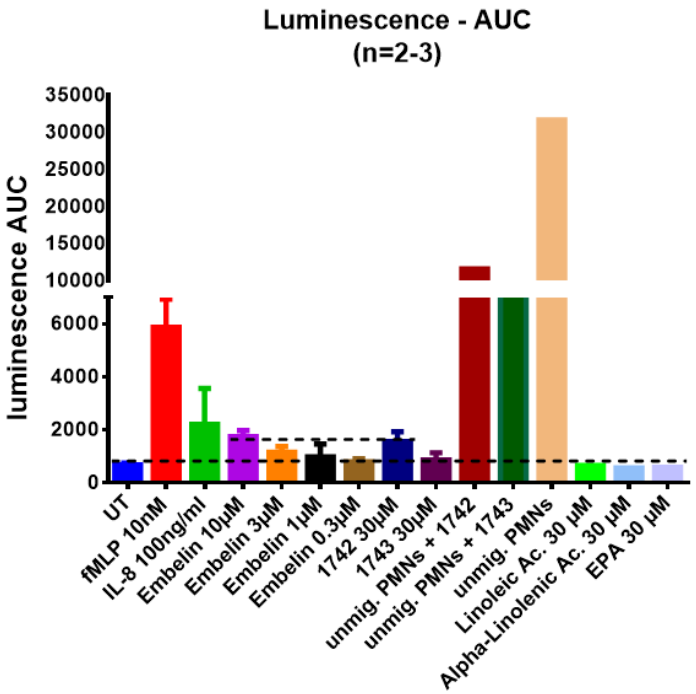

Figure 55 Summary of the data of the luminol oxidation assays. When tested at different concentrations, Embelin exhibited concentration-dependent activity. The effect of 1742 was comparable to that of Embelin at 10 µM, while the other test substances (1743, LA, ALA, and EPA) showed almost no effect. Co-treating with 1742 and 1743 led to reduced numbers of unmigrated PMNs. Figure was made in GraphPad Prism

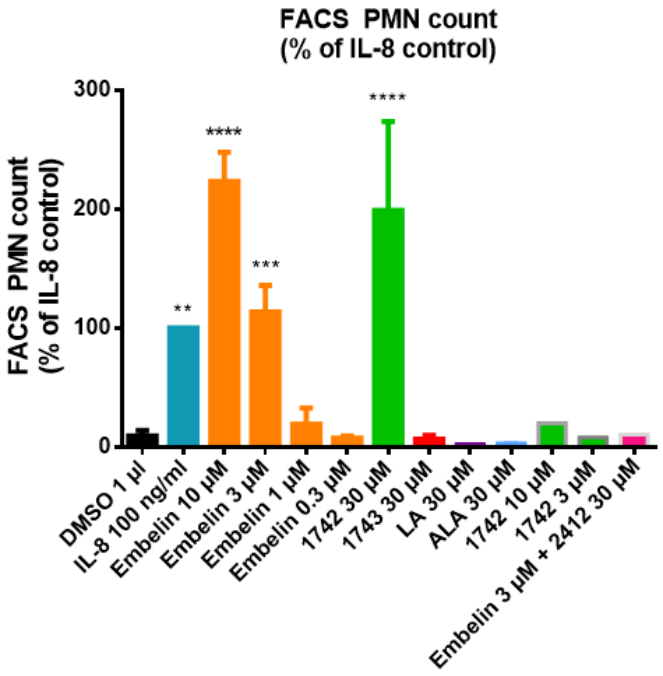

Figure 56 Summary of the data of the FACS – PMN measurements. This figure summarizes the concentration-dependent effects of embelin at different concentrations. At a concentration of 30 µM, 1742 showed a promising effect in the migration assay. An activity was also visible at 10 µM, but it was greatly reduced. The other substances (1743, LA, and ALA) were ineffective in the migration assay. Co-treating with 2412 and Embelin at a concentration of 3 µM resulted in a reduced number of migrated neutrophils compared to Embelin at a concentration of 3 µM alone. Figure was made in GraphPad Prism

Figures 67 and 68 summarize the data on the most relevant substances tested: 1742 (9-Oxo-ODE), 1743 (9-HODE), LA, ALA, and the potential antagonist 2412 (imbricaric acid). The results from the EPAC assay prove that 9-Oxo-ODE (1742) has agonistic effects on the GPR84 receptor and induces neutrophil granulocyte migration. However, related substances, such as 9-HODE (1743), LA, and ALA, did not cause enhanced neutrophil migration. The antagonistic effect of substance 2412 (imbricaric acid) seems promising, but more repeats of the migration assay are necessary to confirm this, which was not possible during the course of this thesis.

5 Discussion

5.1 General discussion

The project aimed to screen a large collection of compounds to identify those with agonistic or antagonistic activity on the GRP84 receptor. A neutrophil migration assay was performed on positively screened compounds to confirm their agonistic or antagonistic effect. Interestingly, several substances exhibited notable activity in the EPAC assay, and some of these substances were verified as agonists/antagonists using the migration assay. The OXLAM substance group, which includes 9-HODE and 9-Oxo-ODE, stood out in multiple rounds of the EPAC assay, as did other linoleic acid-related compounds. This is interesting because other researchers, such as Wang et al., found that long-chain fatty acids, including LA and ALA, had no visible effect on the GRP84 receptor in their experiments[11]. Our results showed effects that are somehow opposing to those reported. According to Ramsden et al., OXLAMs are associated with diseases such as Alzheimer's dementia, non-alcoholic steatohepatitis (NASH), and the pathogenesis of atherosclerosis, which are all inflammatory illnesses[24]. The observed effects of the tested OXLAMs, especially 9-oxo-ODE, suggest that the GPR84 receptor may be involved in inflammatory processes. According to Puengel et al., GPR84 plays an important role in the pathogenesis of non-alcoholic steatohepatitis, and antagonists of GPR84 could be a promising therapeutic intervention for steatohepatitis and fibrosis[40]. Ohue-Kitano et al.'s study also proved the connection between nonalcoholic steatohepatitis (NASH) and the GPR84 receptor. However, the researchers claim that GPR84 has a protective effect, suppressing the overreaction of macrophages to lipotoxicity. In their experiments, they observed that GPR84-deficient mice on a high-fat diet had a higher progression of NASH than wild-type mice. They hypothesize that the receptor senses the increased intake of medium-chain fatty acids (MCFAs) and suppresses the toxicity induced by high-fat intake[9]. Perhaps the protective effect they observed is related to the recruitment of β-arrestins, which causes GPR84 to be downregulated with excessive activation[16,23].

Studies have also shown a correlation between the GPR84 receptor and the development of Alzheimer’s disease. Contrary to expectations, Audoy-Rémus et al. found that activation of the receptor decelerates dendritic degeneration[41]. Ieremias et al. suggested that GPR84 agonists might have therapeutic potential in treating Alzheimer’s disease and atherosclerosis[42]. Other researchers have also suggested that agonism at GPR84 is beneficial in combating atherosclerosis[8,43]. This leads to more questions, since atherosclerosis is an inflammatory disease[44] and GPR84 is considered a proinflammatory receptor[6]. Another

similarity between OXLAMs and GPR84 activation is that high OXLAM consumption leads to high NLRP3 inflammasome and caspase-1 activation[26]. Zhang et al. discovered that GPR84 modulates the pro-inflammatory function of macrophages by promoting the activation of the NLRP3 inflammasome. This pathway also causes the activation of caspase-1 and the release of several interleukins[1].

Many references support our finding that OXLAMs and the GPR84 receptor may be connected. Nonetheless, much more research is necessary to prove this assumption. Therefore, multiple experiments with adequate concentrations of 9-Oxo-ODE and 9-HODE in solvent should be performed. Additionally, testing the other OXLAM structures, such as 13-HODE and 13-Oxo-ODE, for possible GPR84-agonistic effects would be interesting. While further investigation is necessary, these results could help improve our understanding of the relevance of the GPR84 receptor, as well as the pro-inflammatory effects of linoleic acid and its oxidation products.

Although there was little time left to investigate other potentially antagonistic substances, the few experiments conducted with compounds 1721, 1763, 2412, and 2543 yielded promising results. In the migration assay, the combination of 2412 and Embelin was compared with Embelin alone to test the potential agonistic activity of 2412. Adding imbricaric acid clearly attenuated Embelin's agonistic effect. According to Oettl et al., imbricaric acid suppresses NF-κB activation, among other pathways[32]. As previously mentioned, the induction of GPR84 amplifies the inflammatory response in macrophages by promoting the phosphorylation of Akt and ERK, as well as the nuclear translocation of NF-κB. This leads to the upregulation of important inflammatory cytokines[19]. Consequently, the suppression of NF-κB activation through GPR84 antagonism may explain the anti-inflammatory effects of imbricaric acid. Pinoresinol (DNTI 1763) is also reported to suppress the p65 subunit of NF-κB, which may link it to GPR84 signaling. Furthermore, it has been proven to decrease the release of IL-1β, IL-6, TNF-α, and ROS[33–36]. Pinoresinol, as well as the other two substances (1721 and 2543), seemed to reduce the number of migrated neutrophils in the pictures taken. Unfortunately, quantification was not possible. Therefore, more experiments quantifying all substances are needed to collect more information about their relevance to this topic.

5.2 Limitations of the thesis

The thesis yielded interesting new insights into the nature of the GPR84 receptor. However, there are some factors that could make the data less reliable.

5.2.1 Testing substances

First, it is important to note that the DNTI project substances were old. Some were extracted 15 years before the experiments for this thesis were conducted. Although the stock solutions were frozen at -80°C, it is difficult to determine whether they still contain the original concentrations or if the substances have already undergone chemical transformation. Furthermore, most of the stock solutions were nearly depleted, so a structural analysis would not have been possible. In any case, the aim of the thesis was to conduct a broad screening rather than a detailed analysis of a few substances. Additionally, not all stock solutions had the same molar concentrations. Most compounds were dissolved in dimethyl sulfoxide (DMSO) at a concentration of 30 mM. However, some substances were dissolved in other solvents, such as ethanol, or had different concentrations, such as 20 mM, or values declared in milligrams per milliliter, which makes comparisons more difficult and unreliable. For this reason, 9-Oxo-ODE and 9-HODE were ordered to compare the results of the new substance with those of the DNTI project compound. However, testing the newly ordered substances was problematic due to their low concentration and the use of ethanol as a solvent. This means they didn't prove the effect of DNTI substances 1742 and 1743.

5.2.2 EPAC assay

Overall, the EPAC assay performed well, but there were a few issues with finding the right measurement settings on the TECAN Spark. First, an initial incubation time of 30 minutes for the prepared well plates was attempted. This means that the photometer waits the set time before measuring the plate. A previous project with TGR5-transfected cells yielded good results with this incubation step; however, with GPR84 cells, the values exhibited significant variability. It appeared that a long waiting time affected the cAMP levels under these assay conditions. Consequently, the incubation step was removed, which led to deviations only for

the first few measurements in the first row of the well plate. To ensure this wouldn't affect the evaluation, the first value of each measurement was excluded.

Initially, full 96-well plates were analyzed, but the results suggested that the long measurement time (approximately one hour per plate) affected the second half of the plate due to the extended waiting period. To counteract this, half-filled plates were analyzed from that point on. Although the results improved with this adaptation, only biological duplicates of each compound were obtained. For environmental and economic reasons, the method was adapted once more. Full 96-well plates were seeded again, but measured in two steps. When removed from the incubator, rows A–D were treated with substances and prepared for measurement, while rows E–H remained filled with 1x FURA buffer to ensure cell survival. After analyzing row A-D (which took around half an hour), the second step began and rows E-H were treated with substances for measurement. This adaptation worked well because all treated cells were measured within half an hour, and the well plates were also saved.
One trial was conducted with the direct injection of forskolin into each well before measurement, but it was unsuccessful.
In summary, no ideal measuring method was found, but with a few adaptations and limitations, the original method worked for this thesis.

5.2.3 Neutrophil Migration assay

First, it is important to note that the migration assay is unreliable and prone to error. Two of the seven trials did not work properly, and one more trial could not be quantified due to technical problems with the FACS machine. In conclusion, only four of the seven experiments could be evaluated, but the results were good and convincing. Retrospectively, it would have been better to always extract neutrophils from the same donor person. This would have reduced interpersonal variability and potentially made the data more comparable. Nevertheless, the experiments produced interesting results that warrant further investigation. Unfortunately, a lot of data is still missing due to time constraints and technical issues with this thesis.
Testing some possible antagonists in the migration assay was interesting, but it was more of a shot in the dark because a comparable positive control was missing. Despite extensive research, we were unable to find a working, proven antagonist of GRP84 that could be ordered as a positive control for our testing substances, such as imbricaric acid (DNTI 2412).

5.3 Conclusion

This thesis tested many substances for their effects on the GPR84 receptor. The results showed that the OXLAM compounds 9-HODE and 9-OxoODE, as well as related structures, had agonistic effects on the target receptor. This finding contrasts with the observations of other researchers. These results suggest that the effects of oxidized linoleic acid metabolites may occur via GPR84. While some references support the idea that OXLAMs are connected to the GPR84 receptor, inconsistencies remain in the literature. Some investigators have reported observing beneficial effects of GPR84 activation, including anti-inflammatory activities. Therefore, more research is necessary to prove our hypothesis and learn more about the pathophysiological purpose of this orphan receptor.

Additionally, potential antagonistic substances were identified during this project. Imbricaric acid and Pinoresinol were found to have promising inhibitory activity at GPR84. Both compounds have previously been reported to have anti-inflammatory effects, so an interaction with the target receptor is plausible. To determine whether these natural products could be used for therapeutic purposes, more information needs to be collected.

6 Appendix

6.1 List of screened substances

Table 4: List of screened substances

DNTI Number	IUPAC Name	Trivial name	GPR84 agonistic activity in the screening	GPR84 antagonistic activity in the screening
640			141% (raw) 83,4% (related to Forskolin)	101,8% (related to Embelin) 78,6% (related to Forskolin)
641	5-[(2E)-3,7-dimethylocta-2,6-dienoxy]-7-methoxychromen-2-one	5-Geranyloxy-7-methoxycoumarin	178,9% (raw) 105,7% (related to Forskolin)	102,9% (related to Embelin) 79,4% (related to Forskolin)
693	4-hydroxy-5-[(E)-indol-3-ylidenemethyl]-1,3-dihydroimidazol-2-one	-	171,9% (raw) 101,6% (related to Forskolin)	96,2% (related to Embelin) 74,3% (related to Forskolin)
694	2-amino-9-(furan-2-ylmethyl)-1H-purin-6-one	-	175,4% (raw) 103,7% (related to Forskolin)	104,4% (related to Embelin) 80,7% (related to Forskolin)
695	8-[(3-aminophenyl)methylsulfanyl]-1,7-dihydropurin-6-one	-	172,1% (raw) 101,7% (related to Forskolin)	105% (related to Embelin) 81,1% (related to Forskolin)
696	ethyl 2-amino-6-benzyl-5,7-dihydro-4H-thieno[2,3-c]pyridine-3-carboxylate	Tinoridine	168,1% (raw) 99,4% (related to Forskolin)	112% (related to Embelin) 86,5% (related to Forskolin)
697	2-[3-[[4-[(3-nitroacridin-9-yl)amino]phenyl]sulfamoyl]propyl]guanidine	-	187,6% (raw) 110,8% (related to Forskolin)	121,4% (related to Embelin) 93,8% (related to Forskolin)
698	5-(2,5-dimethoxyphenyl)-N-(4-piperidin-1-ylsulfonylphenyl)-1,3,4-thiadiazol-2-amine	-	162,1% (raw) 95,8% (related to Forskolin)	107% (related to Embelin) 82,6% (related to Forskolin)
699	ethyl 4-[[4-amino-3-cyano-5-(3-nitrobenzoyl)thiophen-2-yl]amino]benzoate	-	156,3% (raw) 92,4% (related to Forskolin)	103,2% (related to Embelin) 79,7% (related to Forskolin)
700	2-amino-7-(2-phenylethyl)-3H-pteridin-4-one	-	146,8% (raw) 86,8%	95,2% (related to

			(related to Forskolin)	Embelin) 73,5% (related to Forskolin)
701	3-benzoyl-N-(4,6-diaminopyrimidin-5-yl)benzamide	-	155,1% (raw) 102,2% (related to Forskolin)	111,4% (related to Embelin) 73,5% (related to Forskolin)
702	6-pyridin-3-yl-1H-pteridine-2,4-dione	-	171,9% (raw) 113,3% (related to Forskolin)	130,7% (related to Embelin) 86,3% (related to Forskolin)
703	6-(4-hydroxy-3-methoxyphenyl)-1-methylpteridine-2,4-dione	-	163,6% (raw) 107,8% (related to Forskolin)	114,2% (related to Embelin) 75,4% (related to Forskolin)
704	4-(quinolin-3-ylmethylamino)benzenesulfonamide	-	165,4% (raw) 109% (related to Forskolin)	127,6% (related to Embelin) 84,2% (related to Forskolin)
705	2-hydroxy-5-(7-oxochromen-2-yl)-1H-pyrimidin-3-ium-6-one;4-methylbenzenesulfonate	-	150,3% (raw) 99,1% (related to Forskolin)	119,6% (related to Embelin) 79% (related to Forskolin)
706	4-[[2-[(E)-2-(4-methoxyphenyl)ethenyl]quinazolin-4-yl]amino]benzenesulfonamide	-	135,7% (raw) 89,4% (related to Forskolin)	122,5% (related to Embelin) 80,9% (related to Forskolin)
707	2-[[6-[(4-methoxyphenyl)methyl]-1,3-benzodioxol-5-yl]oxy]acetohydrazide	-	167,7% (raw) 110,5% (related to Forskolin)	143,4% (related to Embelin) 94,6% (related to Forskolin)
708	5-amino-2-[(5-phenyl-1,3,4-thiadiazol-2-yl)methyl]-4H-pyrazol-3-one	-	143,6% (raw) 94,6% (related to Forskolin)	116,4% (related to Embelin) 76,9% (related to Forskolin
709	N-methyl-9-(methylcarbamoylamino)imidazo[4,5-f]quinoline-3-carboxamide	-	144,2% (raw) 95% (related to Forskolin)	113,5% (related to Embelin) 75% (related to Forskolin)
710	(E)-1-phenyl-3-[(5-phenyl-1,2,4-oxadiazol-3-yl)amino]but-2-en-1-one	-	142,5% (raw) 93,9% (related to Forskolin)	115,4% (related to Embelin) 76,2% (related to Forskolin)
711	4-(4-imidazol-1-ylbenzoyl)-5-methyl-1,3-dihydroimidazol-2-one	-	151,3% (raw) 98,4% (related to Forskolin)	111,9% (related to Embelin) 73,2% (related to Forskolin)
712	N-(4,6-dimethylpyrimidin-2-yl)-4-[[4-(3-nitrophenyl)-1,3-thiazol-2-yl]amino]benzenesulfonamide	-	168% (raw) 109,3% (related to Forskolin)	151,8% (related to Embelin) 99,3% (related to Forskolin)
727	2-(2-hydroxy-5-prop-2-enylphenyl)-4-prop-2-enylphenol	Magnolol	155,2% (raw) 100,9% (related to	117,9% (related to Embelin) 77,2% (related

			Forskolin)	to Forskolin)
730	2-(2-hydroxy-3-methoxy-5-propyl-phenyl)-6-methoxy-4-propyl-phenol	Tetrahydrodieugenol	154,3% (raw) 100,3% (related to Forskolin)	120,1% (related to Embelin) 78,6% (related to Forskolin)
753	2-(2-hydroxy-5-propyl-phenyl)-4-propyl-phenol	-	159,1% (raw) 103,4% (related to Forskolin)	123,7% (related to Embelin) 81% (related to Forskolin)
754	2-amino-6-(4-methoxy-3-propyl-phenyl)-4-propyl-phenol	-	172,2% (raw) 111,9% (related to Forskolin)	147,6% (related to Embelin) 96,6% (related to Forskolin)
755			155,6% (raw) 101,1% (related to Forskolin)	135% (related to Embelin) 88,4% (related to Forskolin)
756			148,3% (raw) 96,4% (related to Forskolin)	128,4% (related to Embelin) 84% (related to Forskolin)
757	N-[5-allyl-3-(3-allyl-4-hydroxy-phenyl)-2-hydroxy-phenyl]acetamide	-	167,7% (raw) 109,1% (related to Forskolin)	143,3% (related to Embelin) 93,8% (related to Forskolin)
758	4,4-diallyl-1-methoxy-2-phenyl-cyclohexa-2,5-dien-1-ol	-	160,9% (raw) 104,6% (related to Forskolin)	133,6% (related to Embelin) 87,4% (related to Forskolin)
759	3,3-diallyl-6,6-dimethoxy-1-phenyl-cyclohexa-1,4-diene	-	160,4% (raw) 101,9% (related to Forskolin)	126,2% (related to Embelin) 81,4% (related to Forskolin)
760	2,4-bis(2-hydroxyethyl)-3-methoxy-6-phenyl-phenol	-	169% (raw) 107,3% (related to Forskolin)	128,2% (related to Embelin) 82,6% (related to Forskolin)
761	[4-allyl-2-(3-allyl-4-methoxy-phenyl)phenoxy]-tert-butyl-dimethyl-silane	-	153,4% (raw) 97,4% (related to Forskolin)	118,5% (related to Embelin) 76,4% (related to Forskolin)
763	3-methoxy-6-phenyl-2,4-dipropyl-phenol	-	153,7% (raw) 97,6% (related to Forskolin)	135,8% (related to Embelin) 87,5% (related to Forskolin)
764	2-allyl-4-(2-bromopropyl)-6-phenyl-benzene-1,3-diol	-	166,8% (raw) 105,9% (related to Forskolin)	132% (related to Embelin) 85,1% (related to Forskolin)
765	2,4-diallyl-3-ethoxy-6-phenyl-phenol	-	159% (raw) 100,9% (related to Forskolin)	137,3% (related to Embelin) 88,5% (related

				to Forskolin)
766	2-allyl-6-phenyl-phenol	-	172,5% (raw) 109,5% (related to Forskolin)	139,6% (related to Embelin) 90% (related to Forskolin)
767	2-allyl-4-phenyl-phenol	-	161% (raw) 102,2% (related to Forskolin)	133,5% (related to Embelin) 86% (related to Forskolin)
768	6,6-diallyl-2-phenyl-cyclohexa-2,4-diene-1,1-diol	-	165,9% (raw) 105,4% (related to Forskolin)	135,2% (related to Embelin) 87,2% (related to Forskolin)
769	2-allyl-4-(3-allyl-4-hydroxy-phenyl)phenol	-	169,8% (raw) 107,8% (related to Forskolin)	148,3% (related to Embelin) 95,6% (related to Forskolin)
770	2-allyl-6-[(3-allyl-2-hydroxy-phenyl)methyl]phenol	-	165,7% (raw) 108,5% (related to Forskolin)	125,6% (related to Embelin) 80% (related to Forskolin)
771	4,6-diallyl-6-amino-1-methoxy-2-phenyl-cyclohexa-2,4-dien-1-ol	-	157,9% (raw) 103,4% (related to Forskolin)	114,5% (related to Embelin) 72,9% (related to Forskolin)
772	[3-(3-allyl-4-methoxy-phenyl)-2-hydroxy-5-(2-hydroxypropyl)phenyl]azinic acid	-	166,2% (raw) 108,8% (related to Forskolin)	166,3% (related to Embelin) 105,9% (related to Forskolin)
773	1,3-diallyl-2,4-dipentoxy-5-phenyl-benzene	-	150,4% (raw) 98,5% (related to Forskolin)	118% (related to Embelin) 75,1% (related to Forskolin)
774	4,4-dimethyl-2-phenyl-cyclohexa-2,5-diene-1,1-diol	-	162,5% (raw) 106,4% (related to Forskolin)	123,5% (related to Embelin) 78,6% (related to Forskolin)
775			153,3% (raw) 100,3% (related to Forskolin)	116,3% (related to Embelin) 74,1% (related to Forskolin)
776	4-tert-butyl-2-(5-tert-butyl-2-hydroxy-phenyl)phenol	-	150,1% (raw) 98,3% (related to Forskolin)	129,4% (related to Embelin) 82,4% (related to Forskolin)
777	4-allyl-2-[4-methoxy-3-[(E)-prop-1-enyl]phenyl]phenol	-	155,3% (raw) 101,7% (related to Forskolin)	137,3% (related to Embelin) 87,4% (related to Forskolin)
778	3-[3-[3-(2,3-dihydroxypropyl)-4-methoxy-phenyl]-4-hydroxy-phenyl]propane-1,2-diol	-	140,7% (raw) 92,1% (related to Forskolin)	116% (related to Embelin) 73,8% (related

				to Forskolin)
779	2-allyl-4-(5-allyl-2-methoxy-phenyl)-1-methoxy-benzene	-	154,2% (raw) 100,9% (related to Forskolin)	112,5% (related to Embelin) 71,6% (related to Forskolin)
780	1-methoxy-2-(4-methoxy-3-propyl-phenyl)-4-propyl-benzene	-	148,3% (raw) 99,8% (related to Forskolin)	121,3% (related to Embelin) 75,2% (related to Forskolin)
783	5-allyl-3-(4-allylphenoxy)benzene-1,2-diol	-	130,5% (raw) 87,8% (related to Forskolin)	121,9% (related to Embelin) 75,6% (related to Forskolin)
793			148,2% (raw) 99,7% (related to Forskolin)	119% (related to Embelin) 73,8% (related to Forskolin)
795			155,8% (raw) 104,9% (related to Forskolin)	133,6% (related to Embelin) 82,8% (related to Forskolin)
799			151% (raw) 101,7% (related to Forskolin)	117,1% (related to Embelin) 72,6% (related to Forskolin)
800			165,2% (raw) 111,2% (related to Forskolin)	127,2% (related to Embelin) 78,8% (related to Forskolin)
801			149,3% (raw) 100,5% (related to Forskolin)	118,6% (related to Embelin) 73,6% (related to Forskolin)
802			167,6% (raw) 112,8% (related to Forskolin)	179% (related to Embelin) 111% (related to Forskolin)
803			165,7% (raw) 111,5% (related to Forskolin)	174,3% (related to Embelin) 108,1% (related to Forskolin)
804			155,4% (raw) 104,6% (related to Forskolin)	134,1% (related to Embelin) 83,1% (related to Forskolin)
805			163,6% (raw) 104,9% (related to Forskolin)	108,1% (related to Embelin) 75,3% (related to Forskolin)
806			169,6% (raw)	112% (related to

			108,8% (related to Forskolin)	Embelin) 78% (related to Forskolin)
807			169,5% (raw) 108,7% (related to Forskolin)	150,1% (related to Embelin) 104,6% (related to Forskolin)
808			160% (raw) 102,6% (related to Forskolin)	104,7% (related to Embelin) 72,9% (related to Forskolin)
850	4-[(2E)-3,7-dimethylocta-2,6-dienoxy]furo[3,2-g]chromen-7-one	Bergamottin	168,8% (raw) 108,2% (related to Forskolin)	109,3% (related to Embelin) 76,2% (related to Forskolin)
851	4-hydroxyfuro[3,2-g]chromen-7-one	Bergaptol	169,5% (raw) 108,7% (related to Forskolin)	102,8% (related to Embelin) 71,6% (related to Forskolin)
852	4-methoxyfuro[3,2-g]chromen-7-one	Bergapten	167% (raw) 107,1% (related to Forskolin)	104% (related to Embelin) 72,5% (related to Forskolin)
853	5-methoxyfuro[2,3-h]chromen-2-one	Isobergapten	144,5% (raw) 92,7% (related to Forskolin)	107,5% (related to Embelin) 74,9% (related to Forskolin)
854	9-(3-methylbut-2-enoxy)furo[3,2-g]chromen-7-one	Imperatorin	164,9% (raw) 105,7% (related to Forskolin)	138,4% (related to Embelin) 96,4% (related to Forskolin)
855	4,9-dimethoxyfuro[3,2-g]chromen-7-one	Isopimpinellin	153,8% (raw) 98,6% (related to Forskolin)	95% (related to Embelin) 66,2% (related to Forskolin)
856	7-hydroxychromen-2-one	Umbelliferone	163,2% (raw) 103,3% (related to Forskolin)	107,6% (related to Embelin) 70,3% (related to Forskolin)
857	7-hydroxy-6-methoxychromen-2-one	Scopoletine	-	-
931		Umbelliferone	182% (raw) 115,2% (related to Forskolin)	123,4% (related to Embelin) 80,7% (related to Forskolin)
964			154,7% (raw) 97,9% (related to Forskolin)	112,6% (related to Embelin) 73,6% (related to Forskolin)
965			150,3% (raw) 95,2% (related to Forskolin)	112% (related to Embelin) 73,2% (related

				to Forskolin)
966			155,3% (raw) 98,3% (related to Forskolin)	112,4% (related to Embelin) 73,5% (related to Forskolin)
967			156,9% (raw) 99,3% (related to Forskolin)	118,9% (related to Embelin) 77,7% (related to Forskolin)
968			166,2% (raw) 105,2% (related to Forskolin)	134,2% (related to Embelin) 87,8% (related to Forskolin)
969			164,8% (raw) 104,3% (related to Forskolin)	134,2% (related to Embelin) 87,7% (related to Forskolin)
992			139,6% (raw) 88,4% (related to Forskolin)	92,4% (related to Embelin) 60,4% (related to Forskolin)
1002	7-[(2E)-3,7-dimethylocta-2,6-dienoxy]chromen-2-one	Auraptene	169,5% (raw) 101,9% (related to Forskolin)	120,8% (related to Embelin) 73,7% (related to Forskolin)
1003	4-[(3,3-dimethyloxiran-2-yl)methoxy]furo[3,2-g]chromen-7-one	Oxypeucedanin	155,1% (raw) 93,3% (related to Forskolin)	125,7% (related to Embelin) 76,7% (related to Forskolin)
1004 (also 1044)	4-(3-methylbut-2-enoxy)furo[3,2-g]chromen-7-one	Isoimperatorin	156,7% (raw) 94,2% (related to Forskolin)	128,3% (related to Embelin) 78,2% (related to Forskolin)
1005	9-[[(2R)-3,3-dimethyloxiran-2-yl]methoxy]furo[3,2-g]chromen-7-one	Heraclenin	178,4% (raw) 107,3% (related to Forskolin)	155,8% (related to Embelin) 95% (related to Forskolin)
1006			179,2% (raw) 107,7% (related to Forskolin)	148,8% (related to Embelin) 90,7% (related to Forskolin)
1007	7,2',4'-Trihydroxy-8-lavandulyl-5-methoxyflavanone	Kurarinone	180% (raw) 108,2% (related to Forskolin)	145,1% (related to Embelin) 88,5% (related to Forskolin)
1009	9-[(2R)-2,3-dihydroxy-3-methylbutoxy]-4-methoxyfuro[3,2-g]chromen-7-one	Byakangelicin	171,5% (raw) 103,1% (related to Forskolin)	121,9% (related to Embelin) 74,3% (related to Forskolin)
1022	benzene-1,3,5-triol	Phloroglucinol	153,2% (raw) 92,1%	117,1% (related to

			(related to Forskolin)	Embelin) 71,4% (related to Forskolin)
1045	[(E)-1-(5-hydroxyhept-6-en-1,3-diynyl)non-2-enyl] acetate	-	103,6% (raw) 62,3% (related to Forskolin)	102% (related to Embelin) 62,2% (related to Forskolin)
1046	(8S)-8-prop-1-en-2-yl-8,9-dihydrofuro[2,3-h]chromen-2-one	Angenomalin	145,4% (raw) 103,5% (related to Forskolin)	129,8% (related to Embelin) 90,3% (related to Forskolin)
1047			146,6% (raw) 104,3% (related to Forskolin)	135,6% (related to Embelin) 94,3% (related to Forskolin)
1048			99,4% (raw) 70,7% (related to Forskolin)	100% (related to Embelin) 69,6% (related to Forskolin)
1073	[(2R)-3-hydroxy-3-methyl-1-(7-oxofuro[3,2-g]chromen-4-yl)oxybutan-2-yl] (Z)-2-methylbut-2-enoate	Ostruthol	124,2% (raw) 88,3% (related to Forskolin)	111,6% (related to Embelin) 77,7% (related to Forskolin)
1079	(2S)-2-[3-[(1S,5R,6S)-6-(2,4-dihydroxybenzoyl)-5-(2,4-dihydroxyphenyl)-3-methyl-cyclohex-2-en-1-yl]-2,4-dihydroxy-phenyl]-5,7-dihydroxy-chroman-4-one	Kuwanon L	153,9% (raw) 109,5% (related to Forskolin)	149,4% (related to Embelin) 104% (related to Forskolin)
1081	5-[(6R)-6-hydroxy-7,7-dimethyl-5,6-dihydrofuro[3,2-g]chromen-2-yl]benzene-1,3-diol & 5-[(2R)-2-(1-hydroxy-1-methyl-ethyl)-2,3-dihydrofuro[3,2-f]benzofuran-6-yl]benzene-1,3-diol	Moracin O & Moracin P	153,7% (raw) 109,3% (related to Forskolin)	130,2% (related to Embelin) 90,6% (related to Forskolin)
1082	1,3,8,10a-tetrahydroxy-2-(5-hydroxy-9-methyl-8-oxatricyclo[7.3.1.02,7]trideca-2(7),3,5,10-tetraen-11-yl) -5a-(3-methylbut-2-enyl)benzofuro[3,2-b]chromen-11-one	Saggenon B	145,8% (raw) 103,7% (related to Forskolin)	135,5% (related to Embelin) 94,3% (related to Forskolin)
1088	5,7-dihydroxy-3-(4-methoxyphenyl)chromen-4-one	Biochanin A	150,3% (raw) 106,9% (related to Forskolin)	146% (related to Embelin) 101,6% (related to Forskolin)
1089	5,7-dihydroxy-3-(4-methoxyphenyl)-2,3-dihydrochromen-4-one	Dihydrobiochanin A	143,2% (raw) 101,8% (related to Forskolin)	120,1% (related to Embelin) 83,6% (related to Forskolin)
1091	[(1S,4aS,5R,7S,7aS)-4a,5-dihydroxy-7-methyl-1-[(2S,3R,4S,5S,6R)-3,4,5-trihydroxy-6-(hydroxymethyl)tetrahydropyran-2-yl]oxy-1,5,6,7a-	8-O-Acetyl Harpagoside	137,9% (raw) 98,1% (related to Forskolin)	104,9% (related to Embelin) 73% (related to Forskolin)

	tetrahydrocyclopenta[c]pyran-7-yl] acetate			
1094	2-(2,4-dichlorophenoxy)-N-(3-fluoro-4-methyl-phenyl)propanamide	-	143,3% (raw) 102,2% (related to Forskolin)	119,9% (related to Embelin) 81,1% (related to Forskolin)
1096	2-(2,4-dichlorophenoxy)-N-(3,4-difluorophenyl)propanamide	-	143,9% (raw) 102,6% (related to Forskolin)	118,4% (related to Embelin) 80,1% (related to Forskolin)
1097	N-(3-hydroxy-4-methyl-phenyl)-2-(4-methylphenoxy)propanamide	-	143,7% (raw) 102,5% (related to Forskolin)	132,9% (related to Embelin) 89,9% (related to Forskolin)
1098	3-{[(3-iodo-4-methylphenyl)imino]methyl}-1,2-benzenediol	-	129,1% (raw) 92% (related to Forskolin)	116% (related to Embelin) 78,5% (related to Forskolin)
1099	3-{[(4-ethoxyphenyl)imino]methyl}-1,2-benzenediol	-	105,7% (raw) 75,4% (related to Forskolin)	112% (related to Embelin) 75,7% (related to Forskolin)
1100	N-(4-fluorobenzyl)-N-[2-(trifluoromethyl)benzyl]amine	-	145% (raw) 103,4% (related to Forskolin)	141,2% (related to Embelin) 95,5% (related to Forskolin)
1101	2-(4-methylphenoxy)-N-[3-(methylsulfanyl)phenyl]propanamide	-	148,2% (raw) 105,7% (related to Forskolin)	125,2% (related to Embelin) 84,7% (related to Forskolin)
1102	5-bromo-2-methoxy-N-[2-(trifluoromethyl)phenyl]benzenesulfonamide	-	137,4% (raw) 97,9% (related to Forskolin)	124% (related to Embelin) 83,9% (related to Forskolin)
1103	N-[(5-bromo-2-pyridyl)carbamothioyl]-2,6-dimethoxy-benzamide	-	134,2% (raw) 95,7% (related to Forskolin)	132,8% (related to Embelin) 89,8% (related to Forskolin)
1140			136,6% (raw) 97,4% (related to Forskolin)	113,2% (related to Embelin) 76,6% (related to Forskolin)
1141	Methyl 2,4-dihydroxy-3,6-dimethylbenzoate	-	154,8% (raw) 103,8% (related to Forskolin)	104,8% (related to Embelin) 74,1% (related to Forskolin)
1142	(3-hydroxy-4-methoxycarbonyl-2,5-dimethylphenyl) 3-formyl-2,4-dihydroxy-6-methylbenzoate	Atranorin	153,9% (raw) 103,2% (related to Forskolin)	107,5% (related to Embelin) 76% (related to Forskolin)
1143	4-[[(E)-3-carboxyprop-2-enoyl]oxymethyl]-10-	Fumarprotocetraric	155,7% (raw)	111,1% (related to

	formyl-3,9-dihydroxy-1,7-dimethyl-6-oxo-benzo[b][1,4]benzodioxepine-2-carboxylic acid	acid	104,4% (related to Forskolin)	Embelin) 78,5% (related to Forskolin)
1144	5,18-dihydroxy-7-methyl-2,10,15-trioxatetracyclo[9.7.0.03,8.013,17]octadeca-1(11),3(8),4,6,12,17-hexaene-9,16-dione	Variolaric acid	160,4% (raw) 107,5% (related to Forskolin)	123% (related to Embelin) 86,9% (related to Forskolin)
1145	4-[2,4-dihydroxy-6-(2-oxoheptyl)benzoyl]oxy-2-hydroxy-6-pentylbenzoic acid	Olivetoric acid	165,5% (raw) 111% (related to Forskolin)	156,8% (related to Embelin) 110,8% (related to Forskolin)
1146	5,13,17-trihydroxy-12-(hydroxymethyl)-7-methyl-9,15-dioxo-2,10,16-trioxatetracyclo[9.7.0.03,8.014,18]octadeca-1(11),3(8),4,6,12,14(18)-hexaene-4-carbaldehyde	Salazinic acid	153,2% (raw) 102,7% (related to Forskolin)	110,8% (related to Embelin) 78,3% (related to Forskolin)
1147	2-hydroxy-4-(2-hydroxy-4-methoxy-6-pentylbenzoyl)oxy-6-pentylbenzoic acid	Perlatolinic acid	156,7% (raw) 105% (related to Forskolin)	111,7% (related to Embelin) 79% (related to Forskolin)
1148	2-hydroxy-4-(2-hydroxy-4-methoxy-6-methylbenzoyl)oxy-6-methylbenzoic acid	Evernic acid	162% (raw) 108,6% (related to Forskolin)	125,4% (related to Embelin) 88,6% (related to Forskolin)
1150	2,8-dichloro-3,9-dimethoxy-1,7-dimethylbenzo[b][1,4]benzodioxepin-6-one	Scensidin	153,6% (raw) 102,9% (related to Forskolin)	117,1% (related to Embelin) 82,8% (related to Forskolin)
1151			150,8% (raw) 101,1% (related to Forskolin)	105,9% (related to Embelin) 74,8% (related to Forskolin)
1152			148,4% (raw) 101,7% (related to Forskolin)	120,5% (related to Embelin) 84,1% (related to Forskolin)
1153			151,4% (raw) 103,7% (related to Forskolin)	108,9% (related to Embelin) 76% (related to Forskolin)
1154			154,8% (raw) 106,1% (related to Forskolin)	123,6% (related to Embelin) 86,2% (related to Forskolin)
1155			154,8% (raw) 106% (related to Forskolin)	114,7% (related to Embelin) 80% (related to Forskolin)
1213 & 1228	N-(4-fluorophenyl)-2-methoxy-5-methylbenzenesulfonamide	-	153,8% (raw) 105,4% (related to Forskolin)	113,1% (related to Embelin) 78,9% (related to Forskolin)

1214 & 1229	5-ethyl-N-(4-fluorophenyl)-2-methoxybenzene-1-sulfonamide	-	146,9% (raw) 100,7% (related to Forskolin)	129% (related to Embelin) 90% (related to Forskolin)
1215 & 1230	N-(2-hydroxyphenyl)-5-isopropyl-2-methoxybenzenesulfonamide	-	154,4% (raw) 105,8% (related to Forskolin)	120,7% (related to Embelin) 84,2% (related to Forskolin)
1216 & 1231	N-(2-ethoxyphenyl)-5-isopropyl-2-methoxybenzenesulfonamide	-	156,7% (raw) 107,4% (related to Forskolin)	122% (related to Embelin) 85,1% (related to Forskolin)
1217 & 1232	N-(2-hydroxyphenyl)-2-methoxy-5-methyl-benzenesulfonamide	-	154% (raw) 105,5% (related to Forskolin)	131,4% (related to Embelin) 91,7% (related to Forskolin)
1218 & 1233	N-(2-hydroxyphenyl)-2,5-dimethoxybenzenesulfonamide	-	147,4% (raw) 101% (related to Forskolin)	117,3% (related to Embelin) 81,9% (related to Forskolin)
1219 & 1234	2,5-dimethoxy-N-[3-(trifluoromethyl)phenyl]benzenesulfonamide	-	140,3% (raw) 99,9% (related to Forskolin)	108,9% (related to Embelin) 75,2% (related to Forskolin)
1220 & 1235	N-[4-chloro-3-(trifluoromethyl)phenyl]-2-methoxy-5-methyl-benzenesulfonamide	-	142,4% (raw) 101,4% (related to Forskolin)	108% (related to Embelin) 74,6% (related to Forskolin)
1221 & 1236	2,5-dimethoxy-N-[2-(trifluoromethyl)phenyl]benzenesulfonamide	-	139,9% (raw) 99,7% (related to Forskolin)	108,6% (related to Embelin) 75% (related to Forskolin)
1222 & 1237	[(4-Chloro-2,5-dimethoxyphenyl)sulfonyl][2-(trifluoromethyl)phenyl]amine	-	146,6% (raw) 104,4% (related to Forskolin)	152,8% (related to Embelin) 105,6% (related to Forskolin)
1223 & 1238	[(5-Bromo-2-methoxyphenyl)sulfonyl](phenylethyl)amine	-	146,2% (raw) 104,2% (related to Forskolin)	115,9% (related to Embelin) 80,1% (related to Forskolin)
1224 & 1239	5-bromo-2-ethoxy-N-(3-methyl-2-pyridinyl)benzenesulfonamide	-	145,2% (raw) 103,5% (related to Forskolin)	121,1% (related to Embelin) 83,7% (related to Forskolin)
1225 & 1240	5-chloro-2-methoxy-N-(2-methylphenyl)benzenesulfonamide	-	136,9% (raw) 97,5% (related to Forskolin)	108,8% (related to Embelin) 75,2% (related to Forskolin)
1226 & 1241	5-ethyl-2-methoxy-N-(o-tolyl)benzenesulfonamide	-	145,8% (raw) 103,9% (related to Forskolin)	111% (related to Embelin) 76,7% (related to Forskolin)

1227 & 1242	5-bromo-2-ethoxy-N-(2-ethoxyphenyl)benzenesulfonamide	-	135,5% (raw) 96,5% (related to Forskolin)	105,8% (related to Embelin) 73,1% (related to Forskolin)
1329	[(S)-[(4aR,5S,7aS)-5-hydroxy-1,4a,5,7a-tetrahydrocyclopenta[c]pyran-7-yl]-[(2S,3S,4S,5S,6S)-3,4,5-trihydroxy-6-(hydroxymethyl)tetrahydropyran-2-yl]oxy-methyl] benzoate	Melampyrosid	129,7% (raw) 92,4% (related to Forskolin)	101,3% (related to Embelin) 70% (related to Forskolin)
1330	methyl (1S,4aS,7R,7aS)-4'-(hydroxymethyl)-5'-oxo-1-[(2S,3R,4S,5S,6R)-3,4,5-trihydroxy-6-(hydroxymethyl)tetrahydropyran-2-yl]oxy-spiro[4a,7a-dihydro-1H-cyclopenta[c]pyran-7,2'-furan]-4-carboxylate	Iridoid	126% (raw) 92,4% (related to Forskolin)	97,5% (related to Embelin) 73,7% (related to Forskolin)
1331			118,2% (raw) 86,7% (related to Forskolin)	105,8% (related to Embelin) 80% (related to Forskolin)
1332			125,6% (raw) 92% (related to Forskolin)	102,1% (related to Embelin) 77,2% (related to Forskolin)
1360	methyl 1-hydroxy-4'-(1-hydroxyethyl)-5'-oxo-spiro[4a,7a-dihydro-1H-cyclopenta[c]pyran-7,2'-furan]-4-carboxylate	Plumieridin	138,3% (raw) 101,4% (related to Forskolin)	102,8% (related to Embelin) 77,7% (related to Forskolin)
1399 & 1401	7-methoxy-8-(3-methylbut-2-enyl)chromen-2-one	Osthol	165,6% (raw) 121,4% (related to Forskolin)	145,7% (related to Embelin) 110,1% (related to Forskolin)
1400 & 1402	4-[(2R)-2,3-dihydroxy-3-methylbutoxy]furo[3,2-g]chromen-7-one	Oxypeucedanin hydrate	138,7% (raw) 101,7% (related to Forskolin)	101,3% (related to Embelin) 76,6% (related to Forskolin)
1414	8-hydroxy-pentadeca-9E-ene-11,13-diyn-2-one	-	114,4% (raw) 78,1% (related to Forskolin)	123,4% (related to Embelin) 78,2% (related to Forskolin)
1415	(Z)-tetradec-8-en-11,13-diyn-2-one	-	111,1% (raw) 81,4% (related to Forskolin)	112,6% (related to Embelin) 85,1% (related to Forskolin)
1416	(Z)-pentadec-8-en-11,13-diyn-2-one	-	112,1% (raw) 82,2% (related to Forskolin)	126,4% (related to Embelin) 95,5% (related to Forskolin)
1417	(8Z,13Z)-pentadeca-8,13-dien-11-yn-2-one	-	109,6% (raw) 80,3% (related to Forskolin)	117,1% (related to Embelin) 88,5% (related to Forskolin)

1418			127,3% (raw) 93,3% (related to Forskolin)	91,9% (related to Embelin) 69,5% (related to Forskolin)
1419	(Z)-pentadec-8-en-2-one	-	112,1% (raw) 76,6% (related to Forskolin)	116,9% (related to Embelin) 74,1% (related to Forskolin)
1420	(Z)-pentadec-8-en-2-one	-	130,8% (raw) 89,3% (related to Forskolin)	122,2% (related to Embelin) 77,4% (related to Forskolin)
1441 & 1449	(E)-3-[3,5-dimethoxy-4-(3-methylbut-2-enoxy)phenyl]prop-2-enal	-	141,2% (raw) 96,4% (related to Forskolin)	133% (related to Embelin) 84,3% (related to Forskolin)
1444 & 1452	(E)-3-[4-[(2E)-3,7-dimethylocta-2,6-dienoxy]-3,5-dimethoxy-phenyl]prop-2-en-1-ol	-	139,1% (raw) 95% (related to Forskolin)	126,8% (related to Embelin) 80,4% (related to Forskolin)
1445 & 1453	(E)-3-[3-methoxy-4-(3-methylbut-2-enoxy)phenyl]prop-2-enal	-	155,3% (raw) 106% (related to Forskolin)	137% (related to Embelin) 86,9% (related to Forskolin)
1446 & 1454	(E)-3-[3-methoxy-4-(3-methylbut-2-enoxy)phenyl]prop-2-en-1-ol	-	144,2% (raw) 98,5% (related to Forskolin)	128,1% (related to Embelin) 81,2% (related to Forskolin)
1447 & 1455	(E)-3-[4-[(2E)-3,7-dimethylocta-2,6-dienoxy]-3-methoxy-phenyl]prop-2-enal	-	154,7% (raw) 105,7% (related to Forskolin)	135,7% (related to Embelin) 86% (related to Forskolin)
1448 & 1456	(E)-3-[4-[(2E)-3,7-dimethylocta-2,6-dienoxy]-3-methoxy-phenyl]prop-2-en-1-ol	-	139,9% (raw) 95,6% (related to Forskolin)	110,9% (related to Embelin) 70,3% (related to Forskolin)
1503	(Z)-heptadec-9-en-4,6-diyn-1-ol	-	103,5% (raw) 70,7% (related to Forskolin)	102,3% (related to Embelin) 64,9% (related to Forskolin)
1504	(2E,9Z)-heptadeca-2,9-dien-4,6-diyn-1-ol	-	102% (raw) 71,1% (related to Forskolin)	98% (related to Embelin) 74,8% (related to Forskolin)
1507	(1R,2S,3R,6S,7S,10R)-10-isopropyl-3,7-dimethyl-11-oxatricyclo[5.3.1.02,6]undecan-3-ol	-	123% (raw) 85,7% (related to Forskolin)	105,7% (related to Embelin) 80,7% (related to Forskolin)
1508	(2R,3R,4S,5S,6R)-2-[[(3S,5S,9R,10S,13R,14R,17R)-17-[(E,1R,4S)-4-ethyl-1,5-dimethyl-hex-2-enyl]-10,13-dimethyl-2,3,4,5,6,9,11,12,14,15,16,17-dodecahydro-1H-	alpha-Spinasterol glucoside	142,4% (raw) 99,3% (related to Forskolin)	109,8% (related to Embelin) 83,8% (related to Forskolin)

	cyclopenta[a]phenanthren-3-yl]oxy]-6-(hydroxymethyl)tetrahydropyran-3,4,5-triol			
1509	2-[(5-tert-butyl-2-methoxy-phenyl)sulfonylamino]benzoic acid	-	173,4% (raw) 120,9% (related to Forskolin)	146,1% (related to Embelin) 111,5% (related to Forskolin)
1510	2-[(5-ethyl-2-methoxyphenyl)sulfonylamino]benzoic acid	-	165,3% (raw) 115,2% (related to Forskolin)	122,5% (related to Embelin) 93,4% (related to Forskolin)
1513	4-[(3S,3aR,6S,6aR)-6-(4-hydroxy-3-methoxyphenyl)-1,3,3a,4,6,6a-hexahydrofuro[3,4-c]furan-3-yl]-2-methoxyphenol	Pinoresinol	165% (raw) 115% (related to Forskolin)	151,7% (related to Embelin) 115,7% (related to Forskolin)
1514			137,8% (raw) 96,1% (related to Forskolin)	122,4% (related to Embelin) 93,3% (related to Forskolin)
1516			155,9% (raw) 108,7% (related to Forskolin)	133,7% (related to Embelin) 102% (related to Forskolin)
1517			165% (raw) 115% (related to Forskolin)	142,6% (related to Embelin) 108,8% (related to Forskolin)
1518	3-(2,4-dihydroxyphenyl)-5,7-dihydroxy-2,3-dihydrochromen-4-one	Dalbergioidin	157,5% (raw) 109,8% (related to Forskolin)	128,9% (related to Embelin) 98,4% (related to Forskolin)
1519	(2S)-5,7-dihydroxy-2-(4-hydroxyphenyl)-2,3-dihydrochromen-4-one	Naringenin	166,5% (raw) 117,5% (related to Forskolin)	137,9% (related to Embelin) 94,7% (related to Forskolin)
1529	3H-1,3-benzoxazol-2-one	2-Benzoxazolinone	152,7% (raw) 107,8% (related to Forskolin)	121,6% (related to Embelin) 83,5% (related to Forskolin)
1531	(9Z)-3-[(1R,4aR,7R,8aR)-7-(hydroxymethyl)-1,4a-dimethyl-decalin-1-yl]oxyheptadeca-1,9-dien-4,6-diyn-8-ol	-	105,9% (raw) 74,8% (related to Forskolin)	119,2% (related to Embelin) 81,8% (related to Forskolin)
1532	(9Z)-8-[(1R,4aR,7R,8aR)-7-(hydroxymethyl)-1,4a-dimethyl-decalin-1-yl]oxyheptadeca-1,9-dien-4,6-diyn-3-ol	-	108,1% (raw) 76,3% (related to Forskolin)	115,3% (related to Embelin) 79,1% (related to Forskolin)
1534	(2S,4aR,5R,8R,8aS)-8-[(Z)-6-hydroxy-1-vinyl-pentadec-7-en-2,4-diynoxy]-2-isopropyl-4a,8-dimethyl-decalin-1,5-diol	-	113,2% (raw) 79,9% (related to Forskolin)	118,4% (related to Embelin) 81,3% (related to Forskolin)

1537 & 1548	(1S,3aR,4R,7S,8R,8aR)-4-[(Z)-1-(5-hydroxyhept-6-en-1,3-diynyl)dec-2-enoxy]-7-isopropyl-1,4-dimethyl-2,3,3a,5,6,7,8,8a-octahydroazulene-1,8-diol	-	109,1% (raw) 77% (related to Forskolin)	119,3% (related to Embelin) 81,9% (related to Forskolin)
1555			113,7% (raw) 80,2% (related to Forskolin)	134,1% (related to Embelin) 92% (related to Forskolin)
1554 & 1557	(2S,3S,4R)-2-aminooctadecane-1,3,4-triol	Phytosphingosine	111,5% (raw) 78,7% (related to Forskolin)	121,6% (related to Embelin) 83,4% (related to Forskolin)
1682	5,7-dihydroxy-2-(4-hydroxy-3,5-dimethoxyphenyl)chromen-4-one	Tricin	141,4% (raw) 99,8% (related to Forskolin)	123,7% (related to Embelin) 84,9% (related to Forskolin)
1684	4,6,7-trimethoxy-5-methylchromen-2-one	-	152,4% (raw) 107,6% (related to Forskolin)	124% (related to Embelin) 85,1% (related to Forskolin)
1686	5,7-dihydroxy-2-[4-[(1S,2S)-2-hydroxy-2-(4-hydroxy-3-methoxy-phenyl)-1-(hydroxymethyl)ethoxy]-3,5-dimethoxy-phenyl]chromen-4-one	Salcolin A	153% (raw) 108% (related to Forskolin)	135,1% (related to Embelin) 86% (related to Forskolin)
1689			107,5% (raw) 75,8% (related to Forskolin)	117,2% (related to Embelin) 74,6% (related to Forskolin)
1705	1-benzyl-N-(4-ethoxyphenyl)pyrazolo[3,4-d]pyrimidin-4-amine	-	164,7% (raw) 116,2% (related to Forskolin)	182,1% (related to Embelin) 115,9% (related to Forskolin)
1706	6-bromo-2-(3-isopropoxyphenyl)quinoline-4-carboxylic acid	-	162% (raw) 114,3% (related to Forskolin)	176,3% (related to Embelin) 112,3% (related to Forskolin)
1707	2-(1,3-benzodioxol-5-yl)-N-[(2-ethoxyphenyl)methyl]-N-[(2,4,5-trimethoxyphenyl)methyl]ethanamine	-	152,1% (raw) 107,3% (related to Forskolin)	139,4% (related to Embelin) 88,7% (related to Forskolin)
1708	2-ethoxy-4-[(E)-[3-sulfanyl-5-(trifluoromethyl)-1,2,4-triazol-4-yl]iminomethyl]phenol	-	160,3% (raw) 113,1% (related to Forskolin)	151,7% (related to Embelin) 96,6% (related to Forskolin)
1709	2,5-dichloro-N-(5-methyl-2,1,3-benzothiadiazol-4-yl)benzamide	-	145,3% (raw) 102,5% (related to Forskolin)	124,3% (related to Embelin) 79,2% (related to Forskolin)
1710	6-(3,4-Dimethylphenyl)-3-(trifluoromethyl)[1,2,4]triazolo[3,4-	-	146,1% (raw) 103,1% (related to	123,2% (related to Embelin) 78,5% (related

	b][1,3,4]thiadiazole		Forskolin)	to Forskolin)
1711	N-(4-ethoxyphenyl)-2-[(5-methyl-[1,2,4]triazino[5,6-b]indol-3-yl)sulfanyl]acetamide	-	136,3% (raw) 96,2% (related to Forskolin)	113% (related to Embelin) 71,9% (related to Forskolin)
1712	N-[4-chloro-3-(trifluoromethyl)phenyl]-4-[(2,4-dichlorophenoxy)methyl]benzamide	-	145,8% (raw) 102,9% (related to Forskolin)	115,6% (related to Embelin) 73,6% (related to Forskolin)
1713	4,5-bis[(3,4-dichlorophenyl)methylsulfanyl]-2-phenyl-pyridazin-3-one	-	145,4% (raw) 99,3% (related to Forskolin)	108,2% (related to Embelin) 72,8% (related to Forskolin)
1714	N-[(E)-1-(4-ethoxyphenyl)ethylideneamino]-4-methyl-benzenesulfonamide	-	152,8% (raw) 104,4% (related to Forskolin)	110,3% (related to Embelin) 74,2% (related to Forskolin)
1715	4-bromo-N-[(E)-(3-ethoxy-4-hydroxy-phenyl)methyleneamino]benzenesulfonamide	-	172,9% (raw) 118% (related to Forskolin)	151,6% (related to Embelin) 102% (related to Forskolin)
1716	N-[4-[[4-(4-tert-butylphenyl)thiazol-2-yl]sulfamoyl]phenyl]acetamide	-	171% (raw) 116,8% (related to Forskolin)	135,3% (related to Embelin) 91,1% (related to Forskolin)
1717	2-(4-Ethylphenyl)-2-oxoethyl 2-hydroxy-3-methylbenzoate	-	140,2% (raw) 95,7% (related to Forskolin)	121,2% (related to Embelin) 81,5% (related to Forskolin)
1718	6-amino-9-[2-(4-ethoxyphenoxy)ethyl]purine-8-thiol	-	155,5% (raw) 106,2% (related to Forskolin)	137,4% (related to Embelin) 92,5% (related to Forskolin)
1719	1-[2-(4-ethoxyphenoxy)ethyl]benzimidazole-2-thiol	-	163,5% (raw) 111,7% (related to Forskolin)	122,7% (related to Embelin) 82,6% (related to Forskolin)
1720	N-[2-[[6-(3,5-dimethylpyrazol-1-yl)pyridazin-3-yl]amino]ethyl]-2-fluoro-benzamide	-	155,3% (raw) 106,1% (related to Forskolin)	115,4% (related to Embelin) 77,6% (related to Forskolin)
1721	2-{[(4-Ethoxy-3-methylphenyl)sulfonyl]amino}benzoic acid	-	165,1% (raw) 112,7% (related to Forskolin)	140,5% (related to Embelin) 94,5% (related to Forskolin)
1739	5,7-dihydroxy-2-[4-[(1S,2S)-2-hydroxy-2-(4-hydroxy-3-methoxy-phenyl)-1-(hydroxymethyl)ethoxy]-3,5-dimethoxy-phenyl]chromen-4-one	SALCOLIN B	163,8% (raw) 111,9% (related to Forskolin)	130,5% (related to Embelin) 87,8% (related to Forskolin)

1740	5,7-dihydroxy-2-[(2S,3S)-2-(4-hydroxy-3-methoxy-phenyl)-3-(hydroxymethyl)-2,3-dihydro-1,4-benzodioxin-6-yl]chromen-4-one & 5,7-dihydroxy-2-[(2R,3R)-3-(4-hydroxy-3-methoxy-phenyl)-2-(hydroxymethyl)-2,3-dihydro-1,4-benzodioxin-6-yl]chromen-4-one	(-)-Hydnocarpin & Hydnocarpin D	132,1% (raw) 97,4% (related to Forskolin)	128,1% (related to Embelin) 84,5% (related to Forskolin)
1741	4,7-dimethoxy-5-methyl-chromen-2-one	Siderin	130,5% (raw) 96,2% (related to Forskolin)	126,7% (related to Embelin) 83,6% (related to Forskolin)
1742	(10E,12Z)-9-oxooctadeca-10,12-dienoic acid	9-oxoODE	110,5% (raw) 81,5% (related to Forskolin)	113,1% (related to Embelin) 74,6% (related to Forskolin)
1743	(10E,12Z)-9-hydroxyoctadeca-10,12-dienoic acid	9-HODE	137,9% (raw) 80,2% (related to Forskolin)	-
1763	4-[(3S,3aR,6S,6aR)-6-(4-hydroxy-3-methoxy-phenyl)-1,3,3a,4,6,6a-hexahydrofuro[3,4-c]furan-3-yl]-2-methoxy-phenol	Pinoresinol	167% (raw) 123,2% (related to Forskolin)	166,5% (related to Embelin) 109,9% (related to Forskolin)
1764	5-[(3S,3aR,6S,6aR)-6-(1,3-benzodioxol-5-yl)-1,3,3a,4,6,6a-hexahydrofuro[3,4-c]furan-3-yl]-1,3-benzodioxole	Sesamin	148,5% (raw) 109,5% (related to Forskolin)	134,3% (related to Embelin) 88,6% (related to Forskolin)
1765	5-[[(3S,3aR,6R,6aR)-3-(1,3-benzodioxol-5-yl)-1,3,3a,4,6,6a-hexahydrofuro[3,4-c]furan-6-yl]oxy]-1,3-benzodioxole	Sesamolin	151,1% (raw) 111,4% (related to Forskolin)	141,4% (related to Embelin) 93,3% (related to Forskolin)
1766	(3S,4S)-4-[hydroxy-(4-hydroxy-3-methoxy-phenyl)methyl]-3-[(4-hydroxy-3-methoxy-phenyl)methyl]tetrahydrofuran-2-one	7-Hydroxymatairesinol	138,6% (raw) 102,2% (related to Forskolin)	120,9% (related to Embelin) 79,7% (related to Forskolin)
1767	4-[[(3R,4R,5S)-5-(4-hydroxy-3-methoxy-phenyl)-4-(hydroxymethyl)tetrahydrofuran-3-yl]methyl]-2-methoxy-phenol	Lariciresinol	154,8% (raw) 114,2% (related to Forskolin)	140,2% (related to Embelin) 92,5% (related to Forskolin)
1850	(3S,4S,5S,10S,13S,14R,17S)-17-acetyl-3-hydroxy-10,13-dimethyl-2,3,4,5,6,7,11,12,14,15,16,17-dodecahydro-1H-cyclopenta[a]phenanthrene-4-carboxylic acid	-	116,9% (raw) 86,3% (related to Forskolin)	111,2% (related to Embelin) 73,4% (related to Forskolin)
1851	(4S,10R,11R,15R,18S,20R)-18,25,31-trihydroxy-11,15,29-trimethyl-27-(3-methylbut-2-enoxy)-10-[(E,1R,4R)-1,4,5-trimethylhex-2-enyl]-3-oxa-21-azaoctacyclo[22.7.1.02,22.04,20.06,14.07,11.015,20.028,32]dotriaconta-1(32),2(22),5,13,24,26,28,30-octaen-23-one	-	115,6% (raw) 85,3% (related to Forskolin)	104,1% (related to Embelin) 68,7% (related to Forskolin)

1852	(4S,10R,11R,15R,18S,20R,28S)-18,25,34-trihydroxy-11,15,27,27,28,32-hexamethyl-10-[(E,1R,4R)-1,4,5-trimethylhex-2-enyl]-3,29-dioxa-21-azanonacyclo[22.10.1.02,22.04,20.06,14.07,11.015,20.026,30.031,35]pentatriaconta-1(34),2(22),5,13,24,26(30),31(35),32-octaen-23-one	-	119% (raw) 83,1% (related to Forskolin)	108,7% (related to Embelin) 81% (related to Forskolin)
1876	(E)-8-hydroxypentadec-9-en-11,13-diyn-2-one	-	127,7% (raw) 89,2% (related to Forskolin)	137,4% (related to Embelin) 102,4% (related to Forskolin)
1877	(Z)-tetradec-8-en-11,13-diyn-2-one	-	122,1% (raw) 85,2% (related to Forskolin)	121% (related to Embelin) 90,1% (related to Forskolin)
1878	(Z)-pentadec-8-en-11,13-diyn-2-one	-	122,2% (raw) 85,3% (related to Forskolin)	120,9% (related to Embelin) 90,1% (related to Forskolin)
1879	(8Z,13Z)-pentadeca-8,13-dien-11-yn-2-one	-	132,8% (raw) 92,7% (related to Forskolin)	122,5% (related to Embelin) 91,3% (related to Forskolin)
1880	(8E,11E,13E)-pentadeca-8,11,13-trien-2-one	-	136,6% (raw) 95,4% (related to Forskolin)	119,4% (related to Embelin) 89% (related to Forskolin)
1881	(8Z)-Pentadeca-8,11-dien-2-on	-	143,7% (raw) 100,3% (related to Forskolin)	118,1% (related to Embelin) 88% (related to Forskolin)
1882	(8Z)-Pentadec-8-en-2-on	-	146,4% (raw) 102,2% (related to Forskolin)	118% (related to Embelin) 87,9% (related to Forskolin)
1899	4-[(3-butanoyl-2,4,6-trihydroxy-5-methyl-phenyl)methyl]-3,5-dihydroxy-6,6-dimethyl-2-propanoyl-cyclohexa-2,4-dien-1-one	Flavaspidic acid PB	153,4% (raw) 113,6% (related to Forskolin)	162,5% (related to Embelin) 110,9% (related to Forskolin)
1916	(1R,2S,4aR,5R,8R,8aS)-8-[(Z,1S)-1-[(5R)-5-hydroxyhept-6-en-1,3-diynyl]dec-2-enoxy]-2-isopropyl-4a,8-dimethyl-decalin-1,5-diol	-	105,5% (raw) 78,1% (related to Forskolin)	117,3% (related to Embelin) 80,1% (related to Forskolin)
1917	(1S)-9-[(3R)-3-hydroxypent-4-en-1-ynyl]-6-methoxy-1-[(Z)-non-1-enyl]-1,3-dihydrobenzo[f]isobenzofuran-7-ol	-	102,4% (raw) 75,9% (related to Forskolin)	133,3% (related to Embelin) 91% (related to Forskolin)
1918	(3S,8S,9Z)-heptadeca-1,9-dien-4,6-diyne-3,8-diol	-	114,3% (raw) 84,6% (related to Forskolin)	127,2% (related to Embelin) 86,8% (related

				to Forskolin)
1919	[2-hydroxy-3-[hydroxy-[2-(trimethyl-λ⁵-azanyl)ethoxy]phosphoryl]oxy-propyl] (9Z,12Z)-octadeca-9,12-dienoate	-	116,9% (raw) 86,5% (related to Forskolin)	118,9% (related to Embelin) 81,1% (related to Forskolin)
1921	4-[[(3R,4R,5S)-5-(4-hydroxy-3-methoxy-phenyl)-4-(hydroxymethyl)tetrahydrofuran-3-yl]methyl]-2-methoxy-phenol	Lariciresinol	147,6% (raw) 109,3% (related to Forskolin)	133,4% (related to Embelin) 91,1% (related to Forskolin)
1922	4-(4-hydroxy-3-methoxy-phenyl)-2,3-bis(hydroxymethyl)-7-methoxy-tetralin-6-ol	(+)-Cyclo-lariciresinol	133,8% (raw) 99,1% (related to Forskolin)	118,1% (related to Embelin) 80,6% (related to Forskolin)
1923	4-[(3S,3aR,6S,6aR)-6-(4-hydroxy-3-methoxy-phenyl)-1,3,3a,4,6,6a-hexahydrofuro[3,4-c]furan-3-yl]-2-methoxy-phenol	Pinoresinol	157,8% (raw) 116,8% (related to Forskolin)	156,8% (related to Embelin) 107% (related to Forskolin)
1951	5,7-dihydroxy-2-phenylchromen-4-one	Chrysin	142,8% (raw) 105,7% (related to Forskolin)	123,4% (related to Embelin) 84,2% (related to Forskolin)
1952	5,6,7-trihydroxy-2-phenylchromen-4-one	Baicalein	140,6% (raw) 104,1% (related to Forskolin)	107,3% (related to Embelin) 73,2% (related to Forskolin)
1953	5,7-dihydroxy-2-(4-hydroxyphenyl)-6-methoxy-chromen-4-one	Hispidulin	133,4% (raw) 97,1% (related to Forskolin)	130,9% (related to Embelin) 85,2% (related to Forskolin)
1954	methyl 3,4,5-trihydroxy-6-(5-hydroxy-6-methoxy-4-oxo-2-phenyl-chromen-7-yl)oxy-tetrahydropyran-2-carboxylate	Oroxylin A 7-O-beta-D-glucuronide methyl ester	146,7% (raw) 106,8% (related to Forskolin)	119,6% (related to Embelin) 77,9% (related to Forskolin)
1955	methyl (2S,3S,4S,5R,6S)-6-(5,6-dihydroxy-4-oxo-2-phenyl-chromen-7-yl)oxy-3,4,5-trihydroxy-tetrahydropyran-2-carboxylate	Baicalein 7-O-beta-D-methylglucuronide	128,8% (raw) 93,8% (related to Forskolin)	122,5% (related to Embelin) 79,8% (related to Forskolin)
1956	(2S,3S,4S,5R,6S)-3,4,5-trihydroxy-6-(5-hydroxy-6-methoxy-4-oxo-2-phenyl-chromen-7-yl)oxy-tetrahydropyran-2-carboxylic acid	Oroxylin A glucoronide	126,7% (raw) 92,2% (related to Forskolin)	124% (related to Embelin) 80,8% (related to Forskolin)
1957	3,4,5-trihydroxy-6-(5-hydroxy-4-oxo-2-phenyl-chromen-7-yl)oxy-tetrahydropyran-2-carboxylic acid	Chrysin-7-O-beta-D-glucoronide	133,1% (raw) 96,9% (related to Forskolin)	124,9% (related to Embelin) 81,4% (related to Forskolin)
1958	5,6-dihydroxy-2-phenyl-7-[(2S,3R,4S,5S,6R)-3,4,5-trihydroxy-6-(hydroxymethyl)tetrahydropyran-2-yl]oxy-chromen-4-one	Baicalein 7-O-glucoside	128,5% (raw) 93,5% (related to Forskolin)	122,6% (related to Embelin) 79,9% (related to Forskolin)

1959	(2S,3S,4S,5R,6S)-6-(5,6-dihydroxy-4-oxo-2-phenyl-chromen-7-yl)oxy-3,4,5-trihydroxy-tetrahydropyran-2-carboxylic acid	Baicalin	136% (raw) 99% (related to Forskolin)	128,8% (related to Embelin) 83,9% (related to Forskolin)
2097	(2S,3R,4R,5R,6S)-2-(4,8-dimethoxyfuro[2,3-b]quinolin-7-yl)oxy-6-methyl-tetrahydropyran-3,4,5-triol	Glycoperine	139,9% (raw) 101,8% (related to Forskolin)	143,6% (related to Embelin) 93,5% (related to Forskolin)
2098	methyl (1S,4aS,5aR,6R,10aS)-6',7'-dimethoxy-1-methyl-2'-oxo-spiro[1,4a,5,5a,7,8,10,10a-octahydropyrano[3,4-f]indolizine-6,3'-indoline]-4-carboxylate	Elegantissine	135,1% (raw) 98,3% (related to Forskolin)	127,1% (related to Embelin) 82,8% (related to Forskolin)
2099	2-[(2E,5E,7E,9R,10R,11E)-10-hydroxy-3,7,9,11-tetramethyl-trideca-2,5,7,11-tetraenyl]-5,6-dimethoxy-3-methyl-1H-pyridin-4-one	Piericidin A	143,7% (raw) 104,6% (related to Forskolin)	164,9% (related to Embelin) 107,4% (related to Forskolin)
2100	1-[(3,4-dimethoxyphenyl)methyl]-6,7-dimethoxy-2-methyl-isoquinolin-2-ium iodide	N-Methylpapaverine	158,1% (raw) 109,5% (related to Forskolin)	135,8% (related to Embelin) 85,9% (related to Forskolin)
2102	2-[(3,4-dimethoxyphenyl)methyl]-6,7-dimethoxy-3,4-dihydro-1H-isoquinoline	-	155,1% (raw) 107,4% (related to Forskolin)	123,9% (related to Embelin) 78,3% (related to Forskolin)
2103	5,7-dimethoxy-2-(3,4,5-trimethoxyphenyl)chroman-4-one	-	159,8% (raw) 110,7% (related to Forskolin)	145,5% (related to Embelin) 92% (related to Forskolin)
2123	5-hydroxy-2-(4-methoxyphenyl)-8-(3-methylbut-2-enyl)-7-[(2S,3R,4S,5S,6R)-3,4,5-trihydroxy-6-(hydroxymethyl)tetrahydropyran-2-yl]oxy-3-[(2S,3R,4R,5R,6S)-3,4,5-trihydroxy-6-methyl-tetrahydropyran-2-yl]oxy-chromen-4-one	Icariin	150,3% (raw) 104,1% (related to Forskolin)	119,4% (related to Embelin) 75,5% (related to Forskolin)
2127	1,3,7-trimethylpurine-2,6-dione	Coffein	146,5% (raw) 101,5% (related to Forskolin)	107,9% (related to Embelin) 68,2% (related to Forskolin)
2128	1,7-dihydroxy-3-methoxyxanthen-9-one	Gentisin	156,2% (raw) 108,1% (related to Forskolin)	122% (related to Embelin) 77,1% (related to Forskolin)
2129	(6aR,9R)-N-[(1S,2S,4R,7S)-7-benzyl-2-hydroxy-4-methyl-5,8-dioxo-3-oxa-6,9-diazatricyclo[7.3.0.02,6]dodecan-4-yl]-7-methyl-6,6a,8,9-tetrahydro-4H-indolo[4,3-fg]quinoline-9-carboxamide	Ergotamine	138% (raw) 95,5% (related to Forskolin)	117,8% (related to Embelin) 74,5% (related to Forskolin)
2130	methyl (1S,4aS,7S,7aR)-7-methyl-5-oxo-1-[(2S,3R,4S,5S,6R)-3,4,5-trihydroxy-6-	Verbenalin	135,2% (raw) 93,6% (related to Forskolin)	108,9% (related to Embelin) 68,9% (related

	(hydroxymethyl)tetrahydropyran-2-yl]oxy-4a,6,7,7a-tetrahydro-1H-cyclopenta[c]pyran-4-carboxylate			to Forskolin)
2131			124,5% (raw) 86,2% (related to Forskolin)	114,6% (related to Embelin) 72,4% (related to Forskolin)
2132			114,2% (raw) 79,1% (related to Forskolin)	103% (related to Embelin) 65,2% (related to Forskolin)
2133			151,9% (raw) 114,4% (related to Forskolin)	113,1% (related to Embelin) 84,4% (related to Forskolin)
2135	(2S,4aR,5S,8aR)-5-[2-[(1S,4aR,6S,8aR)-6-hydroxy-5,5,8a-trimethyl-2-methylene-decalin-1-yl]ethyl]-1,1,4a-trimethyl-6-methylene-decalin-2-ol	alpha-Onocerin	129% (raw) 97,2% (related to Forskolin)	112,9% (related to Embelin) 84,3% (related to Forskolin)
2136	6-methyl-2-oxa-6-azatricyclo[3.3.1.03,7]nonan-4-ol	Scopoline	140% (raw) 105,4% (related to Forskolin)	110,4% (related to Embelin) 82,4% (related to Forskolin)
2285	4-allyl-2-(4-nitrophenyl)phenol	-	155,5% (raw) 117,1% (related to Forskolin)	134,3% (related to Embelin) 100,2% (related to Forskolin)
2352	(3S,4R,4aR,6aR,6bS,8R,8aS,14aR,14bS)-4,8a-bis(hydroxymethyl)-4,6a,6b,11,11,14b-hexamethyl-1,2,3,4a,5,6,7,8,9,10,12,14a-dodecahydropicene-3,8-diol	Saikogenin D	140% (raw) 105,4% (related to Forskolin)	110,4% (related to Embelin) 82,4% (related to Forskolin)
2353	(2S,3R,4S,5S,6R)-2-[(2R,3R,4S,5S,6R)-2-[[(3S,4R,4aR,6aR,6bS,8S,8aS,12aS,14R,14aR,14bS)-8-hydroxy-4,8a-bis(hydroxymethyl)-14-methoxy-4,6a,6b,11,11,14b-hexamethyl-1,2,3,4a,5,6,7,8,9,10,12,12a,14,14a-tetradecahydropicen-3-yl]oxy]-3,5-dihydroxy-6-methyl-tetrahydropyran-4-yl]oxy-6-(hydroxymethyl)tetrahydropyran-3,4,5-triol	Saikosaponin B3	127,7% (raw) 96,1% (related to Forskolin)	110,4% (related to Embelin) 82,4% (related to Forskolin)
2354	(2S,3R,4S,5S,6R)-2-[(2R,3R,4S,5S,6R)-2-[[(3S,4R,4aR,6aR,6bS,8R,8aS,12aS,14R,14aR,14bS)-8-hydroxy-4,8a-bis(hydroxymethyl)-14-methoxy-4,6a,6b,11,11,14b-hexamethyl-1,2,3,4a,5,6,7,8,9,10,12,12a,14,14a-tetradecahydropicen-3-yl]oxy]-3,5-dihydroxy-6-methyl-tetrahydropyran-4-yl]oxy-6-(hydroxymethyl)tetrahydropyran-3,4,5-triol	Saikosaponin B4	141,4% (raw) 106,5% (related to Forskolin)	108,5% (related to Embelin) 81% (related to Forskolin)

2355	(2S,3R,4S,5S,6R)-2-[(2R,3R,4S,5S,6R)-2-[[(3S,4aR,6aR,6bS,8R,8aS,12aS,14R,14aR,14bS)-8-hydroxy-8a-(hydroxymethyl)-14-methoxy-4,4,6a,6b,11,11,14b-heptamethyl-1,2,3,4a,5,6,7,8,9,10,12,12a,14,14a-tetradecahydropicen-3-yl]oxy]-3,5-dihydroxy-6-methyl-tetrahydropyran-4-yl]oxy-6-(hydroxymethyl)tetrahydropyran-3,4,5-triol	Saikosaponin T	124,9% (raw) 94% (related to Forskolin)	106,1% (related to Embelin) 79,2% (related to Forskolin)
2356	(2S,3R,4S,5S,6R)-2-[(2R,3R,4S,5S,6R)-3,5-dihydroxy-2-[[(1S,2S,4S,5R,8R,9R,10S,13S,14R,17S,18R)-2-hydroxy-9-(hydroxymethyl)-4,5,9,13,20,20-hexamethyl-24-oxahexacyclo[15.5.2.01,18.04,17.05,14.08,13]tetracos-15-en-10-yl]oxy]-6-methyl-tetrahydropyran-4-yl]oxy-6-(hydroxymethyl)tetrahydropyran-3,4,5-triol	Saikosaponin A	102,2% (raw) 77% (related to Forskolin)	96,1% (related to Embelin) 71,7% (related to Forskolin)
2357	(2S,3R,4S,5S,6R)-2-[(2R,3R,4S,5S,6R)-2-[[(3S,4R,4aR,6aR,6bS,8R,8aS,14aR,14bS)-8-hydroxy-4,8a-bis(hydroxymethyl)-4,6a,6b,11,11,14b-hexamethyl-1,2,3,4a,5,6,7,8,9,10,12,14a-dodecahydropicen-3-yl]oxy]-3,5-dihydroxy-6-methyl-tetrahydropyran-4-yl]oxy-6-(hydroxymethyl)tetrahydropyran-3,4,5-triol	Saikosaponin B2	96,7% (raw) 72,8% (related to Forskolin)	96,1% (related to Embelin) 71,7% (related to Forskolin)
2359	3,9,12-trihydroxy-2,6,10,16-tetramethyl-14-oxatetracyclo[11.2.1.02,11.05,10]hexadec-6-ene-8,15-dione	-	142,3% (raw) 109% (related to Forskolin)	116,3% (related to Embelin) 87,4% (related to Forskolin)
2360	9,12-dihydroxy-2,6,10,16-tetramethyl-14-oxatetracyclo[11.2.1.02,11.05,10]hexadeca-4,6-diene-3,8,15-trione	-	136,3% (raw) 104,4% (related to Forskolin)	116,1% (related to Embelin) 87,2% (related to Forskolin)
2361	9,12-dihydroxy-2,6,10,16-tetramethyl-14-oxatetracyclo[11.2.1.02,11.05,10]hexadec-4-ene-3,8,15-trione	-	129,6% (raw) 99,3% (related to Forskolin)	118,5% (related to Embelin) 89% (related to Forskolin)
2363	3,12,13,15,16-pentahydroxy-2,6,14,17-tetramethyl-10-oxatetracyclo[7.7.1.02,7.013,17]heptadec-5-ene-4,11-dione	-	132,2% (raw) 101,2% (related to Forskolin)	118,7% (related to Embelin) 89,2% (related to Forskolin)
2364	methyl 9H-pyrido[3,4-b]indole-1-carboxylate	-	159,9% (raw) 122,5% (related to Forskolin)	127% (related to Embelin) 95,5% (related to Forskolin)
2365	3-hydroxy-4-methoxy-1,6-diazatetracyclo[7.6.1.05,16.010,15]hexadeca-3,5(16),6,8,10,12,14-heptaen-2-one	-	114,5% (raw) 87,7% (related to Forskolin)	113% (related to Embelin) 85% (related to Forskolin)

2367	13-methoxy-1,6-diazatetracyclo[7.6.1.05,16.010,15]hexadeca-3,5(16),6,8,10,12,14-heptaen-2-one	-	146,1% (raw) 111,9% (related to Forskolin)	125,6% (related to Embelin) 94,4% (related to Forskolin)
2368	7-hydroxy-6-methoxy-chromen-2-one	-	-	-
2369	8-hydroxy-6,7-dimethoxy-chromen-2-one	-	154,9% (raw) 118,6% (related to Forskolin)	138,6% (related to Embelin) 104,2% (related to Forskolin)
2370	3-(5-carboxy-2-hydroxy-phenyl)-4-hydroxy-benzoic acid	-	117,9% (raw) 90,3% (related to Forskolin)	102,1% (related to Embelin) 76,7% (related to Forskolin)
2371	4-hydroxy-3-methoxy-benzoic acid	-	149,7% (raw) 103,1% (related to Forskolin)	108,8% (related to Embelin) 77,1% (related to Forskolin)
2372	4-hydroxy-3-methoxy-benzaldehyde	-	143,7% (raw) 99% (related to Forskolin)	108,9% (related to Embelin) 77,2% (related to Forskolin)
2373	4-hydroxy-3,5-dimethoxy-benzoic acid	-	149,4% (raw) 102,9% (related to Forskolin)	110,3% (related to Embelin) 78,2% (related to Forskolin)
2412	2-hydroxy-4-(2-hydroxy-4-methoxy-6-pentylbenzoyl)oxy-6-propylbenzoic acid	Imbricaric acid	162,2% (raw) 111,7% (related to Forskolin)	162,6% (related to Embelin) 115,2% (related to Forskolin)
2413	3-(1-chloro-4-piperidyl)-6-fluoro-1,2-benzoxazole	-	151,3% (raw) 104,2% (related to Forskolin)	106,5% (related to Embelin) 75,5% (related to Forskolin)
2414	3-[1-(benzenesulfonyl)-4-piperidyl]-6-fluoro-1,2-benzoxazole	-	150,4% (raw) 103,6% (related to Forskolin)	120,7% (related to Embelin) 85,6% (related to Forskolin)
2415	(2R)-2-[(2R,3R)-3-[(1R)-1-[tert-butyl(dimethyl)silyl]oxyethyl]-1-chloro-4-oxo-azetidin-2-yl]oxypropanoic acid	-	128,4% (raw) 88,5% (related to Forskolin)	101,3% (related to Embelin) 71,8% (related to Forskolin)
2418	[(2S,3R,4R)-2-(3,4-dimethoxyphenyl)-4-[(3,4-dimethoxyphenyl)methyl]tetrahydrofuran-3-yl]methyl (Z)-2-methylbut-2-enoate	Leoligin S	168,3% (raw) 115,9% (related to Forskolin)	160,1% (related to Embelin) 113,5% (related to Forskolin)
2419	[(2S,3R,4R)-4-[(3,4-dimethoxyphenyl)methyl]-2-(3,4,5-trimethoxyphenyl)tetrahydrofuran-3-yl]methyl (Z)-2-methylbut-2-enoate	5-Methoxy-Leoligin	161,7% (raw) 111,4% (related to Forskolin)	154,2% (related to Embelin) 109,3% (related to Forskolin)
2422	11-hydroxy-2,6,9,15-tetramethyl-13-	-	140,6% (raw) 96,8%	100,2% (related to

	oxatetracyclo[10.2.1.02,10.05,9]pentadeca-4,6-diene-3,8,14-trione		(related to Forskolin)	Embelin) 71,1% (related to Forskolin)
2423	11-hydroxy-2,6,9,15-tetramethyl-13-oxatetracyclo[10.2.1.02,10.05,9]pentadec-6-ene-3,8,14-trione	-	155,6% (raw) 106,8% (related to Forskolin)	115% (related to Embelin) 79% (related to Forskolin)
2424	[4-acetoxy-1,4-bis[5-(1-hydroxy-1,5-dimethyl-hex-4-enyl)-2-methyl-tetrahydrofuran-2-yl]butyl] acetate	-	150% (raw) 102,9% (related to Forskolin)	116,8% (related to Embelin) 80,2% (related to Forskolin)
2445	(2R,3R)-3,5,7-trihydroxy-2-[(2R,3R)-3-(4-hydroxy-3-methoxy-phenyl)-2-(hydroxymethyl)-2,3-dihydro-1,4-benzodioxin-6-yl]chroman-4-one	Silybin A	169,7% (raw) 116,4% (related to Forskolin)	150% (related to Embelin) 103% (related to Forskolin)
2446	(2R,3R)-3,5,7-trihydroxy-2-[(2S,3S)-3-(4-hydroxy-3-methoxy-phenyl)-2-(hydroxymethyl)-2,3-dihydro-1,4-benzodioxin-6-yl]chroman-4-one	Silibinin B	163,1% (raw) 111,9% (related to Forskolin)	134,5% (related to Embelin) 92,4% (related to Forskolin)
2447	(2R,3R)-3,5,7-trihydroxy-2-[(2R,3R)-2-(4-hydroxy-3-methoxy-phenyl)-3-(hydroxymethyl)-2,3-dihydro-1,4-benzodioxin-6-yl]chroman-4-one	Isosilybin A	150% (raw) 102,9% (related to Forskolin)	118,5% (related to Embelin) 81,4% (related to Forskolin)
2448	(2R,3R)-3,5,7-trihydroxy-2-[(2S,3S)-2-(4-hydroxy-3-methoxy-phenyl)-3-(hydroxymethyl)-2,3-dihydro-1,4-benzodioxin-6-yl]chroman-4-one	Isosilybin B	152,2% (raw) 104,5% (related to Forskolin)	128,5% (related to Embelin) 88,3% (related to Forskolin)
2449	3,5,7-trihydroxy-2-[7-hydroxy-2-(4-hydroxy-3-methoxy-phenyl)-3-(hydroxymethyl)-2,3-dihydrobenzofuran-5-yl]chroman-4-one	Silychrystin	162,4% (raw) 111,4% (related to Forskolin)	150,5% (related to Embelin) 103,4% (related to Forskolin)
2450	(2R,3R)-3,5,7-trihydroxy-2-[(2R,3S)-7-hydroxy-2-(4-hydroxy-3-methoxy-phenyl)-3-(hydroxymethyl)-2,3-dihydrobenzofuran-5-yl]chroman-4-one	Silicristin	145,6% (raw) 99,9% (related to Forskolin)	119,5% (related to Embelin) 82,1% (related to Forskolin)
2451	(1R,3R,6R,7R,10R)-3-hydroxy-10-(4-hydroxy-3-methoxy-phenyl)-8-[(2R,3R)-3,5,7-trihydroxy-4-oxo-chroman-2-yl]-4-oxatricyclo[4.3.1.03,7]dec-8-en-2-one	Silidianin	161% (raw) 110,5% (related to Forskolin)	135,4% (related to Embelin) 93% (related to Forskolin)
2452	(2R,3R)-2-(3,4-dihydroxyphenyl)-3,5,7-trihydroxy-chroman-4-one	Taxifolin	165,3% (raw) 105,6% (related to Forskolin)	114,3% (related to Embelin) 78,9% (related to Forskolin)
2454	5,7-dihydroxy-2-[7-hydroxy-2-(4-hydroxy-3-methoxy-phenyl)-3-(hydroxymethyl)-2,3-dihydrobenzofuran-5-yl]chromen-4-one	Isohydnocarpin	159,3% (raw) 101,8% (related to Forskolin)	111,2% (related to Embelin) 76,8% (related to Forskolin)
2455	2-(3,4-dihydroxyphenyl)-5,7-dihydroxy-chromen-4-one	Luteolin	163,1% (raw) 104,2% (related to Forskolin)	130,1% (related to Embelin) 89,9% (related to Forskolin)

2456	3,5,7-trihydroxy-2-[3-(4-hydroxy-3-methoxy-phenyl)-2-(hydroxymethyl)-2,3-dihydro-1,4-benzodioxin-6-yl]chroman-4-one	Silymarin	169,2% (raw) 108,1% (related to Forskolin)	131,2% (related to Embelin) 90,6% (related to Forskolin)
2459	13-[(2S,3R,4S,5S,6R)-3,4,5-trihydroxy-6-(hydroxymethyl)tetrahydropyran-2-yl]oxy-1,6-diazatetracyclo [7.6.1.05,16.010,15]hexadeca-3,5(16),6,8,10,12,14-heptaen-2-one	-	150% (raw) 95,8% (related to Forskolin)	117,1% (related to Embelin) 80,9% (related to Forskolin)
2460	3,4,9,12-tetrahydroxy-2,6,10,16-tetramethyl-14-oxatetracyclo[11.2.1.02,11.05,10]hexadec-6-ene-8,15-dione	-	145,8% (raw) 93,1% (related to Forskolin)	123,2% (related to Embelin) 85,1% (related to Forskolin)
2461	4,5,7,8,17-pentahydroxy-6,14,18-trimethyl-3,10-dioxapentacyclo[9.8.0.01,7.04,19.013,18]nonadec-14-ene-9,16-dione	-	152,1% (raw) 97,2% (related to Forskolin)	115,8% (related to Embelin) 80% (related to Forskolin)
2462	3,15-dihydroxy-2,6,14,17-tetramethyl-10-oxatetracyclo[7.7.1.02,7.013,17]heptadec-5-ene-4,11,16-trione	-	144,8% (raw) 92,5% (related to Forskolin)	113,9% (related to Embelin) 78,6% (related to Forskolin)
2538	[(2S,3R,4R)-2-(3,4-dimethoxyphenyl)-4-[(3,4-dimethoxyphenyl)methyl]tetrahydrofuran-3-yl]methyl prop-2-enoate	-	174,1% (raw) 111,2% (related to Forskolin)	153,1% (related to Embelin) 105,7% (related to Forskolin)
2539	[(2S,3R,4R)-2-(3,4-dimethoxyphenyl)-4-[(3,4-dimethoxyphenyl)methyl]tetrahydrofuran-3-yl]methyl (E)-2-methylbut-2-enoate	-	167,2% (raw) 106,8% (related to Forskolin)	142,5% (related to Embelin) 98,4% (related to Forskolin)
2543	[(2S,3R,4R)-2-(3,4-dimethoxyphenyl)-4-[(3,4-dimethoxyphenyl)methyl]tetrahydrofuran-3-yl]methyl cyclopropanecarboxylate	-	176,8% (raw) 115,7% (related to Forskolin)	150% (related to Embelin) 100,3% (related to Forskolin)
2544	[(2S,3R,4R)-2-(3,4-dimethoxyphenyl)-4-[(3,4-dimethoxyphenyl)methyl]tetrahydrofuran-3-yl]methyl cyclopentanecarboxylate	-	175% (raw) 114,5% (related to Forskolin)	150,4% (related to Embelin) 100,6% (related to Forskolin)
2545	[(2S,3R,4R)-2-(3,4-dimethoxyphenyl)-4-[(3,4-dimethoxyphenyl)methyl]tetrahydrofuran-3-yl]methyl cyclohexanecarboxylate	-	172,5% (raw) 112,9% (related to Forskolin)	142,5% (related to Embelin) 95,3% (related to Forskolin)
2547	[(2S,3R,4R)-4-[(3,4-dimethoxyphenyl)methyl]-2-phenyl-tetrahydrofuran-3-yl]methyl (Z)-2-methylbut-2-enoate	-	176,4% (raw) 115,5% (related to Forskolin)	133,8% (related to Embelin) 89,5% (related to Forskolin)
2550	[(2S,3R,4R)-2-(3,4-dimethoxyphenyl)-4-[(3,4-dimethoxyphenyl)methyl]tetrahydrofuran-3-yl]methyl propanoate	-	175,3% (raw) 114,7% (related to Forskolin)	157,4% (related to Embelin) 105,3% (related to Forskolin)
2551	[(2S,3R,4R)-2-(3,4-dimethoxyphenyl)-4-[(3,4-dimethoxyphenyl)methyl]tetrahydrofuran-3-	-	175,9% (raw) 115,1% (related to	164,8% (related to Embelin) 110,2%

	yl]methyl butanoate		Forskolin)	(related to Forskolin)
2552	methyl (1S,4S,8R,10S,11E,14S)-11-ethylidene-12-oxo-7,9,13-trioxatetracyclo[6.5.1.01,10.04,14]tetradeca-2,5-diene-5-carboxylate	Plumericin	162,2% (raw) 106,1% (related to Forskolin)	116,6% (related to Embelin) 78% (related to Forskolin)
2553	4,5,7,8,17-pentahydroxy-14,18-dimethyl-6-methylene-3,10-dioxapentacyclo[9.8.0.01,7.04,19.013,18]nonadec-14-ene-9,16-dione	-	148% (raw) 96,8% (related to Forskolin)	115% (related to Embelin) 76,9% (related to Forskolin)
2554	8,9,12-trihydroxy-2,6,10,16-tetramethyl-14-oxatetracyclo[11.2.1.02,11.05,10]hexadec-6-ene-3,15-dione	-	152,6% (raw) 99,9% (related to Forskolin)	113,8% (related to Embelin) 76,1% (related to Forskolin)
2555	[4,5-dihydroxy-6-(hydroxymethyl)-2-[2-(2-hydroxypropyl)-7-methoxy-5-methyl-4-oxo-chromen-8-yl]tetrahydropyran-3-yl] (E)-3-(4-hydroxyphenyl)prop-2-enoate	-	159,1% (raw) 104,1% (related to Forskolin)	116% (related to Embelin) 77,5% (related to Forskolin)
2556	2-(3,4-dimethoxyphenyl)-3,5,6,7,8-pentamethoxy-chromen-4-one	-	179,9% (raw) 114,3% (related to Forskolin)	137,6% (related to Embelin) 79,4% (related to Forskolin)
2557	[3,4,5-trihydroxy-6-(hydroxymethyl)tetrahydropyran-2-yl] 1,10-dihydroxy-9-(hydroxymethyl)-1,2,6a,6b,9,12a-hexamethyl-2,3,4,5,6,6a,7,8,8a,10,11,12,13,14b-tetradecahydropicene-4a-carboxylate	-	147,4% (raw) 93,7% (related to Forskolin)	111,2% (related to Embelin) 64,2% (related to Forskolin)
2558	(E)-3-(3,4-dihydroxyphenyl)-N-[2-(4-hydroxyphenyl)ethyl]prop-2-enamide	N-Caffeoyltyramine	161,9% (raw) 102,9% (related to Forskolin)	114,5% (related to Embelin) 66,1% (related to Forskolin)
2559	6-hydroxy-7-methoxy-chromen-2-one	Isoscopoletin	156,6% (raw) 99,5% (related to Forskolin)	116,7% (related to Embelin) 67,3% (related to Forskolin)
2560	7-hydroxy-6-methoxy-chromen-2-one	Scopoletin	-	-
2569	5,7-dihydroxy-2-(4-methoxyphenyl)chromen-4-one	-	156,1% (raw) 99,2% (related to Forskolin)	115% (related to Embelin) 66,3% (related to Forskolin)
2570	3,5-dihydroxy-2-(3-hydroxy-4-methoxy-phenyl)-7-methoxy-chromen-4-one	-	163% (raw) 103,6% (related to Forskolin)	115,2% (related to Embelin) 66,5% (related to Forskolin)
2571	2-(3,4-dimethoxyphenyl)-5-hydroxy-6,7-dimethoxy-	-	177,4% (raw)	145,5% (related to

	chroman-4-one		112,7% (related to Forskolin)	Embelin) 83,9% (related to Forskolin)
2573	5,6,7-trimethoxy-2-(4-methoxyphenyl)chroman-4-one	-	177,9% (raw) 113,1% (related to Forskolin)	140,4% (related to Embelin) 81% (related to Forskolin)
2574			164% (raw) 104,2% (related to Forskolin)	112,6% (related to Embelin) 64,9% (related to Forskolin)
2575	(E)-3-(4-hydroxyphenyl)-N-[2-(4-hydroxyphenyl)ethyl]prop-2-enamide	Paprazine & N-p-trans-Coumaroyltyramine	160,8% (raw) 111,2% (related to Forskolin)	111,2% (related to Embelin) 70,9% (related to Forskolin)
2576	3-(3,4-dihydroxyphenyl)-N-[2-(4-hydroxyphenyl)ethyl]propanamide	Dihydro-N-Caffeoyltyramine	159,7% (raw) 110,5% (related to Forskolin)	109,9% (related to Embelin) 70,1% (related to Forskolin)
2626	[(2S,3R,4R)-4-[(3,4-dimethoxyphenyl)methyl]-2-(3,4,5-trimethoxyphenyl)tetrahydrofuran-3-yl]methanol	-	171,1% (raw) 118,3% (related to Forskolin)	136,7% (related to Embelin) 87,2% (related to Forskolin)
2627	[(2S,3R,4R)-4-[(3,4-dimethoxyphenyl)methyl]-2-(3,4,5-trimethoxyphenyl)tetrahydrofuran-3-yl]methyl (Z)-2-methylbut-2-enoate	-	175,1% (raw) 121,2% (related to Forskolin)	147,3% (related to Embelin) 94% (related to Forskolin)
2628	[(2S,3R,4R)-4-[(3,4-dimethoxyphenyl)methyl]-2-(3,4,5-trimethoxyphenyl)tetrahydrofuran-3-yl]methyl (E)-2-methylbut-2-enoate	-	174,1% (raw) 120,5% (related to Forskolin)	146,4% (related to Embelin) 93,4% (related to Forskolin)
2629	[(2S,3R,4R)-4-[(3,4-dimethoxyphenyl)methyl]-2-(3,4,5-trimethoxyphenyl)tetrahydrofuran-3-yl]methyl butanoate	-	174,5% (raw) 120,7% (related to Forskolin)	144,3% (related to Embelin) 92,1% (related to Forskolin)
2630	[(2S,3R,4R)-4-[(3,4-dimethoxyphenyl)methyl]-2-(3,4,5-trimethoxyphenyl)tetrahydrofuran-3-yl]methyl 3-methylbut-2-enoate & [(2S,3R,4R)-4-[(3,4-dimethoxyphenyl)methyl]-2-(3,4,5-trimethoxyphenyl)tetrahydrofuran-3-yl]methyl 3-methylbut-3-enoate	-	172,8% (raw) 119,5% (related to Forskolin)	159,4% (related to Embelin) 101,7% (related to Forskolin)
2634	[(2S,3R,4R)-4-[(3,4-dimethoxyphenyl)methyl]-2-(3,4,5-trimethoxyphenyl)tetrahydrofuran-3-yl]methyl cyclohexene-1-carboxylate	-	170,8% (raw) 118,2% (related to Forskolin)	124,2% (related to Embelin) 79,2% (related to Forskolin)
2635	[(2S,3R,4R)-4-[(3,4-dimethoxyphenyl)methyl]-2-(3,4,5-trimethoxyphenyl)tetrahydrofuran-3-yl]methyl cyclopentanecarboxylate	-	168,5% (raw) 116,6% (related to Forskolin)	131,3% (related to Embelin) 83,8% (related to Forskolin)

2636	[(2S,3R,4R)-4-[(3,4-dimethoxyphenyl)methyl]-2-(3,4,5-trimethoxyphenyl)tetrahydrofuran-3-yl]methyl cyclopentene-1-carboxylate	-	168% (raw) 116,2% (related to Forskolin)	140,3% (related to Embelin) 89,5% (related to Forskolin)
2637	[(2S,3R,4R)-4-[(3,4-dimethoxyphenyl)methyl]-2-(3,4,5-trimethoxyphenyl)tetrahydrofuran-3-yl]methyl cyclopropanecarboxylate	-	164,6% (raw) 110,4% (related to Forskolin)	146% (related to Embelin) 91,4% (related to Forskolin)
2638	[(2S,3R,4R)-4-[(3,4-dimethoxyphenyl)methyl]-2-(3,4,5-trimethoxyphenyl)tetrahydrofuran-3-yl]methyl benzoate	-	168,3% (raw) 112,9% (related to Forskolin)	139,4% (related to Embelin) 87,2% (related to Forskolin)
2639	(2S,3R,4R)-3-(allyloxymethyl)-4-[(3,4-dimethoxyphenyl)methyl]-2-(3,4,5-trimethoxyphenyl)tetrahydrofuran	-	168,2% (raw) 112,9% (related to Forskolin)	124,4% (related to Embelin) 77,8% (related to Forskolin)
2640	dimethyl 2,3-bis(1,3-benzodioxol-5-ylmethyl)butanedioate	Heliobuphthalmin	163,2% (raw) 109,5% (related to Forskolin)	122,6% (related to Embelin) 76,7% (related to Forskolin)
2641	dimethyl (3E)-2-(1,3-benzodioxol-5-ylmethyl)-3-(1,3-benzodioxol-5-ylmethylidene)butanedioate	Dehydroheliobupht halmin	163% (raw) 109,3% (related to Forskolin)	122,3% (related to Embelin) 76,5% (related to Forskolin)
2642	5-[7-methoxy-5-(3-methoxypropyl)benzofuran-2-yl]-1,3-benzodioxole	-	150,9% (raw) 101,2% (related to Forskolin)	121,3% (related to Embelin) 75,9% (related to Forskolin)
2643	5-[7-methoxy-5-(3-methoxypropyl)benzofuran-2-yl]-1,3-benzodioxole	-	150,7% (raw) 101,1% (related to Forskolin)	107,3% (related to Embelin) 67,1% (related to Forskolin)
2644	10-(1,3-benzodioxol-5-yl)-9H-isobenzofuro[6,5-g][1,3]benzodioxol-7-one	Helioxanthin	169,5% (raw) 113,7% (related to Forskolin)	137,8% (related to Embelin) 86,2% (related to Forskolin)
2654	(E)-3-(4-hydroxy-3-methoxy-phenyl)-N-[2-(4-hydroxyphenyl)ethyl]prop-2-enamide	N-Trans-feruloyltramine	154,1% (raw) 103,4% (related to Forskolin)	107% (related to Embelin) 67% (related to Forskolin)
2655	(2S)-1-(3,4-dihydroxyphenyl)-7-hydroxy-N2,N3-bis[2-(4-hydroxyphenyl)ethyl]-6,8-dimethoxy-1,2-dihydronaphthalene-2,3-dicarboxamide	-	112,9% (raw) 75,7% (related to Forskolin)	102,1% (related to Embelin) 63,9% (related to Forskolin)
2656	(E)-N-(4-acetamidobutyl)-2-[4,5-dihydroxy-2-[3-[2-(4-hydroxyphenyl)ethylamino]-3-oxo-propyl]phenyl]-3-(4-hydroxy-3,5-dimethoxy-phenyl)prop-2-enamide	-	151,1% (raw) 101,3% (related to Forskolin)	111,5% (related to Embelin) 70,7% (related to Forskolin)
2657	(E)-N-(4-acetamidobutyl)-2-[4,5-dihydroxy-2-[3-[2-(4-hydroxyphenyl)ethylamino]-3-oxo-propyl]phenyl]-3-(4-hydroxy-3-methoxy-	-	154,3% (raw) 103,5% (related to Forskolin)	119,2% (related to Embelin) 75,6% (related to Forskolin)

	phenyl)prop-2-enamide			
2658	(1S)-N3-(4-acetamidobutyl)-1-(3,4-dihydroxyphenyl)-7-hydroxy-N2-[2-(4-hydroxyphenyl)ethyl]-6,8-dimethoxy-1,2-dihydronaphthalene-2,3-dicarboxamide	-	137,6% (raw) 92,2% (related to Forskolin)	104,3% (related to Embelin) 66,2% (related to Forskolin)
2659	(E)-2-[4,5-dihydroxy-2-[3-[2-(4-hydroxyphenyl)ethylamino]-3-oxo-propyl]phenyl]-3-(4-hydroxy-3,5-dimethoxy-phenyl)-N-[2-(4-hydroxyphenyl)ethyl]prop-2-enamide	-	152,3% (raw) 102,1% (related to Forskolin)	118,3% (related to Embelin) 75,1% (related to Forskolin)
2733	[(2S,3R,4R)-4-[(3,4-dimethoxyphenyl)methyl]-2-(4-fluorophenyl)tetrahydrofuran-3-yl]methanol	-	168% (raw) 112,6% (related to Forskolin)	145,8% (related to Embelin) 92,5% (related to Forskolin)
2736	[(2S,3R,4R)-4-[(3,4-dimethoxyphenyl)methyl]-2-phenyl-tetrahydrofuran-3-yl]methanol	-	165,8% (raw) 111,2% (related to Forskolin)	137,4% (related to Embelin) 87,2% (related to Forskolin)
2739	[(2S,3R,4R)-2-(3,4-dimethoxyphenyl)-4-[(3,4-dimethoxyphenyl)methyl]tetrahydrofuran-3-yl]methyl (E)-3-phenylprop-2-enoate	-	157,3% (raw) 105,4% (related to Forskolin)	118,2% (related to Embelin) 75% (related to Forskolin)
2740	[(2S,3R,4R)-2-(3,4-dimethoxyphenyl)-4-[(3,4-dimethoxyphenyl)methyl]tetrahydrofuran-3-yl]methyl 4-phenylbenzoate	-	148,1% (raw) 99,3% (related to Forskolin)	107,9% (related to Embelin) 68,5% (related to Forskolin)
2741	[2-(3,4-dimethoxyphenyl)-4-[(3,4-dimethoxyphenyl)methyl]tetrahydrofuran-3-yl]methyl adamantane-1-carboxylate	-	149,1% (raw) 100% (related to Forskolin)	109,3% (related to Embelin) 69,4% (related to Forskolin)
2742	[(2S,3R,4R)-4-[(3,4-dimethoxyphenyl)methyl]-2-phenyl-tetrahydrofuran-3-yl]methyl cyclopentanecarboxylate	-	157,8% (raw) 105,8% (related to Forskolin)	114% (related to Embelin) 72,3% (related to Forskolin)
2743	[(2S,3R,4R)-2-(3,4-dimethoxyphenyl)-4-[(3,4-dimethoxyphenyl)methyl]tetrahydrofuran-3-yl]methyl naphthalene-1-carboxylate		156,5% (raw) 103,2% (related to Forskolin)	123% (related to Embelin) 78,2% (related to Forskolin)
2744	[(2S,3R,4R)-2-(3,4-dimethoxyphenyl)-4-[(3,4-dimethoxyphenyl)methyl]tetrahydrofuran-3-yl]methyl cycloheptanecarboxylate	-	166,6% (raw) 109,9% (related to Forskolin)	140,8% (related to Embelin) 89,5% (related to Forskolin)
2746	[(2S,3R,4R)-4-[(3,4-dimethoxyphenyl)methyl]-2-phenyl-tetrahydrofuran-3-yl]methyl cyclohexanecarboxylate	-	160% (raw) 105,6% (related to Forskolin)	131,7% (related to Embelin) 83,7% (related to Forskolin)
2748	[(2S,3R,4R)-4-benzyl-2-(3,4-dimethoxyphenyl)tetrahydrofuran-3-yl]methanol	-	168,9% (raw) 111,4% (related to Forskolin)	148,7% (related to Embelin) 94,5% (related to Forskolin)

2749	[(2S,3R,4R)-4-[(4-tert-butylphenyl)methyl]-2-(3,4-dimethoxyphenyl)tetrahydrofuran-3-yl]methanol	-	167,8% (raw) 110,7% (related to Forskolin)	135% (related to Embelin) 85,8% (related to Forskolin)
2750	ethyl 4-[[(3R,4R,5S)-5-(3,4-dimethoxyphenyl)-4-(hydroxymethyl)tetrahydrofuran-3-yl]methyl]benzoate	-	171,2% (raw) 112,9% (related to Forskolin)	168,7% (related to Embelin) 107,2% (related to Forskolin)
2752	[(2S,3R,4R)-2-(3,4-dimethoxyphenyl)-4-[(4-methoxyphenyl)methyl]tetrahydrofuran-3-yl]methanol	-	166,4% (raw) 109,8% (related to Forskolin)	145,7% (related to Embelin) 92,6% (related to Forskolin)
2753	[(2S,3R,4R)-2-(3,4-dimethoxyphenyl)-4-[(4-phenylphenyl)methyl]tetrahydrofuran-3-yl]methanol	-	149,2% (raw) 98,4% (related to Forskolin)	111,9% (related to Embelin) 71,1% (related to Forskolin)
2754	[(2S,3R,4R)-2-(3,4-dimethoxyphenyl)-4-(p-tolylmethyl)tetrahydrofuran-3-yl]methanol	-	163,5% (raw) 107,9% (related to Forskolin)	145,9% (related to Embelin) 92,7% (related to Forskolin)
2756	[(2S,3R,4R)-4-benzyl-2-(3,4,5-trimethoxyphenyl)tetrahydrofuran-3-yl]methanol	-	159,1% (raw) 105% (related to Forskolin)	111,3% (related to Embelin) 70,7% (related to Forskolin)
2758	[(2S,3R,4R)-4-[(4-methoxyphenyl)methyl]-2-(3,4,5-trimethoxyphenyl)tetrahydrofuran-3-yl]methanol	-	170,8% (raw) 110,5% (related to Forskolin)	170,8% (raw) 110,5% (related to Forskolin)
2759	[(2S,3R,4R)-4-[(4-fluorophenyl)methyl]-2-(3,4,5-trimethoxyphenyl)tetrahydrofuran-3-yl]methanol	-	169,1% (raw) 109,4% (related to Forskolin)	169,1% (raw) 109,4% (related to Forskolin)
2761	ethyl 4-[[(3R,4R,5S)-4-(hydroxymethyl)-5-(3,4,5-trimethoxyphenyl)tetrahydrofuran-3-yl]methyl]benzoate	-	174,2% (raw) 112,7% (related to Forskolin)	174,2% (raw) 112,7% (related to Forskolin)
2763	4-[[(3R,4R,5S)-4-(hydroxymethyl)-5-(3,4,5-trimethoxyphenyl)tetrahydrofuran-3-yl]methyl]benzonitrile	-	161,3% (raw) 104,4% (related to Forskolin)	161,3% (raw) 104,4% (related to Forskolin)
2764	[(2S,3R,4R)-4-benzyl-2-(3,4,5-trimethoxyphenyl)tetrahydrofuran-3-yl]methyl (Z)-2-methylbut-2-enoate	-	169,5% (raw) 109,7% (related to Forskolin)	169,5% (raw) 109,7% (related to Forskolin)
2765	[(2S,3R,4R)-4-[(4-tert-butylphenyl)methyl]-2-(3,4,5-trimethoxyphenyl)tetrahydrofuran-3-yl]methyl (Z)-2-methylbut-2-enoate	-	149,2% (raw) 96,6% (related to Forskolin)	149,2% (raw) 96,6% (related to Forskolin)
2766	[(2S,3R,4R)-4-(p-tolylmethyl)-2-(3,4,5-trimethoxyphenyl)tetrahydrofuran-3-yl]methanol	-	170,9% (raw) 110,6% (related to Forskolin)	170,9% (raw) 110,6% (related to Forskolin)

2769	[(2S,3R,4R)-4-[[4-(trifluoromethyl)phenyl]methyl]-2-(3,4,5-trimethoxyphenyl)tetrahydrofuran-3-yl]methyl (Z)-2-methylbut-2-enoate	-	155,4% (raw) 100,5% (related to Forskolin)	155,4% (raw) 100,5% (related to Forskolin)
2770	[(2S,3R,4R)-4-[(4-methoxyphenyl)methyl]-2-(3,4,5-trimethoxyphenyl)tetrahydrofuran-3-yl]methyl (Z)-2-methylbut-2-enoate	-	162,9% (raw) 105,4% (related to Forskolin)	162,9% (raw) 105,4% (related to Forskolin)
2771	[(2S,3R,4R)-4-[(4-acetylphenyl)methyl]-2-(3,4,5-trimethoxyphenyl)tetrahydrofuran-3-yl]methyl (Z)-2-methylbut-2-enoate	-	159,3% (raw) 103,1% (related to Forskolin)	159,3% (raw) 103,1% (related to Forskolin)
2772	[(2S,3R,4R)-4-[(4-cyanophenyl)methyl]-2-(3,4,5-trimethoxyphenyl)tetrahydrofuran-3-yl]methyl (Z)-2-methylbut-2-enoate	-	169,6% (raw) 114% (related to Forskolin)	108,2% (related to Embelin) 70,1% (related to Forskolin)
2776	[(2S,3R,4R)-4-(1-naphthylmethyl)-2-(3,4,5-trimethoxyphenyl)tetrahydrofuran-3-yl]methyl (Z)-2-methylbut-2-enoate	-	162,3% (raw) 109,1% (related to Forskolin)	114,6% (related to Embelin) 74,3% (related to Forskolin)
2777	[(2S,3R,4R)-4-benzyl-2-(3,4-dimethoxyphenyl)tetrahydrofuran-3-yl]methyl (Z)-2-methylbut-2-enoate	-	170,4% (raw) 114,5% (related to Forskolin)	116,8% (related to Embelin) 75,7% (related to Forskolin)
2779	[(2S,3R,4R)-2-(3,4-dimethoxyphenyl)-4-[(4-methoxyphenyl)methyl]tetrahydrofuran-3-yl]methyl (Z)-2-methylbut-2-enoate	-	168,8% (raw) 113,4% (related to Forskolin)	125% (related to Embelin) 81% (related to Forskolin)
2781	[(2S,3R,4R)-4-[(3,4-dimethoxyphenyl)methyl]-2-(4-fluorophenyl)tetrahydrofuran-3-yl]methyl cyclopentanecarboxylate	-	177,5% (raw) 119,3% (related to Forskolin)	120,2% (related to Embelin) 77,9% (related to Forskolin)
2782	[(2S,3R,4R)-2-(3,4-dimethoxyphenyl)-4-[(4-fluorophenyl)methyl]tetrahydrofuran-3-yl]methanol	-	176,6% (raw) 118,7% (related to Forskolin)	128,1% (related to Embelin) 83% (related to Forskolin)
2783	[(2S,3R,4R)-2-(3,4-dimethoxyphenyl)-4-[(3,4-dimethoxyphenyl)methyl]tetrahydrofuran-3-yl]methyl pyridine-3-carboxylate	-	180,8% (raw) 121,5% (related to Forskolin)	131,2% (related to Embelin) 85% (related to Forskolin)
2784	[(2S,3R,4R)-2-(3,4-dimethoxyphenyl)-4-[(3,4-dimethoxyphenyl)methyl]tetrahydrofuran-3-yl]methyl naphthalene-2-carboxylate	-	160,2% (raw) 107,6% (related to Forskolin)	116,1% (related to Embelin) 75,2% (related to Forskolin)
2785	[(2S,3R,4R)-4-[(3,4-dimethoxyphenyl)methyl]-2-(4-fluorophenyl)tetrahydrofuran-3-yl]methyl cyclohexanecarboxylate	-	162,7% (raw) 109,4% (related to Forskolin)	107,7% (related to Embelin) 69,8% (related to Forskolin)
2787	[(2S,3R,4R)-2-(3,4-dimethoxyphenyl)-4-[(3,4-dimethoxyphenyl)methyl]tetrahydrofuran-3-yl]methyl pyridine-4-carboxylate	-	162,6% (raw) 109,3% (related to Forskolin)	118% (related to Embelin) 76,5% (related to Forskolin)

2788	[(2S,3R,4R)-4-[(4-tert-butylphenyl)methyl]-2-(3,4-dimethoxyphenyl)tetrahydrofuran-3-yl]methyl (Z)-2-methylbut-2-enoate	-	141,5% (raw) 95,1% (related to Forskolin)	111,2% (related to Embelin) 71,9% (related to Forskolin)
2789	[(2S,3R,4R)-2-(3,4-dimethoxyphenyl)-4-[(4-phenylphenyl)methyl]tetrahydrofuran-3-yl]methyl (Z)-2-methylbut-2-enoate	-	143,3% (raw) 96,3% (related to Forskolin)	113% (related to Embelin) 73,1% (related to Forskolin)
2790	[(2S,3R,4R)-4-[(4-cyanophenyl)methyl]-2-(3,4-dimethoxyphenyl)tetrahydrofuran-3-yl]methyl (Z)-2-methylbut-2-enoate	-	166,9% (raw) 112,1% (related to Forskolin)	119,6% (related to Embelin) 77,3% (related to Forskolin)
2791	[(2S,3R,4R)-4-[(4-acetylphenyl)methyl]-2-(3,4-dimethoxyphenyl)tetrahydrofuran-3-yl]methyl (Z)-2-methylbut-2-enoate	-	169% (raw) 113,5% (related to Forskolin)	123,5% (related to Embelin) 79,8% (related to Forskolin)
2792	ethyl 4-[[(3R,4R,5S)-5-(3,4-dimethoxyphenyl)-4-[[(Z)-2-methylbut-2-enoyl]oxymethyl]tetrahydrofuran-3-yl]methyl]benzoate	-	158% (raw) 106,2% (related to Forskolin)	117,9% (related to Embelin) 76,2% (related to Forskolin)
2793	[(2S,3R,4R)-2-(3,4-dimethoxyphenyl)-4-(p-tolylmethyl)tetrahydrofuran-3-yl]methyl (Z)-2-methylbut-2-enoate	-	158,8% (raw) 106,7% (related to Forskolin)	120,1% (related to Embelin) 77,7% (related to Forskolin)
2795	14-acetyl-8,10-dihydroxy-13-[2-(3-hydroxy-2-methyl-5-oxo-cyclopenten-1-yl)-4-methyl-5-oxo-tetrahydrofuran-3-yl]-1,6,10-trimethyl-4-oxatetracyclo[10.2.1.02,11.03,7]pentadec-2(11)-en-5-one	-	138% (raw) 92,7% (related to Forskolin)	109,4% (related to Embelin) 70,7% (related to Forskolin)
2796	3,5,7-trihydroxy-2-(4-hydroxyphenyl)chroman-4-one	-	162,6% (raw) 109,3% (related to Forskolin)	113,8% (related to Embelin) 73,6% (related to Forskolin)
2797	3,5,7-trihydroxy-2-(3-hydroxy-4-methoxy-phenyl)chroman-4-one	-	141,2% (raw) 94,9% (related to Forskolin)	106,1% (related to Embelin) 68,6% (related to Forskolin)
2798	5,7-dihydroxy-2-(4-hydroxyphenyl)chroman-4-one	-	148,3% (raw) 103,3% (related to Forskolin)	115,4% (related to Embelin) 71,1% (related to Forskolin)
2799	5,7-dihydroxy-2-(3-hydroxy-4-methoxy-phenyl)-6-methoxy-chroman-4-one	-	161,1% (raw) 112,2% (related to Forskolin)	125% (related to Embelin) 77,1% (related to Forskolin)
2800	3,5-dihydroxy-2-(4-hydroxyphenyl)-7-methoxy-chroman-4-one	-	153,8% (raw) 107,2% (related to Forskolin)	126,8% (related to Embelin) 78,1% (related to Forskolin)

2802	3,5,7-trihydroxy-6-methoxy-2-(4-methoxyphenyl)chromen-4-one	-	149,6% (raw) 104,2% (related to Forskolin)	126,4% (related to Embelin) 77,9% (related to Forskolin)
2803	4-hydroxybenzoic acid	-	146,6% (raw) 102,1% (related to Forskolin)	119,6% (related to Embelin) 73,7% (related to Forskolin)
2804	8-[(1S,5E)-4-oxo-5-[(Z)-pent-2-enylidene]cyclopent-2-en-1-yl]octanoic acid	-	142,7% (raw) 99,4% (related to Forskolin)	115,3% (related to Embelin) 71% (related to Forskolin)
2805	(8Z)-8-[4-oxo-5-[(Z)-pent-2-enyl]cyclopent-2-en-1-ylidene]octanoic acid	-	132,7% (raw) 92,4% (related to Forskolin)	117,4% (related to Embelin) 72,3% (related to Forskolin)
2806	(8E)-8-[4-oxo-5-[(Z)-pent-2-enyl]cyclopent-2-en-1-ylidene]octanoic acid	-	136,3% (raw) 95% (related to Forskolin)	120,3% (related to Embelin) 74,1% (related to Forskolin)
2807	8-[(1S,5Z)-4-oxo-5-[(Z)-pent-2-enylidene]cyclopent-2-en-1-yl]octanoic acid	-	135,6% (raw) 94,4% (related to Forskolin)	112,6% (related to Embelin) 69,4% (related to Forskolin)
2808	8-[(1S,5R)-4-oxo-5-[(Z)-pent-2-enyl]cyclopent-2-en-1-yl]octanoic acid	-	132,5% (raw) 92,3% (related to Forskolin)	114,4% (related to Embelin) 70,5% (related to Forskolin)
DNTI external substance	(9Z,12Z,15Z)-octadeca-9,12,15-trienoic acid	Alpha linolenic acid	-	-
DNTI external substance	(5Z,8Z,11Z,14Z)-icosa-5,8,11,14-tetraenoic acid	Arachidonic acid	-	-
DNTI external substance	(4Z,7Z,10Z,13Z,16Z,19Z)-docosa-4,7,10,13,16,19-hexaenoic acid	Docosahexaenoic acid	-	-
DNTI external substance	2,5-dihydroxy-3-undecyl-1,4-benzoquinone	Embelin	-	-
DNTI external substanc	(5Z,8Z,11Z,14Z,17Z)-icosa-5,8,11,14,17-pentaenoic acid	Eicosapentaenoic acid	-	-

e				
DNTI external substance	[(3R,4aR,5S,6S,6aS,10S,10aR,10bS)-6,10,10b-trihydroxy-3,4a,7,7,10a-pentamethyl-1-oxo-3-vinyl-5,6,6a,8,9,10-hexahydro-2H-benzo[f]chromen-5-yl] acetate	Forskolin	-	-
DNTI external substance	(9Z,12Z)-octadeca-9,12-dienoic acid	Linoleic acid	-	-

6.2 Abbreviations

5-LO	5-Lipoxygenase
6-OAU	6-(Octylamino)-2,4(1H,3H)-pyrimidinedione
9/13-HODE	9/13-hydroxy-octadecadienoic acid
9/13-OxoODE	9/13-oxo-octadecadienoic acid
AA	Arachidonic acid
ABCA1	ATP-Binding Cassette, Sub-Family A 1
AC	Adenylyl cyclase
AKT	Ak strain transforming
ALA	Alpha linolenic acid
ASA	Acetyl salicylic acid
ATP	Adenosine triphosphate
CIB	Complete induction buffer
cAMP	Cyclic adenosine monophosphate
DHA	Docosahexaenoic acid
DIM	Diindolylmethane
DMEM	Dulbecco’s Modified Eagle’s Medium
DMSO	Dimethyl sulfoxide
EDTA	Ethylenediaminetetraacetic acid
EPA	Eicosapentaenoic acid
EPAC	Exchange protein activated by cAMP
Eppi	Eppendorf tube
ERK1/2	Extracellular signal-regulated kinase 1/2

FACS	Fluorescence-activated cell sorting
FBS	Fetal bovine serum
FMLP	N-Formylmethionyl-leucyl-phenylalanine
FRET	Fluorescence resonance energy transfer
GPR84	G Protein-coupled receptor 84
HEK-cells	Human embryonic kidney cells
HEPES	4-(2-Hydroxyethyl)piperazin-1-ylethanesulphonic acid
HO-1	Heme oxygenase 1
IL-1	Interleukine 1
LA	Linoleic acid
LCFS	Long chained fatty acids
MCFS	Medium chained fatty acids
MPGES-1	Microsomal prostaglandine E synthase-1
MTOR	Mammalian target of rapamycin
NFκB	Nuclear factor kappa-light-chain-enhancer of activated B cells
NLRP3	NOD-like receptor protein-3
Nrf2	nuclear factor E2-related factor 2
OXLAMs	Oxidized linoleic acid metabolites
PBMC	Peripheral blood mononuclear cell
PBS	Phosphate-buffered saline
PDG	Pinoresinol diglucoside
PKA	Protein kinase A
RBC	Red blood cells
ROS	Reactive oxygen species
RPMI	Roswell Park Memorial Institute
SCFS	Short chained fatty acids
TEER	Transepithelial/Transendothelial Electrical Resistance
TGR5	Takeda G protein-coupled receptor 5
TLR-4	Toll-like receptor 4
TNF-α	Tumor necrosis factor alpha

6.3 References

1. Zhang, Q. *et al.* GPR84 signaling promotes intestinal mucosal inflammation via enhancing NLRP3 inflammasome activation in macrophages. *Acta Pharmacol. Sin.* **43**, 2042–2054 (2022).
2. Lh, C. *et al.* Phosphodiesters as GPR84 Antagonists for the Treatment of Ulcerative Colitis. *J. Med. Chem.* **65**, (2022).
3. L, G. *et al.* A Newly Discovered Antifibrotic Pathway Regulated by Two Fatty Acid Receptors: GPR40 and GPR84. *Am. J. Pathol.* **188**, (2018).
4. Wang, S. *et al.* GPR84 regulates pulmonary inflammation by modulating neutrophil functions. *Acta Pharmacol. Sin.* **44**, 1665–1675 (2023).
5. Yin, C. *et al.* Regulatory role of Gpr84 in the switch of alveolar macrophages from CD11blo to CD11bhi status during lung injury process. *Mucosal Immunol.* **13**, 892–907 (2020).
6. Zhang, X. *et al.* Pro-phagocytic function and structural basis of GPR84 signaling. *Nat. Commun.* **14**, 5706 (2023).
7. Li, J. *et al.* Targeting metabolic sensing switch GPR84 on macrophages for cancer immunotherapy. *Cancer Immunol. Immunother. CII* **73**, 52 (2024).
8. Gaidarov, I. *et al.* Embelin and its derivatives unravel the signaling, proinflammatory and antiatherogenic properties of GPR84 receptor. *Pharmacol. Res.* **131**, 185–198 (2018).
9. Ohue-Kitano, R. *et al.* Medium-chain fatty acids suppress lipotoxicity-induced hepatic fibrosis via the immunomodulating receptor GPR84. *JCI Insight* **8**, e165469 (2023).
10. Luscombe, V. B., Wang, P., Russell, A. J. & Greaves, D. R. Biased agonists of GPR84 and insights into biological control. *Br. J. Pharmacol.* **181**, 1509–1523 (2024).
11. Wang, J., Wu, X., Simonavicius, N., Tian, H. & Ling, L. Medium-chain Fatty Acids as Ligands for Orphan G Protein-coupled Receptor GPR84 *. *J. Biol. Chem.* **281**, 34457–34464 (2006).
12. Suzuki, M. *et al.* Medium-chain Fatty Acid-sensing Receptor, GPR84, Is a Proinflammatory Receptor. *J. Biol. Chem.* **288**, 10684–10691 (2013).
13. Sun, X.-N. *et al.* GPR84-mediated signal transduction affects metabolic function by promoting brown adipocyte activity. *J. Clin. Invest.* **133**, e168992 (2023).
14. Wojciechowicz, M. L. & Ma'ayan, A. GPR84: an immune response dial? *Nat. Rev. Drug Discov.* **19**, 374–374 (2020).
15. Marsango, S. & Milligan, G. Regulation of the pro-inflammatory G protein-coupled receptor GPR84. *Br. J. Pharmacol.* **181**, 1500–1508 (2024).
16. Zhang, Q., Yang, H., Li, J. & Xie, X. Discovery and Characterization of a Novel Small-Molecule Agonist for Medium-Chain Free Fatty Acid Receptor G Protein–Coupled Receptor 84. *J. Pharmacol. Exp. Ther.* **357**, 337–344 (2016).
17. Pillaiyar, T. *et al.* Diindolylmethane Derivatives: Potent Agonists of the Immunostimulatory Orphan G Protein-Coupled Receptor GPR84. *J. Med. Chem.* **60**, 3636–3655 (2017).
18. Lee, K. Epac: new emerging cAMP-binding protein. *BMB Rep.* **54**, 149–156 (2021).
19. Recio, C. *et al.* Activation of the Immune-Metabolic Receptor GPR84 Enhances Inflammation and Phagocytosis in Macrophages. *Front. Immunol.* **9**, 1419 (2018).

20. Aktar, R., Rondinelli, S. & Peiris, M. GPR84 in physiology—Many functions in many tissues. *Br. J. Pharmacol.* **181**, 1524–1535 (2024).
21. Nicol, L. S. C. *et al.* The role of G-protein receptor 84 in experimental neuropathic pain. *J. Neurosci. Off. J. Soc. Neurosci.* **35**, 8959–8969 (2015).
22. Calebiro, D., Nikolaev, V. O., Persani, L. & Lohse, M. J. Signaling by internalized G-protein-coupled receptors. *Trends Pharmacol. Sci.* **31**, 221–228 (2010).
23. J, F. *et al.* GRK2 selectively attenuates the neutrophil NADPH-oxidase response triggered by β-arrestin recruiting GPR84 agonists. *Biochim. Biophys. Acta Mol. Cell Res.* **1869**, (2022).
24. Ramsden, C. E. *et al.* Lowering dietary linoleic acid reduces bioactive oxidized linoleic acid metabolites in humans. *Prostaglandins Leukot. Essent. Fatty Acids* **87**, 135–141 (2012).
25. Whelan, J. & Fritsche, K. Linoleic Acid. *Adv. Nutr.* **4**, 311–312 (2013).
26. Schuster, S. *et al.* Oxidized linoleic acid metabolites induce liver mitochondrial dysfunction, apoptosis, and NLRP3 activation in mice. *J. Lipid Res.* **59**, 1597–1609 (2018).
27. Chen, T.-C. *et al.* Effect of omega-6 linoleic acid on neurobehavioral development in Caenorhabditis elegans. *Prostaglandins Leukot. Essent. Fatty Acids* **191**, 102557 (2023).
28. Mercola, J. & D'Adamo, C. R. Linoleic Acid: A Narrative Review of the Effects of Increased Intake in the Standard American Diet and Associations with Chronic Disease. *Nutrients* **15**, 3129 (2023).
29. F, da C. S. *et al.* Oxidized linoleic acid metabolites regulate neuronal morphogenesis in vitro. *Neurochem. Int.* **164**, (2023).
30. Liang, N. *et al.* Feeding mice a diet high in oxidized linoleic acid metabolites does not alter liver oxylipin concentrations. *Prostaglandins Leukot. Essent. Fatty Acids* **172**, (2021).
31. Ramsden, C. E. *et al.* Effects of diets enriched in linoleic acid and its peroxidation products on brain fatty acids, oxylipins, and aldehydes in mice. *Biochim. Biophys. Acta Mol. Cell Biol. Lipids* **1863**, 1206 (2018).
32. Oettl, S. K. *et al.* Imbricaric Acid and Perlatolic Acid: Multi-Targeting Anti-Inflammatory Depsides from Cetrelia monachorum. *PLOS ONE* **8**, e76929 (2013).
33. Zhang, Y., Lei, Y., Yao, X., Yi, J. & Feng, G. Pinoresinol diglucoside alleviates ischemia/reperfusion-induced brain injury by modulating neuroinflammation and oxidative stress. *Chem. Biol. Drug Des.* **98**, 986–996 (2021).
34. Lei, S. *et al.* Pinoresinol diglucoside attenuates neuroinflammation, apoptosis and oxidative stress in a mice model with Alzheimer's disease. *Neuroreport* **32**, 259–267 (2021).
35. Haapakorva, E., Raunio, H., von Wright, A. & Harvima, I. Pinoresinol stimulates keratinocyte proliferation and downregulates TNF-α secretion in peripheral blood mononuclear cells: An experimental in vitro study. *Health Sci. Rep.* **6**, e998 (2022).
36. Chen, Y. *et al.* Pinoresinol diglucoside (PDG) attenuates cardiac hypertrophy via AKT/mTOR/NF-κB signaling in pressure overload-induced rats. *J. Ethnopharmacol.* **272**, 113920 (2021).
37. Perhal, A. Elucidation of Signal Transduction Mechanisms with Pathological Relevance for Cardiovascular Diseases in-vitro and in-vivo. (ETH Zurich, 2020). doi:10.3929/ethz-b-000440925.
38. Swanson, D., Block, R. & Mousa, S. A. Omega-3 Fatty Acids EPA and DHA: Health Benefits Throughout Life1. *Adv. Nutr.* **3**, 1–7 (2012).
39. Kousparou, C., Fyrilla, M., Stephanou, A. & Patrikios, I. DHA/EPA (Omega-3) and LA/GLA (Omega-6) as Bioactive Molecules in Neurodegenerative Diseases. *Int. J. Mol. Sci.* **24**, 10717 (2023).

40. Puengel, T. *et al.* The Medium-Chain Fatty Acid Receptor GPR84 Mediates Myeloid Cell Infiltration Promoting Steatohepatitis and Fibrosis. *J. Clin. Med.* **9**, 1140 (2020).
41. Audoy-Rémus, J. *et al.* GPR84 deficiency reduces microgliosis, but accelerates dendritic degeneration and cognitive decline in a mouse model of Alzheimer's disease. *Brain. Behav. Immun.* **46**, 112–120 (2015).
42. Ieremias, L. *et al.* Structure-Activity Relationship Studies and Optimization of 4-Hydroxypyridones as GPR84 Agonists. *J. Med. Chem.* **67**, 3542–3570 (2024).
43. Mancini, S. J. *et al.* On-target and off-target effects of novel orthosteric and allosteric activators of GPR84. *Sci. Rep.* **9**, 1861 (2019).
44. Zhu, Y. *et al.* Research Progress on the Relationship between Atherosclerosis and Inflammation. *Biomolecules* **8**, 80 (2018).

6.4 List of tables

6.5 Table of figures